An investigation of the activation of protein kinase complexes in the MyD88 signalling network

Jiazhen Zhang

A thesis submitted for the degree of Doctor of Philosophy

MRC Protein Phosphorylation and Ubiquitylation Unit
School of Life Sciences
University of Dundee

March 2017

I. Table of contents

II. List of figures

Chapter 1

Chapter 3

Chapter 4

Chapter 5

III. List of tables

IV. Acknowledgements

First and foremost, I would like to thank my supervisor Philip for providing me with such a great opportunity to study in Dundee and explore these exciting projects over the last four years. In particular, I appreciate his excellent guidance, and conceptual insights, as well as constant support.

Secondly, I want to express my gratitude towards the Cohen lab, both past and present, for providing me with technical and moral support throughout my projects. Especially, I would like to thank Kristopher Clark for sharing invaluable bench experience and practical advice with me.

Thirdly, I am grateful to the members of my thesis committee, Simon Arthur and Yogesh Kulathu, for their support and suggestions.

I would also like to extend my sincere gratitude to the members of the support teams of the MRC-PPU. Special thanks are due to Robert Gourlay and David Campbell for phosphorylation site identification; Rosie Clarke and Arlene Whigham for cell sorting and flow cytometry, and Kirsten McLeod, Janis Stark, Alison Muir and Laura Fin for tissue culture support. I am also grateful to all the Divisional administrative support staff, particularly Alison Hart, Allison Bridges, Hannah Kendall, Judith Hare and Rachel Naismith. They have all made working here a tremendously rewarding experience.

In addition, I owe a great deal to the teams that support the Division of Signal Transduction Therapy. James Hastie and Hilary McLauchlan for running the facility so well; Mark Peggie and Thomas Macartney for the enormous number of clones they generated for my work; Fiona Brown for antibody production, Mark Dorward for protein production and Ryan Traynor for providing kinase inhibitors. My work would have not been possible without their contributions.

Finally, I wish to thank my parents, my friends in the UK and China, my sports mates (both football and badminton). I know the four years of my PhD would not have been the same without you. Most of all, thanks to my girlfriend Shuyu Li and our cats Mimi (RIP I love you) and Bruce Li for being with me, through the light and the dark.

V. Declarations

I hereby declare that the following thesis is based on the results of investigations conducted by myself, and that this thesis is of my own composition. Work other than my own is clearly indicated in the text by reference to the researchers or their publications. This thesis has not in whole or in part been previously presented for a higher degree.

Jiazhen Zhang

I certify that Jiazhen Zhang has spent the equivalent of at least nine terms in research work in the Medical Research Council Protein Phosphorylation and Ubiquitylation Unit (MRC-PPU), School of Life Sciences, University of Dundee and that he has fulfilled the conditions of the Ordinance General No. 14 of the University of Dundee and is qualified to submit the accompanying thesis in application for the degree of Doctor of Philosophy.

Professor Sir Philip Cohen, F.R.S, F.R.S.E

VI. List of Publications

Zhang, J., Clark, K., Lawrence, T., Peggie, M. W. and Cohen, P. (2014) An unexpected twist to the activation of IKKβ: TAK1 primes IKKβ for activation by autophosphorylation. Biochem. J. **461**, 531–7.

Zhang, J., Macartney, T., Peggie, M. and Cohen, P. (2016) Interleukin-1 activates TAK1 kinase complexes by two different mechanisms. Manuscript in preparation.

Strickson, S., Emmerich, C. H., Goh, E. T. H., **Zhang, J.**, Ian, K., Ortiz-Guerrero, J., Macartney, T., Hastie, J., Knebel, A., Peggie, M., et al. (2016) Identification of E3 ligase-dependent and independent roles of TRAF6. Submitted.

VII. Abbreviations

ABIN	A20-binding inhibitor of NF-κB
ABTS	2,2'-Azino-bis[3-ethylbenzothiazoline-6-sulfonicacid]-diammonium salt
ACN	acetonitrile
AP-1	activator protein 1
APS	ammonium persulphate
ASC	apoptosis-associated speck-like protein containing a CARD domain
ATF2	activating transcription factor 2
ATP	adenosine 5'-triphosphate
BMDM	bone marrow-derived macrophage
BMP	bone morphogenetic protein
C1	Compound 1
Cas9	CRISPR associated protein 9
CC	coiled-coil
CD	cluster of differentiation
cIAP	cellular inhibitor of apoptosis protein
CLR	C-type Lectin receptor
cpm	counts per minute
CREB	cAMP response element binding protein
CRISPR	clustered regularly interspaced short palindromic repeat
CT	C-terminal
CTD	C-terminal domain
CYLD	Cylindromatosis
Da	Dalton
DAMP	damage-associated molecular pattern
DD	death domain
DMEM	Dulbecco's modified Eagle's medium
DMSO	dimethyl sulphoxide
DNA	deoxyribonucleic acid
DSB	double-stranded break
DSTT	Division of Signal Transduction Therapy
DTT	dithiothreitol
DUB	deubiquitylase
DUSP1	dual specificity phosphatase 1
E.coli	Escherichia coli
e.g.	exempli gratia
E1	ubiquitin-activating enzyme
E2	ubiquitin-conjugating enzyme
E3	ubiquitin ligase
ECL	enhanced chemiluminescence
EDA-ID	anhidrotic ectodermal dysplasia with immunodeficiency
EDTA	sodium ethylenediaminetetraacetic acid
EGTA	sodium ethylene glycol tetra acetic acid
ELISA	enzyme-linked immunosorbant assay
ERK	extracellular-signal regulated kinase
ES	embryonic stem
FACS	flow-cytometry associated cell sorting
FBS	foetal bovine serum

FHA	fork-head-associated
g	gram
G418	geneticin
GAPDH	glyceraldehyde 3-phosphate dehydrogenase
GCK	germinal centre kinase
gRNA	guide ribonucleic acid
GST	glutathione S-transferase
h	hour
HA	haemagglutinin
HEK	human embryonic kidney
HEPES	4-(2-Hydroxyethyl)piperazine-1-ethanesulfonic acid
HOIL1	heme-oxidized IRP2 ubiquitin ligase 1
HOIP	HOIL1-interacting protein
HPLC	high performance liquid chromatography
HRP	horseradish peroxidase
IFN	interferon
Ig	immunoglobulin
IgG	immunoglobulin G
IKK	IκB kinase
IL	Interleukin
IL-1R	Interleukin-1 receptor
IL-1R1	Interleukin-1 receptor type 1
IL-1RA	Interleukin-1 receptor antagonist protein
IL-1RAcP	Interleukin-1 receptor accessory protein
IRAK	IL-1R-associated kinase
IRF	interferon regulatory factor
IκB	inhibitor of NF-κB
JNK	c-Jun N-terminal kinase
K48-Ub	K48-linked ubiquitin
K63-Ub	K63-linked ubiquitin
kDa	kilodalton
KO	knockout
L	litre
LB	Luria-Bertani medium
LPS	lipopolysaccharide
LRR	leucine-rich repeat
LUBAC	linear ubiquitin assembly complex
LZ	Leucine zipper
m	milli
M	molar
MAL	MyD88 adaptor like
MAP	mitogen-activated protein
MAP3K	mitogen-activated protein kinase kinase kinase
MEF	mouse embryonic fibroblast
MEK	MAP kinase/ERK kinase
MEKK	MAP kinase/ERK kinase kinase
Met1-Ub	Met1-linked/ linear ubiquitin
Min	minute
MK2	MAP kinase-activated protein kinase 2

MKK	MAP kinase kinase
MNK	MAP kinase integrating kinase
MRC-PPU	Medical Research Council Protein Phosphorylation and Ubiquitylation Unit
mRNA	messenger ribonucleic acid
MS	mass spectrometry
MSK	mitogen- and stress-activated protein kinase
MyD88	myeloid differentiation primary response gene 88
n	nano
NaCl	sodium chloride
NBD	NEMO-binding domain
NEMO	NF-κB Essential Modifier
NF-κB	nuclear factor κB
NIK	NF-κB-interacting kinase
NLR	NOD-like receptor
NLRP3	NLR-, LRR- and pyrin-containing protein-3
NLS	nuclear localization sequence
NOD	nucleotide oligomerisation domain
N-terminal	amino terminal
NZF	Npl40 zinc finger
p-	phospho
PAGE	polyacrylamide gel electrophoresis
PAMP	pattern associated molecular pattern
PBS	phosphate-buffered saline
PCR	polymerase chain reaction
pDC	plasmacytoid dendritic cell
PEI	polyethylenimine
PKACα	cAMP-dependent protein kinase catalytic subunit α
PMA	phorbol 12-myristate 13-acetate
PMSF	phenylmethansulphonyl fluoride
PP	protein phosphatase
PRKX	X-linked protein kinase
PRR	pattern recognition receptor
PST	proline/serine/threonine
pUb	poly ubiquitin
PVDF	polyvinylidene fluoride
qRT-PCR	real-time quantitative reverse transcription polymerase chain reaction
RANKL	receptor activator of NF-κB ligand
RBR	RING-in-between-RING
RIG	retinoic acid-inducible gene-1
RING	really interesting new gene
RLR	RIG -I-like receptor
RNA	ribonucleic acid
rpm	revolutions per minute
RSK	ribosomal protein S6 kinase
RT	room temperature
s	second
SARM	sterile α- and HEAT/Armadillo containing protein

$SCF^{\beta TrCP}$	β-TrCP F-box–containing component of a Skp1-Cullin-F-box (SCF)–type E3 ubiquitin-protein ligase complex
SDD	scaffold/dimerization domain
SDS	sodium dodecyl sulphate
SHARPIN	SHANK-associated RH domain-interacting protein
shRNA	short hairpin ribonucleic acid
siRNA	small interfering ribonucleic acid
SMAC	second mitochondrion-derived activator of caspase
STAT3	signal transducer and activator of transcription 3
TAB	TAK1-binding protein
TACE	TNFα-converting enzyme
TAK1	transforming growth factor β-activated kinase 1
TANK	TRAF family member-associated NF-κB activator
TBK1	TANK-binding kinase 1
TBS	tris-buffered saline
TBS-T	tris-buffered saline with Tween 20
TEABC	Triethylammonium bicarbonate
TEMED	tetramethylethylenediamine
TGFβ	transforming growth factor β
TICAM-1/2	TIR domain containing molecule 1/2
TIR	Toll/interleukin-1 receptor
TIRAP	TIR-associated protein
TLR	Toll-like receptor
TM	transmembrane
TNF	tumour necrosis factor
Tollip	Toll-interacting protein
Tpl2	tumour progression locus 2
TRAF	TNF-associated factor
TRAM	TRIF-related adaptor molecule
TRIF	TIR-domain-containing adaptor protein inducing interferon
tris	tris(hydroxymethyl)aminomethane
TTP	tris-tetraprolin
Ub	ubiquitin
ULD	ubiquitin-like domain
USP	Ub-specific peptidase
VSV-G	vesicular stomatitis virus G protein
WT	wild type
XIAP	X-linked inhibitor of apoptosis protein
ZF	zinc finger
β-ME	2-mercaptoethanol
μ	micro

VIII. Amino Acid Code

Amino acid	Three letter symbol	Single letter symbol
Alanine	Ala	A
Arginine	Arg	R
Asparagine	Asn	N
Aspartic acid	Asp	D
Cysteine	Cys	C
Glutamic acid	Glu	E
Glutamine	Gln	Q
Glycine	Gly	G
Histidine	His	H
Isoleucine	Ile	I
Leucine	Leu	L
Lysine	Lys	K
Methionine	Met	M
Proline	Pro	P
Serine	Ser	S
Threonine	Thr	T
Tryptophan	Trp	W
Tyrosine	Tyr	Y
Valine	Val	V
Any amino acid	Xaa	X
Any aromatic or acidic residue	Aaa	

IX. Summary

The TAK1 and canonical IKK complexes are the two master protein kinases of the innate immune system that control the production of inflammatory mediators, but the mechanisms by which they are activated in this system are still unclear. In this thesis, I present the research I have carried out to solve these problems.

The IKKβ component of the canonical IKK complex is required to activate the transcription factors NF-κB and IRF5 and the protein kinase Tpl2, but how IKKβ itself is activated *in vivo* is still unclear. It was found to require phosphorylation by one or more 'upstream' protein kinases in some reports, but by autophosphorylation in others. In the first part of this thesis, I describe my work that has resolved this controversy by demonstrating that the activation of IKKβ induced by IL-1 (interleukin-1) or TNF (tumour necrosis factor) in embryonic fibroblasts, or by ligands that activate Toll-like receptors in macrophages, requires two distinct phosphorylation events: first, the TAK1 catalysed phosphorylation of Ser177 and, secondly, the IKKβ-catalysed autophosphorylation of Ser181. The phosphorylation of Ser177 by TAK1 is a priming event required for the subsequent autophosphorylation of Ser181, which enables IKKβ to phosphorylate exogenous substrates. I also present genetic evidence which indicates that the IL-1-stimulated, LUBAC (linear ubiquitin chain assembly complex)-catalysed formation of Met1-linked/linear ubiquitin (Met1-Ub) chains and their interaction with the NEMO (NF-κB essential modulator) component of the canonical IKK complex permits the TAK1-catalysed priming phosphorylation of IKKβ at Ser177 and IKKα at Ser176. These findings may be of general significance for the activation of other protein kinases.

The activation of the TAK1 complex by inflammatory stimuli is thought to be triggered by the binding of Lys63-linked ubiquitin chains to the TAB2 or TAB3 components of the TAB1-TAK1-TAB2 and TAB1-TAK1-TAB3 complexes. In the second part of the thesis I tested whether this broadly accepted model was correct by knocking out the genes encoding TAK1 and its regulatory subunits TAB1, TAB2 and TAB3 by CRISPR/Cas9 gene-editing technology, alone and in combination, in an IL-1 receptor expressing human cell line. These genetic studies led me to discover that the IL-1-dependent activation of TAK1 occurs by two different mechanisms. The first, involves the previously described interaction of Lys63-linked ubiquitin chains with TAB2 and TAB3, while the second can take place in the complete absence of TAB2 and TAB3. The second mechanism, which involves activation of the TAB1-TAK1 heterodimer is more transient than the first, but is sufficient for the IL-1-dependent transcription of immediate early genes (A20, IκBα). I show that the activation of the TAB1-TAK1 complex requires the expression of the E3 ubiquitin ligase TRAF6 and the TRAF6-generated formation of Lys63-linked ubiquitin chains, which leads to the phosphorylation of TAK1 at Thr187 and activation. However, neither TAB1 nor TAK1 bind directly to Lys63-linked ubiquitin chains. I identify one novel IL-1-dependent phosphorylation site on TAB1 and two on TAK1 and propose that Lys63-linked ubiquitin chains activate an as yet unidentified protein kinase, which phosphorylates one or more of the novel phosphorylation sites on the TAB1-TAK1 heterodimer inducing a conformational change that permits TAK1 to autophosphorylate Thr187.

Chapter 1 Introduction to the thesis

1.1 Preface

Immunity is a host defence system employed by multicellular organisms for protection against invading pathogens. It comprises two major branches: the innate immune system and the adaptive immune system [1].

The innate immune system serves as the first line of defence against microorganisms. It provokes an immediate response to recognised pathogenic components without any prior exposure. This form of defence is established by producing the effector proteins needed to target the pathogens directly but non-specifically (such as components of the complement system [1] and nitric oxide synthase [2]), or by generating inflammatory mediators that rapidly recruit immune cells to the infected site to eliminate the pathogenic infection. Innate immunity also has an important role in activating the adaptive immune response by permitting antigen presentation [3].

The adaptive immune system, also called acquired immunity, is found only in vertebrates [4]. Despite being a slower response, adaptive immunity is highly specific to particular invaders and produces precisely tailored responses to eradicate them. Immunological memory is another feature of the adaptive immune system, so that a subsequent encounter with the same antigen mounts a quicker and enhanced counterattack to remove the pathogens [5,6].

The failure of immunity, termed immunodeficiency, makes people more susceptible to infection [7–9]. The tight regulation of the immune system is also critical, since hyper-activation of the immune system can cause chronic inflammatory and autoimmune diseases, including asthma, lupus, psoriasis, rheumatoid arthritis and

septic shock, and have other severe consequences, such as different types of lymphomas [10–15].

1.2 The innate immune system

1.2.1 The pattern recognition receptor superfamily

The innate immune system is usually considered to be a generic defence mechanism, but it has nevertheless evolved some relatively specific approaches to fight infection by pathogens. One of these is the recognition of conserved pathogenic components, termed pathogen-associated molecular patterns (PAMPs). These unique and invariant modules are essential for the organism's survival and present only on pathogens and not the host [16].

The detection of PAMPs is conducted by pattern recognition receptors (PRRs) [17]. The PRR superfamily can be subdivided into four classes, including Toll-like receptors (TLRs) sensing a wide range of pathogens, NOD-like receptors (NLRs) sensing bacteria, RIG (retinoic acid-inducible gene)-I-like receptors (RLRs) sensing viruses, and C-type Lectin receptors (CLRs) sensing fungi and damaged cells [17–19]. The receptors recognise not only PAMPs, but also endogenous molecules released from damaged host cells, known as damage-associated molecular patterns (DAMPs) [19].

This thesis mainly focuses on the early events in the signalling pathways of the TLRs and the closely related Interleukin-1 receptor (IL-1R). These two types of receptors will be described in the following two subsections.

1.2.1.1 Toll-like receptors

Toll-like receptors (TLRs) are germline-encoded membrane PRRs. They are human orthologues of the Toll receptor in *Drosophila* melanogaster, which has an essential role in detecting fungi and in promoting anti-fungal responses [20,21]. TLRs are widely expressed on immune and epithelial cells. To date, 13 different TLRs have been identified in mammals, 10 of which, namely TLR1-10, are present in human, whereas TLRs 1-9 and 11-13 are expressed in mice [22]. Studies in "knock-out" (KO) mice have revealed that each TLR responds to a distinct set of PAMPs, demonstrating a degree of specificity [23].

TLRs have been divided into two groups based on their subcellular locations. The plasma membrane bound TLRs (TLR1, 2, 4, 5, 6 and 11) detect the surface components of pathogens, whilst the TLRs (TLR3, 7, 8, and 9) expressed in intracellular vesicles (endosomes and endoplasmic reticulum) bind to nuclei acids from pathogens, primarily viruses [22].

All TLRs consist of an extracellular ligand-binding domain, a transmembrane (TM) domain and a cytoplasmic signalling domain (the TLR1/2 is shown as an example in **Fig 1.1**). The tandem copies of leucine-rich repeats (LRRs) at their N-termini form a horseshoe structure in TLR dimers, which permits the engagement of ligands [24]. TLRs can function as homo- or hetero-dimers to broaden the spectrum of ligand recognition [25], and additional diversity is contributed by variable residues distinct from leucine in the LRR regions [26]. In contrast, the cytoplasmic region is highly conserved. The Toll/Interleukin-1 receptor (TIR) domain is present in all TLRs as well as the receptors for Interleukin-1 (IL-1), IL-18 and IL-33 [27]. Since TLRs have no intrinsic catalytic activity, they require adaptor proteins for coupling to signal transduction pathways.

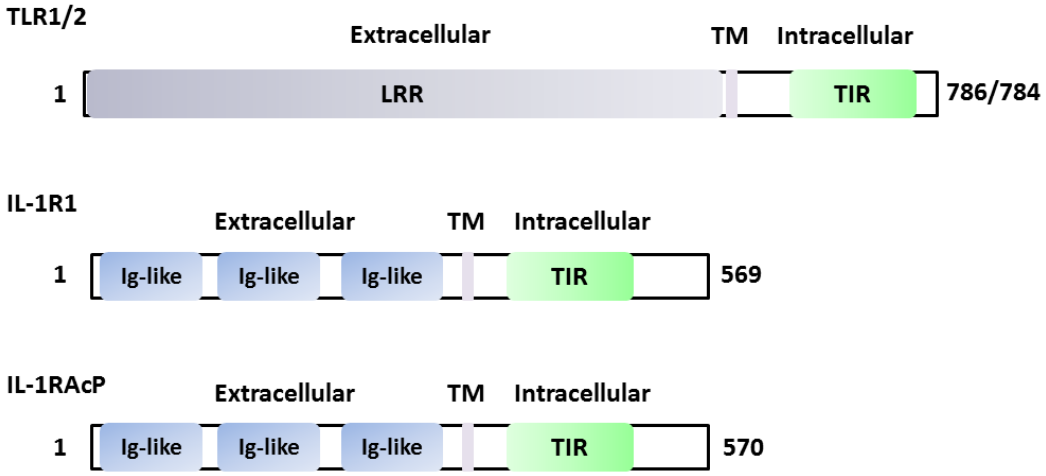

Figure 1.1 Domain organisations of TLR1/2, IL-1R1 and IL-1RAcP. TLR1/2 contains several copies of leucine-rich repeats (LRR) at N terminus, whereas both IL-1R1 and IL-1RAcP share three Ig-like regions in their extracellular portion to sense ligands. TLR1/2, IL-1R1 and IL-1RAcP possess a transmembrane domain (TM), followed by a Toll/Interleukin-1 receptor (TIR) domain for the recruitment of TIR-containing adaptor proteins.

1.2.1.2 IL-1 and the IL-1 receptor

IL-1 is a critical pro-inflammatory cytokine and its generation and secretion is a major outcome of inflammatory responses induced by the activation of TLRs [28]. Three cytokines, IL-1α, IL-1β and IL-1R antagonist (IL-1RA), bind to the type1 IL-1R (IL-1R1). IL-1α is retained in the cytosol and membrane, and only released when cells destruct as a result of necrosis or mechanical damage [29]. In contrast, IL-1β is produced in large amounts and secreted during inflammation [30]. The IL-1β precursor (pro-IL-1β) exists as a biologically inactive propeptide in cytosol, and requires proteolytic cleavage to form an active cytokine. This procedure is performed by a complex termed the NLRP3 (NLR-, LRR- and pyrin-containing protein-3) inflammasome which comprises the NLR protein NLRP3, an adaptor protein ASC (apoptosis-associated speck-like protein containing a CARD domain) and a cysteine protease pro-caspase-1 [31]. The autocatalytic cleavage of pro-caspase-1, which is induced by the formation of the inflammasome in the cytoplasm, activates caspase-1, which then processes pro-IL-1β into an active secreted form. The secretion mechanism of the mature IL-1β remains

elusive, but its export is independent of conventional endoplasmic reticulum (ER)-Golgi complex due to the lack of signal peptide [32,33]. Two separate signals are needed to activate the NLRP3 complex, the first is provided by PAMPs which activates the NF-κB-dependent transcription of NLRP3 and pro-IL-1β, and the second is from DAMPs, including ATP, uric acid and the toxin nigericin, which triggers the specific activation of NLRP3 and assembly of the inflammasome complex [31,34]. The tight regulation of precursor processing prevents the abnormal production of IL-1β and minimizes potential disorder caused by hyper-inflammation. IL-1RA is expressed as two intracellular isoforms, which are present in the cytoplasm and only released upon cell death. They bind to IL-1R1 with higher affinity than IL-1α and IL-1β. IL-1RA is unable to recruit IL-1R accessory protein (IL-1RAcP), and therefore restricts potential tissue damage caused by the action of pro-inflammatory cytokines [29].

Like TLRs, IL-1R1 contains an intracellular TIR domain (**Fig 1.1**). However, its extracellular region consists of three immunoglobulin (Ig)-like domains for the recognition of its ligands [24].

The engagement of IL-1 α/β with IL-1R1 triggers the recruitment of IL-1RAcP forming a heterodimeric complex [35,36]. The TIR domains of the IL-1R1-IL-1RAcP complex can then promote the recruitment of the adaptor protein MyD88 (myeloid differentiation primary response gene 88).

1.2.1.3 TIR adaptor proteins

The binding of ligands induces conformational changes within the intracellular TIR regions of TLRs and IL-1R1, allowing the recruitment of TIR-containing adaptor proteins so that signal propagation is initiated.

Five distinct adaptors have been identified so far, namely MyD88, MAL/TIRAP (MyD88 adaptor like/ TIR-associated protein), TRIF/TICAM-1 (TIR-domain-containing adaptor protein inducing interferon/TIR domain containing molecule 1), TRAM/ TICAM-2 (TRIF-related adaptor molecule/TIR domain containing molecule 2) and SARM (sterile α- and HEAT/Armadillo containing protein) [37].

The IL-1R1 and all TLRs, except TLR3, recruit MyD88 through a TIR-TIR domain interaction in their cytoplasmic region. TLR3 transmits its signal through TRIF, whereas TLR4 signals via both MyD88 and TRIF. TLR2 and TLR4, in particular, employ TIRAP to aid MyD88 recruitment. Once TLR4 has undergone translocation to the endosome, it requires TRAM to recruit TRIF [22]. The role of SARM remains unclear. It has been proposed to negatively regulate TRIF- and MyD88-dependent signalling pathways [38,39].

Signalling via MyD88 leads to the production of pro-inflammatory and anti-inflammatory cytokines through TLR1, TLR2, TLR4, TLR5 and TLR6. The pro-inflammatory cytokines include IL-1β, IL-6, IL-12 and tumour necrosis factor α (TNFα), while the most important anti-inflammatory cytokine is IL-10. In contrast, type 1 interferons (IFNs) are induced through TLR7, TLR8 and TLR9. TRIF-dependent signalling is primarily responsible for the generation of IFNβ [22].

1.2.2 The MyD88-mediated signalling network

The MyD88 adaptor protein is utilized by IL-1R1 and most TLRs, thus their downstream signalling pathways are similar. The pro-inflammatory cytokines produced by these pathways help to eliminate the pathogen and the anti-inflammatory molecules resolve the inflammatory response. The production of pro-inflammatory cytokines requires master transcription factors, such as NF-κB (nuclear

factor κB) and IRFs (interferon regulatory factors) [40,41]. Once activated, they translocate into nucleus and initiate the transcription of target genes encoding pro-inflammatory molecules. In contrast, the generation of anti-inflammatory cytokines is dependent on the activation of the transcription factor CREB (cAMP response element binding protein) [42].

An overview of the MyD88 signalling network is depicted in **Fig 1.2**. The structure, function and regulation of key components of this network will be described in the following sections.

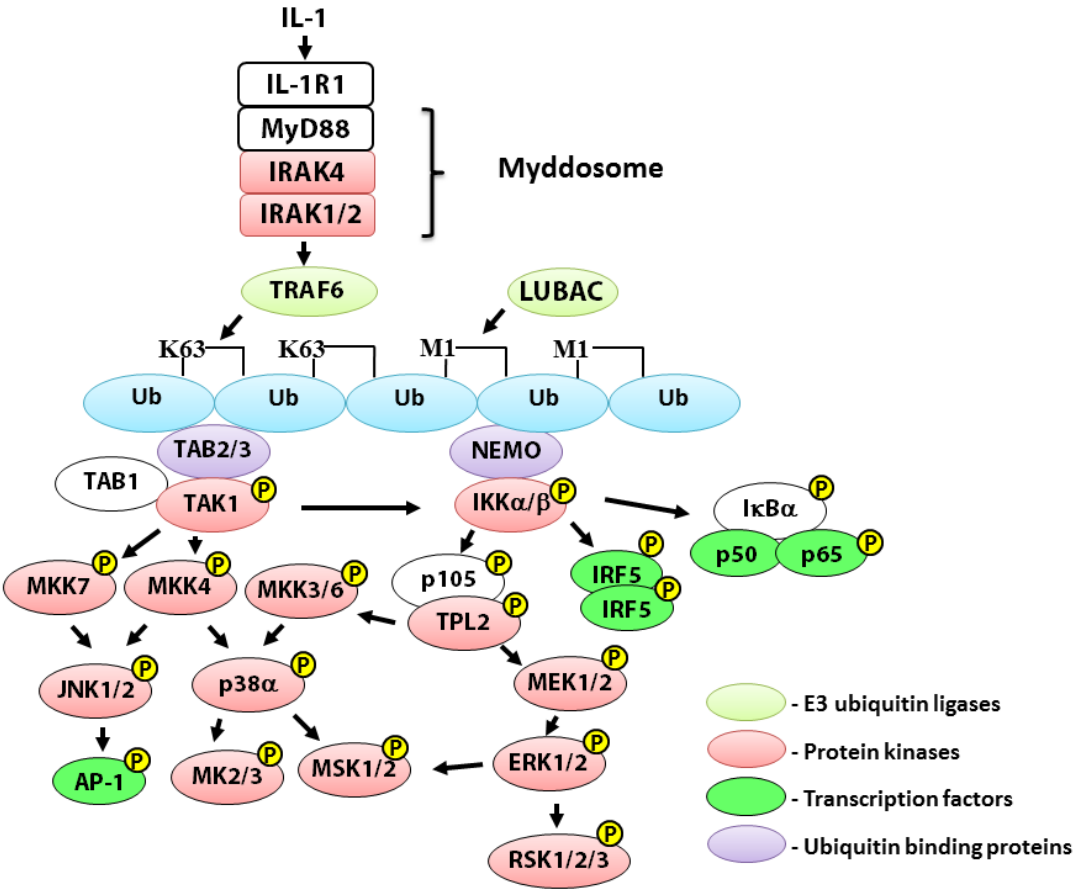

Figure 1.2 An overview of early events in the IL-1-stimulated signalling pathway. The engagement of IL-1 on IL-1R1 induces the formation of Myddosome complex. The E3 ligases including TRAF6 and LUBAC complex generate K63/Met1 hybrid poly-ubiquitin chains, leading to the activation of TAK1 complex and the canonical IKK complex. This is followed by the activation of downstream kinases and transcription factors including AP-1, NF-κB (p50:p65) and IRF5. They regulate the expression of genes encoding inflammatory cytokines. The phosphorylation event is indicated by P, without signifying the phosphorylation sites.

1.2.2.1 MyD88 and the formation of the Myddosome

MyD88 was discovered as an adaptor that recruits members of the IRAK (IL-1R-associated kinase) family to the IL-1 receptor [43]. It comprises an N-terminal death domain (DD), which facilitates its interaction with downstream DD-containing components such as IRAKs (**Fig 1.3**). The C-terminal TIR domain of MyD88 is required for its association with the TIR domain in the cytoplasmic region of TLRs and IL-1R1 (**Fig 1.1, Sections 1.2.1.1 and 1.2.1.2**) [44]. MyD88 KO mice showed resistance against lipopolysaccharide (LPS)-induced endotoxic shock, and peritoneal macrophages from these mice did not respond to IL-1 nor LPS stimulation, suggesting an indispensable role for MyD88 in signal transduction triggered by IL-1 and TLR agonists [45,46]. The binding of MyD88 to TLRs or IL-1R1 induces the recruitment of IRAK4, which interacts with MyD88 via its DD (**Fig 1.3**). This association is thought to promote its oligomerization and auto-activation, followed by further recruitment of IRAKs 1 and 2 to form a complex named the Myddosome (**Fig 1.2**) [47,48]. An X-ray crystallographic structure analysis of the DDs of the Myddosome suggested that six MyD88 molecules were first bound to receptor followed by four IRAK4 proteins, and then four IRAK1 or IRAK2 molecules. The entire Myddosome complex resembles a helical tower-like structure, with hexagonal staggered layers packed on top of one another [48].

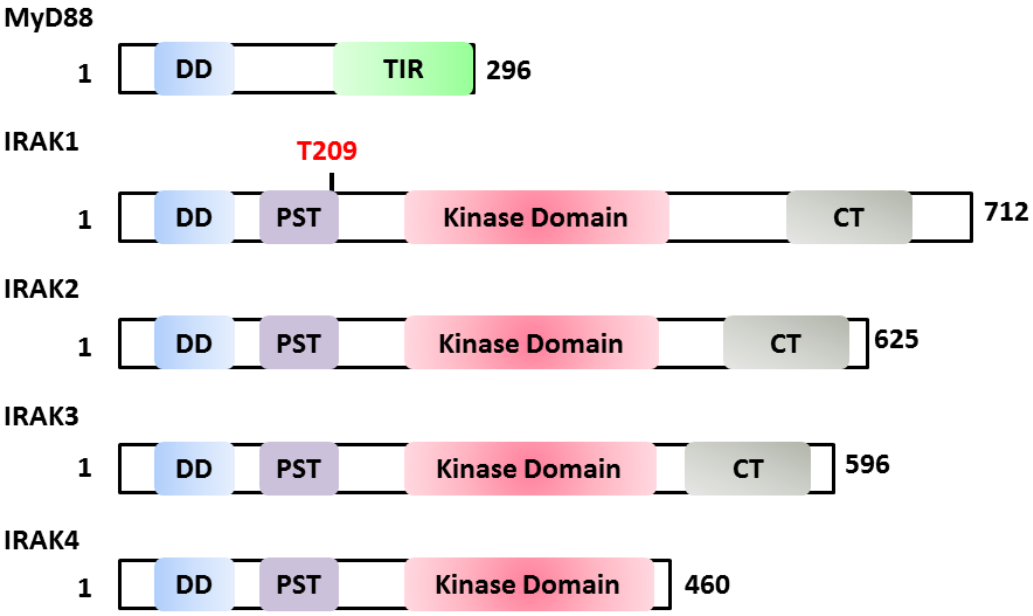

Figure 1.3 Domain organisations of MyD88 and IRAK family. MyD88 and all four IRAKs contain death domain (DD) at their N termini for the association with each other or other DD-containing proteins. The TIR domain at the C-terminal on MyD88 facilitates its interaction with TLRs or IL-1R1 at their cytoplasmic TIR regions. IRAKs contain proline/serine/threonine (PST) rich domain and kinase domain. The C-terminal (CT) domain is essential for TRAF6 binding. IRAK4 lacks CT domain, and IRAKs 2 and 3 are catalytically inactive pseudokinases. The phosphorylation site is highlighted in red.

1.2.2.2 IRAK kinases

IRAK1, originally termed IRAK, is a human orthologue of Pelle, a protein kinase crucial for the activation of NF-κB in *Drosophila* [49]. The IRAK family has four members, namely IRAK1 [49], IRAK2 [50], IRAK3 (also known as IRAKM) [51] and IRAK4 [52], named according to the order in which they were discovered. Each IRAK comprises an N-terminal death domain (DD), which interacts with MyD88 and other DD-containing proteins [53], a proline/serine/threonine (PST) rich domain where multiple sites are thought to be phosphorylated extensively, and a serine/threonine kinase domain [44] (**Fig 1.3**). All IRAKs, apart from IRAK4, additionally possess a C-terminal (CT) Pro-Xaa-Glu-Xaa-Xaa-Aaa motif (where Xaa represents any amino acid, and Aaa is an aromatic or acidic residue), which is required for their interaction with TRAF6 (tumour necrosis factor (TNF)-associated factor 6) [54].

IRAKs 1 and 4 contain intrinsic kinase activity, whereas IRAKs 2 and 3 appear to be catalytically inactive pseudokinases since the critical Asp residue in their Asp-Phe-Gly (DFG) motifs is replaced by Asn and Ser, respectively [51]. IRAK3 is expressed only in monocytes, whereas the other IRAKs are expressed in most cell types [51].

1.2.2.2.1 IRAK4

The expression of IRAK4 and its kinase activity are essential for the inflammatory response. IRAK4 KO mice showed complete resistance to LPS-induced septic shock as well as considerably reduced IL-6 and TNFα levels in serum [55,56]. The mouse embryonic fibroblasts (MEFs) or peritoneal macrophages from mice in which IRAK4 is deleted or replaced by kinase-inactive mutants showed severe reduction in the IL-1 or TLR agonist-induced activation of MAP (mitogen-activated protein) kinases and the canonical IKK (IκB (inhibitor of NF-κB) kinase) complex [55–57]. The activation of IRAK4 is believed to occur through *trans*-autophosphorylation [58], which is prompted by its oligomerization after interaction with MyD88 [59].

1.2.2.2.2 IRAK1

MyD88 signalling and the secretion of inflammatory cytokines were reduced in IRAK1 KO bone marrow-derived macrophages (BMDMs) and MEFs, but re-expression of a catalytically inactive mutant of IRAK1 rescued the signal, indicating that the kinase activity of IRAK1 is not essential for the production of inflammatory cytokines in these cells [60] and suggesting that IRAK1 may function as a scaffold to recruit other proteins. The association between IRAK1 and TRAF6 has been demonstrated *in vitro* [54], but the genetic evidence needed to establish the *in vivo* significance of this interaction has yet to be obtained. The mechanism of IRAK1 activation has also not yet been established. It has been proposed that, like IRAK4, the oligomerization of IRAK1

permits its auto-phosphorylation at Thr209, which is essential for its activation *in vitro* [61].

1.2.2.2.3 IRAKs 2 and 3

Although IRAK2 and IRAK3 are both pseudokinases [51], they play distinct roles in the MyD88 signalling network. Studies in macrophages derived from IRAK2 KO mice revealed the importance of IRAK2 in the TLR-induced activation of NF-κB and the expression of genes encoding pro-inflammatory cytokines after prolonged TLR signalling, though it is dispensable for the initial response to TLR agonists [62]. The mutation of Glu525 in the Pro-Xaa-Glu-Xaa-Xaa motif to Ala in IRAK2 disrupted the interaction between IRAK2 and TRAF6. Interestingly, the loss of this interaction did not affect the MyD88 signalling network in BMDMs during the early phase (0-2 h), but the transcription and secretion of pro-inflammatory mediators was almost completely gone in the late phase (2-8 h), indicating that IRAK2 is a positive regulator for the production of inflammatory cytokines [60]. Given that the deletion of both IRAK1 and IRAK2 leads to substantial defects in the TLR signalling pathway [62] and that IRAK1 is largely degraded 2-4 h after the initial response [60], it is possible that IRAK2 functions redundantly with IRAK1 in the early phase, but the IRAK2-TRAF6 interaction becomes essential for sustaining the signal during the late phase.

As the least investigated member in the IRAK family, IRAK3 is thought to restrict the MyD88 signalling network, since BMDMs lacking IRAK3 expression showed enhanced release of inflammatory cytokines in response to stimulation by TLR agonists [63].

1.2.3 The E3 ligase TRAF6 and the activation of TAK1 by ubiquitin chains

In 1996, Cao *et al* reported TRAF6 as the 6th member in the TRAF family [64]. The TRAF family of proteins were initially identified as molecules associated with the cytoplasmic portion of TNF receptors [65]. The seven members reported so far are characterized by similar structures [66]. All TRAFs, except TRAF1, contain an N-terminal RING (really interesting new gene) domain, followed by several zinc-finger (ZF) domains, and a coiled-coil (CC) region (TRAF6 is shown as an example in **Fig 1.4**). The TRAF-C (C-terminal) domain is present in all TRAFs except TRAF7. An structural analysis revealed that the TRAF-C domain of TRAF6 enables to interact with Pro-Xaa-Glu-Xaa-Xaa-Aaa motif on IRAKs 1, 2 and 3 [54].

The overexpression of TRAF6 in human embryonic kidney 293 (HEK293) cells activated NF-κB, while a dominant-negative mutant of TRAF6, which lacked the RING domain and four ZF domains, failed to trigger IL-1-induced NF-κB activation [64]. The indispensable role of TRAF6 in MyD88-dependent signalling network was further demonstrated in MEFs from TRAF6 KO mice stimulated with IL-1 or LPS [67]. RING domains were subsequently found to possess E3 ubiquitin ligase activity [68], and Zhijian Chen's group then discovered that TRAF6 functioned as an E3 ligase. Together with an E2 enzyme complex Ubc13-Uev1a, which contacts the RING and ZF1 domain in TRAF6 (**Fig 1.4**), the E3 ligase TRAF6 was shown to catalyse the formation of K63-linked ubiquitin (K63-Ub) chains specifically [69]. The pivotal role of TRAF6 E3 ligase activity in cells was established by the finding that IL-1-dependent signalling was restored to TRAF6 KO MEFs reconstituted with wild-type TRAF6, but not with E3 ligase-defective mutants [70,71]. Interestingly, TRAF6 is the only member of the TRAF family which has

been shown convincingly to display E3 ligase activity [69]. Other TRAFs, such as TRAF2, may function as scaffolds to recruit other active E3 ligases [72].

The activation of TRAF6 is thought to result from its dimerization induced by the interaction of TRAF6 with IRAKs 1 and 2 in the Myddosome [73,74]. This is supported by the finding that oligomerization-defective TRAF6 mutants were unable to restore IL-1 signalling when re-expressed in TRAF6 KO MEFs [75].

Further investigation of the role of K63-Ub chains in the MyD88 signalling network by Zhijian Chen's lab led to the now widely accepted model that K63-Ub chains activate the TAK1 (transforming growth factor β (TGFβ)-activated kinase 1) complex. This exciting achievement was made by the famous cell-free assays that he set up to study this system [76], which will be described in the following section.

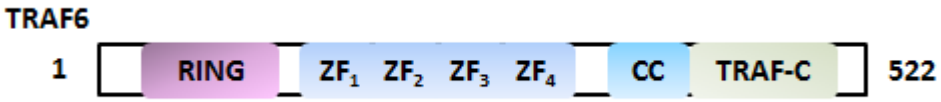

Figure 1.4 Domain organisation of TRAF6. TRAF6 comprises an N-terminal RING domain essential for its E3 ligase activity, followed by four zinc finger (ZF) domains for the interaction with E2. The coiled-coil (CC) domain is required for self-oligomerization, and TRAF-C domain allows its binding to IRAKs.

1.2.4 The TAK1 complex

TAK1 is a member of the mitogen-activated protein (MAP) kinase kinase kinase (MAP3K) family. As indicated by its full name (**Section 1.2.3**), TAK1 was initially identified as an activator of MAP kinases in cells stimulated with transforming growth factor β (TGFβ) or bone morphogenetic protein (BMP) [77]. Soon after, it was shown that TAK1 can be activated by a variety of immune stimuli, including the pro-inflammatory cytokines IL-1 [78], and agonists of TLRs and NLRs [79]. The catalytic subunit TAK1 together with the regulatory subunits namely TAK1-binding protein 1

(TAB1), TAB2 and TAB3, form two separate heterotrimeric complexes under physiological conditions: the TAB1-TAK1-TAB2 complex and the TAB1-TAK1-TAB3 complex, respectively [80].

The TAK1 catalytic subunit contains an N-terminal kinase domain, which is bound by TAB1, and a C-terminal domain (CTD), which interacts with TAB2 or TAB3 [44] (**Fig 1.5**). TAB1 is a pseudophosphatase which carries a protein phosphatase 2C (PP2C)-like domain at its N-terminus [81], followed by a p38 MAP kinase binding (PB) domain and a TAK1-binding (TB) domain at its C terminus [44]. TAB2 and TAB3 are structurally similar. Both carry an N-terminal CUE (Cue1-homologous) domain, a coiled-coil (CC) region, followed by a TAK1-binding domain and a C-terminal Npl40 zinc-finger (NZF) domain [44] (**Fig 1.5**). Both CUE and NZF domains are highly conserved and interact with K63-Ub chains. However, the deletion of the NZF domain, but not the CUE domain, was found to impair the phosphorylation of IκBα by the canonical IKK complex *in vitro* ([82], **Section 1.2.5.1**). This suggests that the NZF domain is the major ubiquitin-binding region of TAB2 and TAB3 involved in activating TAK1.

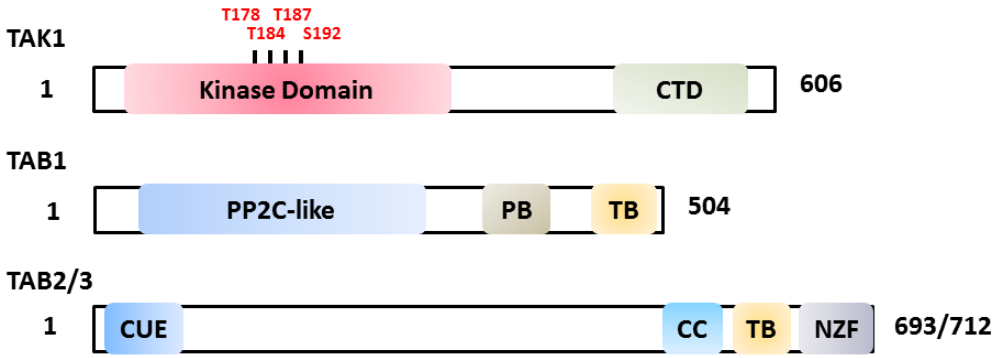

Figure 1.5 Domain organisations of TAK1 and TABs. TAK1 contains an N-terminal kinase domain and C-terminal domain (CTD) for its association with TAB2 or TAB3. TAB1 is a pseudo-phosphatase containing a protein phosphatase 2C (PP2C)-like domain at N terminus, followed by a p38 binding (PB) domain and a TAK1 binding (TB) domain at C terminus. TAB2 and TAB3 comprise an N-terminal ubiquitin binding (CUE) domain, a coiled-coil (CC) region, a TAK1-binding (TB) domain and a C-terminal Npl4 zinc finger (NZF) domain. The phosphorylation sites are highlighted in red.

1.2.4.1 The phosphorylation and activation of TAK1

The protein kinase activity of TAK1 is required for the activation of NF-κB and MAP kinases, because their upstream kinases, including the canonical IKK complex, c-Jun N-terminal kinase (JNK) and p38 MAP kinases, were not activated in IL-1 stimulated fibroblasts that lack TAK1 expression [83] or that express a truncated, inactive version of TAK1 [84].

The activation mechanism of TAK1 has been studied extensively. The IL-1-induced activation of endogenous TAK1 occurs within a few minutes [78,85] and the phosphorylation on TAK1 is required for its activity, since phosphatase treatment of TAK1 prevents it from phosphorylating its physiological substrate MKK6 (MAP kinase kinase 6) *in vitro* [85]. The activation of many protein kinases, including MAP3Ks, requires the phosphorylation of serine and/or threonine residues in the activation loop between subdomains VII (containing the DFG motif) and VIII (terminating in the M(A/S)PE motif) [86]. TAK1 contains four serine/threonine residues in this region that could potentially become phosphorylated, namely Thr178, Thr184, Thr187 and Ser192 which are indicated by asterisks in the following sequence

DFGT*ACDIQT*HMT*NNKGS*AAWMAPE. The use of phospho-specific antibodies that recognise TAK1 at Thr187 revealed that this threonine only becomes phosphorylated when the MyD88 pathway is activated in cells [87]. Moreover, this site does not become phosphorylated and TAK1 is not activated in cells expressing the catalytically inactive TAK1[K63W] mutant in which Lys63 in ATP-binding pocket was mutated to Trp [87], suggesting that TAK1 is activated by the autophosphorylation at Thr187. Furthermore, an antibody developed later that recognises TAK1 phosphorylated at both Thr178 and Thr184 did not detect the phosphorylation of these sites when Thr187 was mutated to Ala [88]. This suggests that phosphorylation at Thr178 and Thr184 may be autophosphorylation events occurring subsequent to the phosphorylation at Thr187. Thr187 phosphorylation is therefore used as the major readout of TAK1 activation throughout this thesis.

1.2.4.2 The role of TAB1 in the activation of TAK1

TAB1 was the first regulatory subunit in the TAK1 complex to be identified [89], and is bound constitutively to TAK1 in cells [78,80,85]. Thus early studies focused on the role of TAB1 in TAK1 phosphorylation and activation [89,90]. The kinase activity of wild type TAK1, but not the catalytically inactive TAK1[K63W] mutant, was greatly enhanced only when TAB1 was co-expressed with TAK1 in yeast [89] or mammalian cells [90], confirming that TAK1 can activate itself in an ATP-dependent manner, and that TAB1 can promote TAK1 autophosphorylation. The C-terminal 68 amino acids of TAB1 is sufficient for association with and activation of TAK1 when it is either overexpressed in unstimulated HeLa cells [90] or fused covalently to the catalytic domain of wild type TAK1 [91]. A mutagenesis study showed that the conserved residue Phe 484 on TAB1 was crucial for TAK1 binding and activation [92], which

further indicated the importance of TAB1 in TAK1 activation. The crystal structure of TAB1-TAK1 chimera provided further details on the molecular basis of TAB1-mediated TAK1 activation [93]. However, two groups reported that the IL-1-induced activation of TAK1, and subsequent activation of MAP kinases and NF-κB occurred normally in the TAB1-deficient MEFs, indicating that TAB1 is dispensable for TAK1 activation [83,94]. The investigation of the role of TAB1 in TAK1 activation was largely discontinued as a result of these observations, and attention switched to the roles of the other two subunits, TAB2 and TAB3.

1.2.4.3 The roles of TAB2 and TAB3 in the activation of TAK1

Early studies showed that TAK1 was recruited to TRAF6 in response to IL-1 stimulation [78], and TAB2 (Fig 5 in [95]) and TAB3 (Fig 5 in [96]) were identified as two adaptors aiding this ligand-dependent association. These studies were also the first to indicate how the activation of the TAK1 complex might be linked to the TRAF6 E3 ligase in the MyD88 signalling network. The discovery that the IL-1-dependent activation of TAK1 was dependent on one or more TRAF6-catalysed ubiquitylation events [76] led Ishitani *et al* to propose that the IL-1-induced TRAF6-mediated ubiquitylation of TAB2 and TAB3 may activate TAK1. However, the data they presented only demonstrated that Ub chains were co-immunoprecipitated with TAB2 or TAB3 [96]. Kanayama *et al* then revealed that the NZF domain was the major Ub-binding region of TAB2 and TAB3 as described earlier (**Section 1.2.4,** [82]). They also demonstrated that the NZF domains of TAB2 and TAB3 interact with K63-Ub chains, which may induce a conformational change in the TAK1 complex, leading to TAK1 auto-phosphorylation and auto-activation *in vitro* [82]. This mechanism for the K63-Ub-dependent activation of TAK1 was supported by the observation that replacing the conserved Cys residues in

the NZF domains with Ala prevented the activation of TAK1, and that the replacement of the NZF domain by a ubiquitin-binding motif from unrelated proteins restored TAK1 activation in a cell-free system (Fig 4 in [82]). The TRAF6-catalysed formation of K63-Ub chains was shown to only activate the TAB2-TAK1 complex *in vitro*, but not the TAB1-TAK1 complex nor the TAK1 catalytic subunit alone [76]. Moreover, the depletion of TAB2 from HEK293 cells abolished the kinase activity of immunoprecipitated TAK1 *in vitro*, which was restored when recombinant TAB2-TAK1 was added in the assay (Fig 2c in [76]). These pieces of evidence further suggested the importance of TAB2 in the activation of TAK1.

As discussed in **Section 1.2.3,** the wild type TAB2 and TAB3, but not mutants lacking the NZF domains, associated with K63-Ub chains synthesized by TRAF6 and Ubc13-Uev1a ([69], Fig 1b in [97]), but not with K48-Ub chains *in vitro* (Fig 3 in [82], Fig 4a in [98]), and the TAK1 complex could only be activated by K63-Ub chains, but not K48- nor Met1-Ub chains *in vitro* (Fig 2f and S10 in [97]). Moreover, the presence of CYLD (Cylindromatosis), a deubiquitylase that only cleaves K63-Ub and Met1-Ub chains [98], completely blocked the activation of TAK1. These data indicate that TAB2, as well as TAB3, activates TAK1 by binding to K63-Ub chains specifically. A recent study on the crystal structures of the TAB2 NZF domain bound to K63-linked di- and tri-ubiquitin molecules demonstrated that the NZF domain contains two ubiquitin-binding sites, which associate with neighbouring Ub molecules at two sites in a K63-Ub oligomer [99]. A Met1-Ub oligomer was unable to bend like a K63-Ub chain to contact the two binding sites in the NZF domain simultaneously, explaining the specificity of TAB2 for K63-Ub chains. Taken together, these findings indicated that TAB2 and TAB3 induce the activation of TAK1 by binding to K63-Ub chains specifically.

Although the model for the activation of TAK1 via the interaction of K63-Ub chains with TAB2/TAB3 is simple and elegant, it was built up mainly based on *in vitro* experiments, and the genetic evidence needed to establish this hypothesis was still lacking when I started my project. TAB2-deficient MEFs showed normal MAP kinase activity and NF-κB DNA binding activity, suggesting that TAB2 alone is not essential for IL-1 signalling [100]. Similar results were obtained from studies in TAB3-deficient MEFs and macrophages after TLR agonists stimulation [101]. The knockdown of both TAB2 and TAB3 (but not either protein alone) using siRNA (small interfering RNA) technology in HeLa cells largely prevented the phosphorylation-induced slower migration of TAK1, as well as the activation of MAP kinases and NF-κB [96], strongly suggesting that TAB2 and TAB3 are functionally redundant in the activation of TAK1. These observations inspired me to generate a cell line in which both TAB2 and TAB3 were genetically ablated and in this thesis to re-express mutated versions of these TAB subunits to try to elucidate the roles of TAB2 and TAB3 in the activation of the endogenous TAK1.

Once TAK1 is activated, it prompts the activation of NF-κB by phosphorylating and activating the canonical IKK complex [76,78]. The next section focuses on the structure of the canonical IKK complex, its functional role in activating the NF-κB transcription factor, and how it was thought to be activated at the time the work described in this thesis was started.

1.2.5 The canonical IKK complex

The canonical IKK complex is composed of two protein kinases, IKKα and IKKβ (also called IKK1 and IKK2) [102–104], and one regulatory subunit called NEMO (NF-κB Essential Modifier, also called IKKγ) [105,106]**.** The IKKα and IKKβ components of the complex display 51% identity in amino acid sequence [102]. They both contain an N-

terminal kinase domain, in which two key serine residues located in the activation loop (Ser176 and Ser180 for IKKα and Ser177 and Ser181 for IKKβ) have to be phosphorylated for the kinases to be activated [102,107,108]. Recent structural analysis of IKKβ revealed that it also carries an ubiquitin-like domain (ULD), a α-helical scaffold/dimerization domain (SDD), and a C-terminal NEMO-binding domain (NBD) [109] (**Fig 1.6**). The ULD is required for kinase activity and the SDD mediates its dimerization. IKKα is predicted to have a similar structural organisation to IKKβ [109].

NEMO was discovered as the third subunit in the canonical IKK complex [105,106]. This 48 kDa polypeptide contains an α-helical region and two coiled-coil (CC) domains. The first CC domain (CC1) promotes NEMO dimerization and its interaction with the IKKs [110] (**Fig 1.6**). The second CC domain (CC2) together with the leucine zipper (LZ) motif is the ubiquitin binding domain [111]. The C-terminal zinc-finger (ZF) domain targets the IKK complex to substrates such as IκBα [112]. The molar ratio IKKα:IKKβ:NEMO is 1:1:2 [113], consistent with a crosslinking experiment indicating that the canonical IKK complex comprises two IKKα, two IKKβ and four NEMO molecules in cells [114–117].

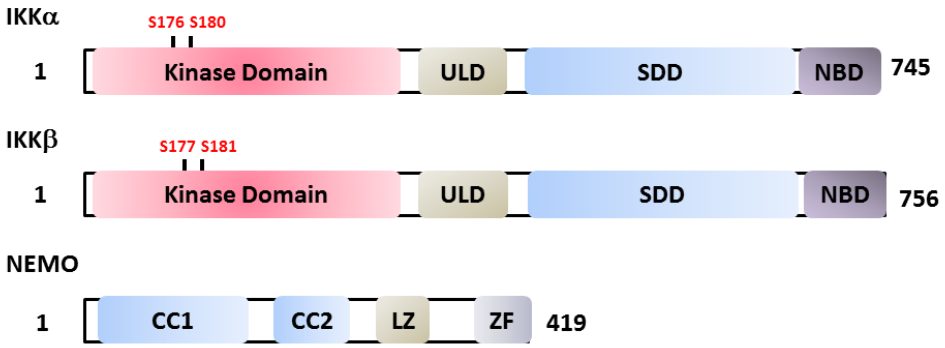

Figure 1.6 Domain organisations of the canonical IKK complex. Both IKKα and IKKβ contain a kinase domain at N terminus, followed by an ubiquitin-like domain (ULD) required for kinase activity, an α-helical scaffold/dimerization domain (SDD) for dimerization, and a C-terminal NEMO-binding domain (NBD). NEMO comprises a coiled-coil domain (CC1) for the dimerization and interaction with IKKs, followed by CC2 and leucine zipper (LZ)

motif forming an ubiquitin binding region. The C-terminal zinc-finger (ZF) domain is for IκBα interaction. The phosphorylation sites are highlighted in red.

1.2.5.1 The activation of NF-κB transcription factors

The canonical IKK complex activates NF-κB by inducing the phosphorylation and subsequent degradation of IκBα [118]. NF-κB is a family of dimeric transcription factors consisting of NF-κB1 (p50 and its precursor p105) or NF-κB2 (p52 and its precursor p100) complexed to c-Rel, RelA (p65) or RelB. NF-κB dimers are implicated in regulating many physiological processes, including not only innate immunity but also the cellular response to DNA damage [116,119,120].

When the innate immune system is not activated, NF-κB dimers (except p52: RelB) are sequestered in the cytoplasm by IκB proteins (IκBα, IκBβ and IκBε) [121–123]. When the MyD88 signalling pathway is activated, IκBα is phosphorylated by the canonical IKK complex on Ser32 and Ser36 [124–126], and the dual-phosphorylated protein is recognised by the β-TrCP F-box–containing component of a Skp1-Cullin-F-box (SCF)–type E3 ubiquitin-protein ligase complex, called $SCF^{\beta TrCP}$. This leads to the K48-linked polyubiquitylation and degradation of IκBα by the 26S proteasome [127–129]. It is followed by the liberation of NF-κB subunits and the exposure of the nuclear localization sequence (NLS) on RelA (p65) [44,117,130], causing the dimeric transcription factors to translocate into nucleus and initiate the transcription of target genes [116]. The canonical IKK complex also enables phosphorylation of RelA at Ser536 in cells [131,132], and a recent study in knock-in mice suggested that this phosphorylation is not required for its nuclear translocation but negatively regulates NF-κB signalling [133].

1.2.5.2 IKKα and IKKβ

Although IKKα is a component of the canonical IKK complex, it is not essential for the MyD88-dependent activation of NF-κB [107]. The mutation of two serine residues to alanine in the activation loop of IKKα did not impair the IL-1-activated IKK complex from phosphorylating IκBα *in vitro* [107]. Moreover, the immunoprecipitated IKK complex from IL-1-stimulated IKKα-deficient MEFs phosphorylated IκBα *in vitro* similarly to the canonical IKK complex from wild type MEFs [134]. In addition, the IL-1-induced phosphorylation of p105 at Ser933 and RelA at Ser536 and degradation of IκBα was comparable in wild type and IKKα-deficient MEFs [135].

IKKα activity is required to activate the alternative (or non-canonical) NF-κB pathway, which is triggered by a subset of TNF superfamily members, including lymphtoxin-α/β, CD40L, BAFF and RANKL (receptor activator of NF-κB ligand) [136–138]. The engagement of these ligands stabilizes the NF-κB-interacting kinase (NIK), which is thought to phosphorylate and activate IKKα homodimers [108]. The active IKKα then phosphorylates p100, triggering its proteolytic processing to p52, which associates with the RelB dimer to stimulate gene transcription [138]. In contrast to the rapid degradation of IκB isoforms in the canonical NF-κB pathway, IKKα-dependent processing of p100 to p52 is much slower [139]. Notably, neither IKKβ nor NEMO is involved in this pathway.

Unlike IKKα, IKKβ is vital for IL-1-induced NF-κB activation. The IKK complex isolated from IL-1-stimulated IKKβ-deficient MEFs and embryonic stem (ES) cells was not capable of phosphorylating IκBα *in vitro*, and no activated NF-κB capable of binding to DNA was detected in the nuclear extracts of these cells [140]. Moreover, the deletion of IKKβ in MEFs resulted in a dramatic reduction in the IL-1-mediated

phosphorylation of p105 and RelA, and the degradation of IκBα was completely abolished [135]. The replacement of Ser177 and Ser181 of IKKβ by Ala residues prevented IκBα phosphorylation *in vitro*, whereas their replacement by Glu residues (to mimic the effect of phosphorylation by introducing negative charges) enhanced its kinase activity [102,107]. These results suggest that phosphorylation of the two serine residues in the activation loop of IKKβ is required for its activation.

1.2.5.3 NEMO

NEMO was established as an indispensable regulator of the activation of IKK complex, by the finding that neither IKK activity nor NF-κB activation was observed in NEMO-deficient MEFs and ES cells in response to IL-1 or LPS [141,142]. Recent work identified NEMO as an ubiquitin-binding protein. NEMO was initially found to associate with K63-linked oligomers [143,144], but more recently was shown to interact with Met1-linked ubiquitin dimers with 100-fold higher affinity than with K63-Ub dimers [111,145,146], which is discussed in more detail in **Section 1.2.6**. The point mutation of Asp311 to Asn or Gly in the CC2-LZ domain (**Section 1.2.5**, **Fig 1.6**) disrupted the noncovalent interaction with Ub chains, and impaired but did not abolish the activation of IKK complex and subsequent NF-κB signalling in response to pro-inflammatory cytokines, including IL-1β [8,147]. Patients carrying these NEMO mutations suffer from a disease termed anhidrotic ectodermal dysplasia with immunodeficiency (EDA-ID) [8,147]. These findings indicate a critical role for ubiquitin-binding to NEMO in the activation of IKK complex.

1.2.5.4 The activation of the canonical IKK complex

Since the canonical IKK complex plays a critical role in the activation of NF-κB, the mechanism by which IKKβ is activated has been investigated extensively. Two

general mechanisms for the activation of this complex have been proposed. Firstly, IKKβ is phosphorylated by one or more upstream kinase(s); secondly, the canonical IKK complex may phosphorylate and activate itself in the absence of any other activating protein kinase. The first mechanism was supported by the finding that IL-1 failed to activate the IKK complex in MEFs lacking TAK1 activity (**Section 1.2.4.1,** [83,84]) or in the presence of relatively specific inhibitors of TAK1 [135,148,149]. The time course of IL-1-induced TAK1 activation is also compatible with being the trigger of IKK activation [135]. Taken together, these results implicate TAK1 as a prominent candidate kinase phosphorylating and activating IKKβ. However, support for the second mechanism comes from the finding that mutation of the two Ser residues in the activation loop of IKKβ to Asp residues resulted in the auto-phosphorylation of IKKβ (probably at phosphorylation sites near the C-terminus), which did not occur if this IKKβ mutant was converted to a catalytically inactive form by the additional mutation of Lys44 to Met or Ala [102,108]. Moreover, in IL-1-stimulated IKKα-deficient MEFs, BI605906, a specific inhibitor of IKKβ that does not inhibit TAK1, prevented IKKβ from being detected by an antibody that recognises IKKβ phosphorylated at both Ser177 and Ser181 [135]. Furthermore, structural analysis has demonstrated that human IKKβ exists as a dimer of dimers under the conditions of crystallisation [109], and the structure is compatible with *trans* auto-phosphorylation being the mechanism of activation.

The following section will detail recent studies indicating that the binding of NEMO to Ub chains, especially Met1-Ub chains, may trigger a conformational change of IKK complex, which might induce autophosphorylation.

1.2.6 The linear ubiquitin assembly complex (LUBAC)

The formation of Met1-Ub chains described in **Section 1.2.5** is catalysed by the Linear UBiquitin Assembly Complex (LUBAC) [150], which is composed of three subunits: HOIL-1 (heme-oxidized IRP2 ubiquitin ligase 1), HOIP (HOIL1-interacting protein) and SHARPIN (SHANK-associated RH domain-interacting protein) [150–153].

HOIP is the catalytic subunit of the complex. It is a RING-in-between-RING (RBR) E3 ligase, which exploits the RING1 domain to associate with the ubiquitin-loaded E2 conjugating enzyme UbcH7 (also known as UBE2L3) [154,155], followed by the transfer of activated ubiquitin from UbcH7 to the catalytic cysteine (C885 of human HOIP) in the RING2 domain, and subsequent conjugation to another ubiquitin molecule [156,157]. The RBR domain alone in HOIP is sufficient for Met1-Ub chains synthesis, but the domains located N-terminal of RBR largely restrict its E3 ligase activity [156]. The interaction of the HOIL-1 and SHARPIN components with HOIP facilitates the formation of Met1-Ub chains *in vitro* (Fig 2 in [151]), which is proposed to release the auto-inhibition of HOIP in the LUBAC complex (Fig 3 in [156]).

LUBAC and its E3 ligase activity are critical for IKK activation in the MyD88-mediated signalling. The IL-1-induced activation of the canonical IKK complex was largely decreased in the MEFs from HOIP [C879S] knock-in mice [158], HOIL1-deficient mice [159] or mice with a mutation in SHARPIN [151–153]. Moreover, the reconstitution of LUBAC with E1 activating enzyme and E2 conjugating enzyme (UbcH5c) to HeLa cell extracts deprived of these components restored the activation of IKK complex *in vitro* [145].

Early studies demonstrated that LUBAC complex interacts with NEMO and catalyses the ubiquitylation of NEMO with linear Ub chains at Lys285 and Lys309 in the

CC2-LZ domain, which were believed to induce the activation of NF-κB [159]. A more recent study showed that the combination of an E2 conjugating enzyme UbcH5C and the TRAF6 E3 ligase synthesized Ub chains of various linkage types *in vitro*, which promoted the phosphorylation and activation of IKK and the subsequent phosphorylation of IκBα (Fig S8 and S10 in [97]). A point mutation within a ubiquitin-binding domain of NEMO (Tyr308Ser) prevented Ub chains from mediating IKK activation *in vitro* (Fig S7 in [97]), strongly suggesting that Ub chains activate IKK via direct binding to NEMO, at least in this cell free system. Moreover, the mutation of Lys270 in the hydrophobic CC2-LZ domain to Ala, which is believed to mimic the conformational change induced by the binding of Ub chains with NEMO, leads to a constitutively activated IKK complex either measured *in vitro* or by the activation of NF-κB in cells [160]. Furthermore, the overexpression of a Met1-linked Ub dimer fused to NEMO induces the phosphorylation of the endogenous IKK complex and the activation of NF-κB in HEK293 cells in which MyD88 signalling has not been activated (Fig 3 in [145]). These data suggest a critical role of Met1-Ub-binding NEMO in the activation of the canonical IKK complex.

1.2.7 The signalling network downstream of TAK1 and the canonical IKK complex

1.2.7.1 The NF-κB pathway downstream of the canonical IKK complex

The activated IKK complex triggers the phosphorylation and activation of NF-κB transcription factors as described in **Section 1.2.5.1**. Additionally, another transcription factor IRF5 is phosphorylated at Ser462 by the IKK complex in TLR7 agonist-stimulated myeloid cells including human plasmacytoid dendritic cells (pDC) and murine macrophages [161]. The phosphorylation induces the dimerization and activation of IRF5, which then translocates into the nucleus and induces transcription of the genes encoding inflammatory cytokines [161,162].

In addition to the activation of transcription factors, the canonical IKK complex also regulates the activation of an essential MAP3K known as Tpl2 (tumour progression locus 2)/MAP3K8. In cells where the MyD88 pathway is not activated, the inactive Tpl2 is complexed with p105 (**Section 1.2.5.1**) and ABIN2 (A20-binding inhibitor of NF-κB 2), both of which are required for Tpl2 stability [163,164]. The stimulation-induced activation of IKK complex results in the IKKβ-catalysed phosphorylation and degradation of p105 as well as the phosphorylation of Tpl2 [165,166], causing the activation of Tpl2.

Tpl2 activates the protein kinases MEK1 and MEK2 (MAP kinase or ERK kinases 1 and 2), which then activate the MAP kinase family members ERK1 and ERK2 (extracellular-signal regulated kinases 1 and 2). This signalling axis is essential for the lipopolysaccharide (LPS)-induced conversion of pre-TNFα to its secreted from [167,168], which is catalysed by TNFα-converting enzyme (TACE) [169].

More recently Tpl2 has been implicated in activating the MAP kinase kinases MKK3 and MKK6, which will be described in the following subsection.

1.2.7.2 MAP kinase cascades

In MAP kinase signalling cascades one or more MAP3Ks activate MAP2Ks (MAP kinase kinases), which then activate the MAP kinases, which can be subdivided to three types, namely, ERK1/2, p38s and JNKs [2,170]. In general, the activation of MAP kinases requires the dual phosphorylation of a Thr–Xaa–Tyr motif in the activation loop by one or more MAP2K(s). MAP2Ks are activated by serine and/or threonine phosphorylation in their activation loops by MAP3Ks [2].

The ERK1/2 kinases can, in turn, activate ribosomal protein S6 kinases (RSK1/2/3) and MSK1 (mitogen- and stress-activated protein kinase) and MSK2 [2] and

MNK1 and MNK2 (MAP kinase integrating kinases) [171]. RSK1/2/3 have been implicated in TLR-mediated endocytosis [172,173], whereas the MSKs are nuclear protein kinases, which phosphorylate and activate the transcription factor CREB. CREB has a key role in stimulating the transcription of anti-inflammatory cytokines, such as IL-10 (**Section 1.2.1.3**) and IL-1 receptor antagonist protein (IL-1RA, **Section 1.2.1.2**) [174–176]. MNKs are reported to phosphorylate a number of components in the translational machinery, including the eukaryotic initiation factor 4F (eIF4F) complex, a critical regulator in the protein synthesis [171].

The p38α MAP kinase also mediates the phosphorylation of MSKs [177]. In addition, it phosphorylates and activates MAP kinase-activated protein kinase-2 (MK2) and MK3, which then stimulate the translation of TNF mRNA and therefore TNF production [178,179]. Interestingly, the p38α MAP kinase negatively regulates TAK1 activity. In this feedback control mechanism, activated p38α MAP kinase phosphorylates three TAB regulatory subunits in the TAK1 complex, and therefore suppress TAK1 activity [180,181]. This may be one mechanism that prevents the overproduction of inflammatory mediators.

The phosphorylation and activation of p38α is carried out by the upstream MAP2Ks, termed MKK3, MKK4 and MKK6. For a number of years it was thought that all three MKKs were direct substrates of TAK1 [170,182]. However, a recent study demonstrated that Tpl2, but not TAK1, is the physiological upstream kinase phosphorylating and activating MKK3 and MKK6 in the TNF and MyD88 signalling pathways [183]. These findings indicate that p38α can be activated by two distinct pathways, namely the TAK1-MKK4 and Tpl2-MKK3/MKK6 axis, respectively (**Fig 1.2**).

The third class of MAP kinases, comprising JNK1, JNK2 and JNK3, are activated by the MAP2Ks, termed MKK4 and MKK7, of which MKK7 appears to be the major contributor in the IL-1 signalling pathway [184]. JNK1 and JNK2 phosphorylate the subunits of transcription factor AP-1 (activator protein 1), including c-Jun and ATF2 (activating transcription factor 2), which then translocate into nucleus and are involved in regulating the production of cytokines [185,186].

1.2.8 Human diseases associated to the deficiency or mutations of the components in the MyD88-mediated signalling pathway.

Many human diseases have been shown to be associated with the defect of key components in the MyD88 signalling network ([9,15,187–190], **Table 1.1**). The loss of essential proteins results in immunodeficiency, whereas the specific mutation which hyper activated the pathway caused inflammatory and autoimmune diseases, or even cancer. It is therefore critical to understand how the activation of MyD88-dependent signalling pathway is tightly regulated, especially the activation and restriction mechanisms of essential protein kinases, such as TAK1 and the canonical IKK complex.

Table 1.1 The genetic defects of the components in the MyD88 signalling network and consequences.

Genetic defects	Molecular effects	Phenotype	Reference
MyD88 deficiency	Unable to activate NF-κB	Recurrent pyogenic bacterial infections	[45,46,191]
MyD88[L265P]	Constitutively activate NF-κB	Diffuse large B-cell lymphoma (DLBCL); Waldenström's	[12,192]

		macroglobulinemia	
IRAK4 deficiency	Unable to activate NF-κB	Susceptible to pyogenic bacterial infections	[56,187,193]
IRAK4 kinase inactive knock-in	Severely Impaired NF-κB activation	Susceptible to pyogenic bacterial infections	[55,57,194]
TRAF6 deficiency	Defective IL-1, CD40 and LPS signalling	Embryonic lethal; enlarged spleen; defective lymph node organogenesis	[67,195]
TAK1 deficiency	Unable to activate NF-κB	Embryonic lethal	[83]
TAK1 kinase inactive mutant	Unable to activate NF-κB	Embryonic lethal; impaired B cell development	[84]
IKKβ deficiency	Unable to activate NF-κB	Embryonic lethal; uncontrolled liver apoptosis	[140]
IκBα[S32I]	Impaired IκBα degradation	Anhidrotic ectodermal dysplasia with immunodeficiency (EDA-ID)	[196,197]
NEMO deficiency	Unable to activate NF-κB	EDA-ID	[141,142]

NEMO[D311N/G]	Unable to interact with Ub chains	EDA-ID	[8,147]
HOIP deficiency	Unable to generate Met1-Ub chains	Autoinflammation, immunodeficiency and lymphangiectasia.	[7]
HOIP[C879S]	Unable to generate Met1-Ub chains	Embryonic lethal.	[158]

1.3 Aim of the thesis

At the time I began the studies described in this thesis, the canonical IKK complex had been identified and studied in great detail for many years [102–104], and its essential role in the response to various inflammatory stimuli was well established [145,147]. However, the molecular mechanism by which it became activated remained controversial. It was widely accepted that the activation of IKKα and IKKβ required their phosphorylation at two serine residues in their activation loops [102,107,108], but whether activation was catalysed by TAK1 or by auto-phosphorylation [97,135] had not been resolved. Moreover, the important role of ubiquitin chains in activating the IKK complex had not become clear adding another tier of complexity to the activation process. I therefore decided to solve this problem, and my results are presented in Chapter 3 of the thesis.

Clarification of the mechanism of IKK activation inspired me to study how TAK1, the master kinase of the innate immune system, was activated. Unlike the IKKs, it was

widely accepted that TAK1 was activated by K63-Ub chains, which interacted with the TAB2 and TAB3 components to induce TAK1 activation. The evidence supporting this elegant model had mainly been based on biochemical studies in cell-free assays [76,82,90]. However, this model had been challenged by a study showing normal activation of MAP kinases and NF-κB in BMDM from mice lacking expression of both TAB2 and TAB3 [101]. The newly developed CRISPR/Cas9 (clustered regularly interspaced short palindromic repeat (CRISPR) associated protein 9 (Cas9)) gene editing technology [198] encouraged me to re-investigate the requirement for the three TAB subunits in the activation of the TAK1 complex in human cells. This study led me to discover that the TAK1 complex is activated by two distinct mechanisms and these results are presented in Chapter 4 of this thesis.

Chapter 2 Materials and methods

2.1 Materials

2.1.1 Chemicals

Reagents used in **tissue culture** were as following: Dulbecco's modified Eagle medium (DMEM), Foetal Bovine Serum (FBS), Opti-MEM reduced serum media, Dulbecco's phosphate buffered saline (PBS), Trypsin/EDTA (0.05%), L-Glutamine, sodium pyruvate, Versene (0.48 mM) and penicillin/streptomycin solution were from **GIBCO (Paisley, UK)**. 6, 12, 24 and 96 well tissue culture plates, 10 cm and 15 cm tissue culture dishes, cell scrapers, cryovials and Spin-X centrifuge tube filters (CLS 8161) were from **Corning Incorporated** (NY, USA). Polyethylenimine (PEI) was from **Polysciences** (Warrington, PA). Lipofectamine 2000 transfection reagent was from **Invitrogen** (MA, USA). GeneJuice transfection reagent was from **EMD Millipore** (Germany). Mouse macrophage colony-stimulating factor (M-CSF) was from R&D systems. The protamine sulphate, geneticin (G418), and puromycin were from **Sigma**. GeneJuice transfection reagent was from **Novagen** (Germany).

Reagents used in **biochemistry techniques** were as following: 40% (w/v) 29:1 Acrylamide: Bis-Acrylamide solution was from **Flowgen Bioscience** (Humberside, UK). Precision Plus protein marker and Bradford reagent were from **BioRad** (Herts, UK). Immobilon Western Cemiluminescent HRP Substrate and Immobilon-P Polyvinylidene fluoride (PVDF) 0.45 µm membrane was from **EMD Millipore** (Germany). Skimmed milk (Marvel) was from **Premier Beverages** (Stafford, UK). Enhanced chemiluminescence (ECL) kit and Hyperfilm MP were from **GE Healthcare** (Piscataway, USA). X-ray films were from **Konica Corporation** (Japan). Photographic developer (LX24) and liquid fixer (FX40) were from **Kodak** (Liverpool, UK). InstantBlue coomassie stain

was from **Expedeon** (Cambridge, UK). The mono-phosphorylated peptide KELDQGpSLCTSFVGTLQ and the diphosphorylated peptide KELDQGpSLCTpSFVGTLQ (where pS is phosphoserine), corresponding to amino acid residues 171-187 of IKKβ with phosphoserine at Ser177 only or at both Ser177 and Ser181, respectively, were synthesized by **Pepceuticals Ltd**. Precast gels (4-12% Bis-Tris, NuPAGE) and NanoDrop spectrophotometer were from **Thermo Scientific**.

Reagents used in **molecular biology techniques** were: Luria Bertani broth (LB) and LB agar plates were from the Central Technical Services team, **University of Dundee**. Plasmid Midi or Maxi kits were from **Qiagen Ltd** (Crawley, UK). Homogenizer mini column (HCR003), RNA MicroElute kit (R6831-01) and DNase I Digestion Set (E1091) were from **Omega.** The iScript cDNA synthesis kit (170-8891) and SsoFast EvaGreen Supermix (172-5204) was from **Bio-Rad**.

Agonists and inhibitors used throughout this thesis were: Murine interleukin 1α (IL-1α), TNF, and cytokine ELISA kits were from **Peprotech** (New Jersey, USA). Lipopolysaccharide (LPS) O55:B5 was from **Enzo Life Sciences** (USA). Pam_3CSK_4 was from **InvivoGen** (San Diego, USA). The IKKβ inhibitor BI605906 [135] was synthesized by Dr Natalia Shpiro, Medical Research Council Protein Phosphorylation and Ubiquitylation Unit (MRC-PPU), University of Dundee, and the TAK1 inhibitor NG25 by Dr Nathanael Gray, Harvard Medical School [199]. The TAK1 inhibitor 5Z-7-oxozeaenol was purchased from **BioAustralis Fine Chemicals** (Australia). KOD Hot Start DNA polymerase was from **Novagen** (Germany).

Other common chemicals include: Ampicillin, adenosine 5'-triphosphate sodium salt (ATP), ammonium persulphate (APS), beta-mercaptoethanol (β-ME), bovine serum albumin (BSA), benzamidine, dimethyl sulphoxide (DMSO), dithiothreitol

(DTT), doxycycline, ethanol, glycerol, glycine, hexadimethrine bromide (polybrene), isopropanol, iodoacetamide, leupeptin, kanamycin, methanol, magnesium acetate (MgAc), magnesium chloride (MgCl2), phenylmethanesulphonylfluoride (PMSF), polyethylene glycol sorbitan monolaurate (Tween-20), polyethylene glycol dodecyl ether (Brij-35), Ponceau S, sodium chloride (NaCl), sodium ethylenediaminetetraacetic acid (EDTA), sodium ethylene glycol tetra acetic acid (EGTA), sodium fluoride, sodium 2-glycerophosphate, sodium orthovanadate, sodium dodecyl sulphate (SDS), toctyl phenoxypolyethoxyethanol (Triton)-X-100, and tetramethylethylenediamine (TEMED) were from **Sigma-Aldrich** (Poole,UK). Protein G-Sepharose and Glutathione Sepharose were from GE **Healthcare** (Piscataway, USA). The monophosphorylated peptide KELDQGpSLCTSFVGTLQ and the diphosphorylated peptide KELDQGpSLCTpSFVGTLQ (where pS is phosphoserine), corresponding to amino acids 171–187 of IKKβ with phosphoserine at Ser^{177} only or at both Ser^{177} and Ser^{181} respectively, were synthesized by **Pepceuticals**. γ^{32}ATP was from **PerkinElmer** (MA, USA).

2.1.2 Buffers and other solutions

The composition of buffers regularly used throughout this thesis is listed in **Table 2.1**.

Table 2.1 List of commonly used buffers

Buffer	Composition
MRC cell lysis buffer	50 mM Tris/HCl pH 7.5, 1 mM EDTA, 1 mM EGTA, 1% (v/v) Triton X-100, 10 mM sodium glycerol 2-phosphate, 50 mM sodium fluoride (NaF), 5 mM sodium pyrophosphate ($Na_2P_2O_7$), 0.27 M sucrose. 1 mM sodium orthovanadate (Na_3VO_4), 1 mM DTT, 1 mM PMSF, 1 μg/ml Aprotinin and 1 μg/ml Leupeptin are added before use.
8-12% acrylamide resolving gels (separating gels)	375 mM Tri-HCl (pH 8.8), 0.1% (w/v) SDS and 6-12% acrylamide (depending on the size of separated proteins). 0.1% (w/v) ammonium persulfate (APS) and 0.1% (v/v) N,N,N',N'-tetramethylethylenediamine (TEMED) were added to initiate polymerisation.
Stacking gels	125 mM Tri-HCl (pH 6.8), 0.1% (w/v) SDS, and 4% (w/v) acrylamide. 0.1% (w/v) APS and 0.1% (v/v) TEMED were added to initiate polymerisation.
SDS sample buffer (1X)	2% (w/v) SDS, 1% (v/v) β-mercaptoethanol (freshly added), 50 mM Tris/HCl pH 6.8 and 10% (v/v) glycerol, 0.02% Bromophenol Blue. Buffer was prepared as a 5x stock.
Tris-glycine SDS/PAGE running buffer (1X)	25 mM Tris, 192 mM Glycine, 0.1% (w/v) SDS. Buffer was prepared as a 10x stock.
Tris-glycine transfer buffer (1X)	25 mM Tris, 192 mM Glycine, 20% (v/v) methanol. Buffer (without methanol) was prepared as 10x stock. Methanol was added before use.
MOPS running buffer	50 mM MOPS, 50 mM Tris base, 0.1% (w/v) SDS, 1 mM EDTA, pH 7.7.
Tris buffered saline-Tween (TBS-T)	50 mM Tris/HCl pH 7.5, 0.15 M NaCl and 0.2% (v/v) Tween-20.
Phosphatase assay buffer (Purchased from New England Biolabs)	50 mM HEPES, 100 mM NaCl, 2 mM DTT, 0.01% (w/v) Brij 35, 1 mM manganese chloride, pH 7.5.
Immunoprecipitation high salt washing buffer	50 mM Tris/HCl, pH 7.5, 1% (v/v) Triton X-100, 0.05% (v/v) βME and 0.2 M NaCl
Immunoprecipitation washing buffer	50 mM Tris/HCl, pH 7.5, 1% (v/v) Triton X-100, 0.05% (v/v) βME
PreScission protease buffer	50mM Tris/HCl pH7.5, 150mM NaCl, 1mM EDTA pH8.0, 1mM DTT, 0.03% Brij 35.
Halo-link resin wash buffer	50 mM Tris/HCl, pH 7.5, 0.5 M NaCl and 1% (v/v) Triton-X100

Notes on MRC cell lysis buffer:

Lysis buffer is used to inhibit protein kinases, phosphatases and proteases immediately during lysis process, in order to fix and remain the phosphorylation state

of proteins in the extracts at the levels present *in vivo*. EDTA was used to chelate divalent cations including Mg^{2+} and thus inhibited metal dependent enzymes such as kinases and many phosphatases. EGTA was used as a chelator with high affinity towards Ca^{2+}. Sodium fluoride (NaF) and sodium pyrophosphate ($Na_2P_2O_7$) were used as Ser/Thr protein phosphatases inhibitors, while sodium orthovanadate (Na_3VO_4) inhibited protein tyrosine phosphatases. PMSF was used as a serine protease inhibitor. Aprotinin inhibited trypsin and related proteolytic enzymes while Leupeptin inhibited cysteine, serine and threonine peptidases. 0.1 M Na_3VO_4 solution was prepared by several successive rounds of boiling, cooling to room temperature (RT) on ice and adjusting to pH 10. This was repeated until the solution remained stable at pH 10 after boiling and became colourless. This procedure ensures that the majority of the Na_3VO_4 is in the monomeric state that favours tyrosine phosphatase inhibition. 0.1 M Na_3VO_4 was stored at -20 °C. Lysis buffer was stored at 4 °C. DTT and protease inhibitors were added freshly before each use.

2.1.3 Commercial antibodies

The antibodies purchased from commercial supplies are listed in **Table 2.2**. The antibodies were diluted 1:1000 in 5% (w/v) BSA in TBS-T (**Table 2.1**). The PVDF membrane was incubated with antibody solution overnight at 4 °C.

Table 2.2 List of commercial antibodies

Antibody	Source	Catalogue No.	Host
IL-1R1	Santa Cruz	SC688	Rabbit
p-IRAK4 (T345/S346)	Pfizer	N/A	Rabbit
TRAF6	Santa Cruz	SC7221	Rabbit
K63-ubiquitin linkage specific	CST	5621	Rabbit
p-TAK1 (T187)	CST	4536	Rabbit
p-TAK1 (S439)	CST	9339	Rabbit
TAK1	CST	4505	Rabbit
TAB1	Abcam	Ab151408	Rabbit
TAB2	CST	3745	Rabbit
TAB3	CST	14211	Rabbit
M1-ubiquitin linkage specific	Genentech	N/A	Human
p-IKKα(S176/S180) p-IKKβ(S177/S181)	CST	2697L	Rabbit
p-IKKα(S176) p-IKKβ(S177)	CST	2078S	Rabbit
p-IKKα(S180) p-IKKβ(S181)	Abcam	AB55341	Rabbit
IKKβ	Merck-Millipore	05-535	Mouse

NEMO	**Santa Cruz**	**SC8330**	**Rabbit**
p-p105/NF-κB (S933)	**CST**	**4806S**	**Rabbit**
p-JNK1/2 (T183/Y185)	**Invitrogen**	**44682**	**Rabbit**
JNK1/2	**CST**	**9258S**	**Rabbit**
p-p38 MAP kinase (T180/Y182)	**CST**	**9211**	**Rabbit**
p38 MAP kinase	**CST**	**9212S**	**Rabbit**
p-ERK1/2 (T202/Y204)	**CST**	**9101s**	**Rabbit**
GAPDH	**CST**	**2118S**	**Rabbit**
XIAP	**CST**	**2042**	**Rabbit**
cIAP1	**CST**	**7065**	**Rabbit**
Anti-Flag	**Sigma**	**F3165**	**Mouse**
Anti-GST	**Sigma**	**G7781**	**Rabbit**
Anti-haemagglutinin (HA)	**Roche**	**12-013-819-001**	**Rat**
Anti-rabbit IgG HRP	**Pierce**	**31210**	**Goat**
Anti-mouse IgA HRP	**Pierce**	**62-6720**	**Goat**

2.1.4 In-house antibodies

The antibodies generated by the antibody production group of Division of Signal Transduction Therapy (DSTT) MRC-PPU, University of Dundee, are listed in **Table 2.3**. All of these antibodies were raised in sheep at Diagnostics Scotland (Carluke, Lanarkshire, UK).

Table 2.3 List of in-house antibodies

Antibody	Sheep No.	Bleed No.
HOIP	S174D	3
TAK1	S828A	1
TAB1	S823A	1
IKKβ	S189C	1
HA epitope tag	Mouse Monoclonal 12CA5	N/A

2.1.5 Plasmids

The plasmids provided by Dr Mark Peggie and Thomas Macartney in the cloning team of DSTT, MRC-PPU, University of Dundee, were presented in **Table 2.4**.

Table 2.4 List of plasmids

Protein/Target	Vector	Source	Code	Resistance marker	Purpose
IL-1R1	pBabe	DSTT	DU46481	G418	Constitutive expression
GST- IKKβ[D166A]	pEBG6P	DSTT	DU43897		Transient expression
GST-TAK1	pEBG6P	DSTT	DU3652		Transient expression
GST-TAK1[D175A]	pEBG6P	DSTT	DU3785		Transient expression
Myc-TAK1	pCMV	DSTT	DU3027		Transient expression
Myc-TAK1[S439A]	pCMV	DSTT	DU3859		Transient expression
Tet-on	Tet-on Advanced	Clontech	630930	G418	Doxycycline-controlled transactivator
Gag/pol	pCMV	DSTT	DU35085		Retrovirus generation
VSV-G	pCMV	DSTT	DU35309		Retrovirus generation
HA-tagged empty vector (EV)	pRetroXTight	DSTT	DU46102	Puromycin	Inducible expression
HA-IKKβ	pRetroXTight	DSTT	DU46079	Puromycin	Inducible expression
HA-IKKβ [S177A]	pRetroXTight	DSTT	DU46080	Puromycin	Inducible expression
HA-IKKβ [S177E]	pRetroXTigh	DSTT	DU4605	Puromyci	Inducible

	t		4	n	expression
HA-IKKβ [D166A/S177E]	pRetroXTight	DSTT	DU46233	Puromycin	Inducible expression
TAK1 *	pRetroXTight	DSTT	DU51270	Puromycin	Inducible expression
TAK1[D175A] *	pRetroXTight	DSTT	DU51293	Puromycin	Inducible expression
HA-TAB1	pRetroXTight	DSTT	DU51103	Puromycin	Inducible expression
HA-TAB1[S395A]	pRetroXTight	DSTT	DU51140	Puromycin	Inducible expression
HA-TAB1[F484A]	pRetroXTight	DSTT	DU51164	Puromycin	Inducible expression
HA-TAB2	pRetroXTight	DSTT	DU46500	Puromycin	Inducible expression
HA-TAB2[T674A/F675A]	pRetroXTight	DSTT	DU46511	Puromycin	Inducible expression
TRAF6	pRetroXTight	DSTT	DU51583	Puromycin	Inducible expression
TRAF6[L74H]	pRetroXTight	DSTT	DU51584	Puromycin	Inducible expression
TRAF6[C70A]	pRetroXTight	DSTT	DU51585	Puromycin	Inducible expression
TRAF6	pBabe	DSTT	DU47223	Puromycin	Constitutive expression
TRAF6[L74H]	pBabe	DSTT	DU47224	Puromycin	Constitutive expression
Flag-TRAF6[120-522]	pBabe	DSTT	DU51445	Puromycin	Constitutive expression
TAB1 (exon 1)	pU6 gRNA	DSTT	DU48411		TAB1 KO
TAB2 (exon 4)	pU6 gRNA	DSTT	DU48654		TAB2 KO
TAB3 (exon 7)	pU6 gRNA	DSTT	DU48354		TAB3 KO
TRAF6 (exon 2)	pU6 gRNA (sense)	DSTT	DU52382	Puromycin	TRAF6 KO
TRAF6 (exon 2)	pU6 gRNA (anti sense)	DSTT	DU52392	Puromycin	TRAF6 KO
TAK1 (exon 1)	pU6 gRNA (sense)	DSTT	DU52138	Puromycin	TAK1 KO
TAK1 (exon 1)	pU6 gRNA (anti sense)	DSTT	DU52141	Puromycin	TAK1 KO
TAB1 (exon 2)	pU6 gRNA (sense)	DSTT	DU52383	Puromycin	TAB1 KO
TAB1 (exon 2)	pU6 gRNA (anti sense)	DSTT	DU52393	Puromycin	TAB1 KO

TAB2 (exon 4)	**pU6 gRNA (sense)**	**DSTT**	**DU52384**	**Puromycin**	**TAB2 KO**
TAB2 (exon 4)	**pU6 gRNA (anti sense)**	**DSTT**	**DU52394**	**Puromycin**	**TAB2 KO**
TAB3 (exon 7)	**pU6 gRNA (sense)**	**DSTT**	**DU52385**	**Puromycin**	**TAB3 KO**
TAB3 (exon 7)	**pU6 gRNA (anti sense)**	**DSTT**	**DU52395**	**Puromycin**	**TAB3 KO**
XIAP (exon 2)	**pU6 gRNA (sense)**	**DSTT**	**DU52462**	**Puromycin**	**XIAP KO**
XIAP (exon 2)	**pU6 gRNA (anti sense)**	**DSTT**	**DU52474**	**Puromycin**	**XIAP KO**
Halo-NEMO	**pFN18A**	**DSTT**	**DU35939**		**Bacterial expression**
Halo-NZF_2 (644-692 TAB2)	**pET28a**	**DSTT**	**DU23839**		**Bacterial expression**

*: Two constructs encode truncated version of TAK1 in which residues 414-430 are missing.

2.1.6 Proteins

The proteins used throughout this thesis, presented in **Table 2.5**, were expressed and purified by the Protein Production Team, headed by James Hastie, DSTT, MRC-PPU, by Sam Strickson, or by myself. All proteins are human based unless otherwise stated.

Table 2.5 List of proteins

Protein	Code	Source
GST-IKKβ[D166A]	**DU43897**	**Jiazhen Zhang**
GST-TAK1	**DU3652**	**Jiazhen Zhang**
GST-TAK1[D175A]	**DU3785**	**Jiazhen Zhang**
His_6-TAK1[1-303]-TAB1[437-504]	**DU753**	**DSTT**
GST- PP1γ	**DU1807**	**DSTT**
GST-MAP4K1 (1-821)	**DU32902**	**DSTT**
His_6-MAP4K2 (2-812)	**DU1760**	**DSTT**
GST-MAP4K3 (1-873)	**DU38666**	**DSTT**
GST-MAP4K5 (2-846)	**DU38642**	**DSTT**
PreScission proteinase	**DU34905**	**DSTT**
Halo-NEMO	**DU35939**	**Sam Strickson**
Halo-NZF_2 (644-692 TAB2)	**DU23839**	**Sam Strickson**

2.2 Methods

2.2.1 Mammalian cell culture

2.2.1.1 Cell culture growth media

The composition of growth media was as following: Dulbecco's modified eagles medium (DMEM), 10% (v/v) foetal bovine serum (FBS), 4 mM L-Glutamine, 100 U/ml penicillin, 100 µg/ml streptomycin and 1 mM sodium pyruvate.

2.2.1.2 Cell maintenance and passaging

Cells were cultured in the growth media at 37 °C under 5% CO_2 atmosphere. Cells were passaged when they were 80% - 90% confluency in 10 or 15 cm tissue culture dishes. The media was removed by aspiration. Cells were washed with PBS and incubated with 1 or 2 ml trypsin/EDTA (0.05%) at 37 °C until they detached (usually 2-3 min). Trypsin was quenched by the addition of serum-containing media and cells were plated onto new tissue culture dishes.

2.2.1.3 Immortalised cell lines

2.2.1.3.1 Human embryonic kidney (HEK) 293 cells

HEK293 cells stably overexpressing the IL-1R, namely IL-1R cells, were kindly provided by Dr Xiaoxia Li (Cleveland Clinic Foundation, Cleveland, Ohio, U.S.A.). The Flp-In™ HEK293 T-Rex cells were originally purchased from Invitrogen, which were engineered by Yosua Kristariyanto (MRC-PPU) to express Flag-tagged Cas9 under a doxycycline-inducible promoter, known as HEK293_Cas9 cell line. The HEK293FT cells were purchased from Invitrogen and used for virus generation.

2.2.1.3.2 Mouse embryonic fibroblasts (MEFs)

The IKKα-deficient MEFs were kindly given by Dr Inder Verma (Salk Institute for Biological Studies, San Diego, USA). The MEFs isolated from knock-in mice expressing

NEMO[D311N] mutant or HOIP[C879S] mutant were generated by Dr Sambit Nanda (Cohen lab) and Dr Christoph Emmerich (Cohen lab), respectively.

2.2.1.4 Bone-marrow-derived macrophages (BMDM)

The bone marrow from the knock-in mice expressing catalytically inactive IKKα was kindly provided by Dr Toby Lawrence (Centre d'Immunologie de Marseille-Luminy, Marseille, France).

The bone marrow was extracted from the tibia and femurs of mice by flushing the bone cavity with L929 media (provided by Dr Sambit Nanda). The bone-marrow-derived macrophages (BMDM) were obtained after filtering the bone marrow through sieve, and incubated for 7 days at 37 °C in the L929 media containing mouse M-CSF.

The media in 10 cm dish was removed by aspiration. BMDM was washed with sterile PBS and incubated for 10 min with 5 ml Versene at RT until they are detached. Cells were collected by scrapping and brief centrifugation for 5 min at 300 xg, and re-seed in the plate with L929 media containing mouse M-CSF 24 h ahead of stimulation.

2.2.1.5 Freezing and thawing of cells

Cells with 90-95% confluency in 15 cm dish were incubated with 2 ml trypsin/EDTA (0.05%) for 3 min at 37 °C. The cell suspension was centrifuged for 5 min at 1200 rpm and resuspended in 3 ml of freezing medium (10% DMSO, 90% FBS) and divided in 3x 1 ml aliquots in cryovials. The tubes were placed into a cell-freezing chamber (Thermo Scientific) for 24 h at -80 °C, and then transferred to liquid nitrogen tank for long term storage.

For thawing, the cryovials were placed in a water bath at 37 °C, and gently mixed with 9 ml growth media followed by brief centrifuge. The pellet was resuspended with 10 ml growth media (**Section 2.2.1.1**) and seed in a 10 cm tissue culture dish.

2.2.1.6 Cell transfection

2.2.1.6.1 PEI

The Polyehylenimine (PEI) stock solution (1 mg/ml) was prepared in 20 mM HEPES buffer (pH 7.5), sterilised by filtration through a 0.22-mm filter, aliquoted and stored at -80 °C. For the transfection of HEK293 cells in 10 cm dishes, 10 µg of plasmid DNA was diluted in 1 ml of Opti-MEM reduced serum media, mixed with 30 µl of 1 mg/ml PEI by brief vortex and incubated at RT for 15 min. The mixture was then added drop-wise to the cells. Cells were lysed after 24 hours.

2.2.1.6.2 Lipofectamine 2000

Lipofectamine 2000 was used to transfect 293FT cells for virus production. 10 µg of plasmid DNA was diluted in 300 µl of Opti-MEM reduced serum media, and then gently mixed with 36 µl of Lipofectamine 2000 diluted in 300 µl of Opti-MEM reduced serum media. This solution was incubated for 15 min at RT and added drop-wise to the cells cultivated in 10 cm dish with antibiotic-free medium.

2.2.1.6.3 GeneJuice

GeneJuice transfection reagent was used to transfect gRNAs into 293 cells for gene knockout. 60 µl GeneJuice reagent was diluted in 1000 µl of Opti-MEM reduced serum media by brief vortex and incubated at RT for 10 min. 10 µg of gRNA plasmid was then added, gently mixed and incubated at RT for extra 10 min. The mixture was then added drop-wise to the cells.

2.2.1.7 Inhibition and stimulation of cells

All the inhibitors used throughout this thesis are listed in **Table 2.6**. 10 mM stock of inhibitors dissolved in DMSO was provided by DSTT, and stored in aliquots at -20 °C. The inhibitor solution was added directly into the cell culture medium and incubated for 1 h at 37 °C. An equivalent volume of DMSO was used as a vehicle control.

Typically the 1000x stock of agonists were prepared after dissolving in PBS, and stored in aliquots at -20 °C. They were added directly into the cell culture medium at the concentrations indicated in the figure legends.

Table 2.6 List of protein inhibitors

Inhibitor	Reported target
NG25	TAK1 [199]
5z-7-oxozeaenol	TAK1 [148]
BI605906	IKKβ [135]
PD 0325901	MEK1/2 [200]
BIRB 0796	p38 [201]

2.2.1.8 Generation of stable cell lines

2.2.1.8.1 Generation of IL-1R* cells

To stably express IL-1 receptor in the HEK293_Cas9 cells, the cDNA encoding the IL-1 receptor was inserted into a pBABE retroviral vector with a neomycin-resistance gene (**Table 2.4**). To generate retroviral particles, 6 μg of retroviral vector, 3.75 μg of vector encoding gag/pol packaging protein (**Table 2.4**) and 2.25 μg of vector encoding vesicular stomatitis virus G protein (VSV-G) envelope proteins (**Table 2.4**) were diluted in 300 μl Opti-MEM reduced serum media. It was gently mixed with 36 μl Lipofectamine 2000 diluted in 300 μl Opti-MEM reduced serum media, and incubated

for 15 min at RT. The solution was added drop-wise into cell culture cultivated in Opti-MEM reduced serum media in 10 cm dish with 90% confluency. The media was replaced with fresh growth media 4 h after transfection. The media containing retrovirus was collected after 48 h, and passed through a 0.45 μm filter to remove cell debris. 1 ml retrovirus was added to 4 ml of HEK293_Cas9 cell culture (roughly 1X 10^5 cells) in a 6 cm dish with 2 μg/ml protamine sulphate to facilitate infection. The media was refreshed 24 h after virus infection, and further 24 h later cells were selected by exposure for 1-2 weeks to media containing 1 mg/ml G418.

2.2.1.8.2 Generation of TAK1 KO, TAB1 KO, TAB2/3 double KO, TAB1/TRAF6 double KO, TAB2/3/TRAF6 triple KO and TAB2/3/XIAP triple KO IL-1R* cells

In the original CRISPR/Cas9 approach, the IL-1R* cells were transfected with TAB1, TAB2 or TAB3 gRNA plasmid (**Table 2.4**) using GeneJuice transfection reagent (**Section 2.2.1.6.3**). After 8 h, the expression of wild type Cas9 was induced with doxycycline (1 μg/ml). After 18 h later, the transfection of gRNA plasmid was repeated. Cells were then diluted and seed on 96-well plate with the density of 1 cell per 100 μl media, and left until colonies began to form (2-3 weeks). The single clones were analysed by immunoblotting of the cell extracts with antibodies indicated in the figures, or by restriction cleavage analysis after polymerase chain reaction (PCR).

Later, a pair of guide RNAs (sense and anti-sense gRNAs) was designed for each gene (**Table 2.4**). The sense gRNA aiming the region upstream of cleavage site was introduced into a plasmid containing a puromycin-resistance gene. The anti-sense gRNA aiming the region downstream of cleavage site was inserted into a plasmid encoding Cas9[D10A] nickase which only cleaves one strand of the DNA complementary to gRNA [198]. To knock out TAK1, TAB1 and TAB2 in the IL-1R* cells

individually, each gRNA plasmid (1.0 μg) was mixed with 1 ml of Opti-MEM reduced serum media and 20 μl of PEI (1 mg/ml, **Section 2.2.1.6.1**). After incubation for 15 min at RT, the solution was added to the cells drop-wise for transfection. After 24 h and 48 h, the medium was replaced with fresh medium containing 2 μg/ml puromycin. The cells were then single cell-plated into 96 well plates and left until colonies began to form (2-3 weeks). The single clones were analysed by immunoblotting of the cell extracts with antibodies indicated in the figures.

Several TAB1-null and TAB3-null clones were obtained, a few of which were selected for further study. Double knock-out (DKO) IL-1R* cells lacking expression of both TAB2 and TAB3 were generated by targeting TAB3-null IL-1R* cells with gRNAs specific for TAB2. Double knock-out (DKO) IL-1R* cells lacking expression of both TAB1 and TRAF6 were generated by targeting TAB1-null IL-1R* cells with gRNAs specific for TRAF6. Triple knock-out IL-1R* cells lacking the expression of TAB2, TAB3, and each of TAB1, TRAF6 and XIAP were generated by targeting the TAB2/TAB3 double KO cells with gRNAs specific for TAB1, TRAF6 and XIAP, respectively.

2.2.1.8.3 Generation of cells stably expressing reconstituted target proteins.

To stably express proteins of interest under the control of an inducible promoter, cDNA of interest was introduced into a pRetroXTight retroviral vector carrying a puromycin-resistance gene (**Table 2.4**). The pRetroXTight retroviral particles and the Tet-On vector encoding a doxycycline-controlled transcriptional transactivator were generated same as pBABE retroviral vector described in **Section 2.2.1.8.1**. Retroviruses were diluted 4-fold with fresh media, and incubated for 24 h with cells of interest in the presence of 2 μg/ml protamine sulphate. Fresh medium containing 1 mg/ml G418 (when Tet-On vector is in use) and 3 μg/ml puromycin (gene of interest)

was added to select the transduced cells. Cells were cultured for 16 h with doxycycline (0.1-1.0 μg/ml) to induce the expression of protein of interest when pRetroXTight vector is in use.

2.2.2 Molecular biology techniques

2.2.2.1 Plasmid transformation, amplification and isolation

Approximately 10 ng of one plasmid (1 μl) were added to 25 μl of thawed *E.coli* DH5α competent cells which were then placed on ice for 15 min. Cells were heat-shocked by incubation at 42 °C for 35 sec in a thermomixer to facilitate the uptake of DNA, and placed back on ice for a further 2 min to recover. All of cells were spread directly onto Luria-Bertani (LB) agar plates containing 100 μg/ml ampicillin. Plates were left in a 37 °C incubator overnight to allow colony growth.

To amplify the plasmid, one colony was inoculated into 250 ml LB media containing 100 μg/ml ampicillin, and incubated for 16 h on a shaking incubator at 37 °C. The cells were pelleted by centrifugation at 3000 rpm for 15 min in a J-6 Beckman centrifuge at 4 °C. The plasmid DNA was isolated using the Qiagen plasmid Midi or Maxi kit according to the manufacturer's instructions. One preparation yielded about 1 mg plasmid DNA.

2.2.2.2 Measurement of DNA and mRNA concentration

NanoDrop spectrophotometer (Thermo Scientific) was calibrated with nuclease-free water, and then used to determine the absorbance of isolated DNA or mRNA in aqueous solution at 260 nm. The concentration was calculated accordingly.

2.2.2.3 DNA cloning techniques

All recombinant DNA procedures, amplifications, restriction digestions and ligations were carried out using standard protocols by the DSTT cloning team, University of Dundee, jointly headed by Mark Peggie and Rachel Toth. The cDNA constructs used during the course of this Thesis are listed in **Table 2.4**. All PCR reactions were performed using KOD Hot Start DNA polymerase (Novagen). DNA sequencing was performed by the DNA Sequencing Service, College of Life Sciences, University of Dundee (www.dnaseq.co.uk).

2.2.2.4 Real-time quantitative reverse transcription PCR (qRT-PCR)

IL-1R* cells were seeded into 24-well plates at a final concentration of 1.5×10^5 and the RNA was extracted using a RNA MicroElute kit from VWR (R6831-01). RNA was reverse transcribed using the iScript cDNA synthesis kit from Bio-Rad (170-8891). PCR was performed using SsoFast EvaGreen Supermix from Bio-Rad (172-5204) in the CFX384 (Bio-Rad). Primer sequences are as following:

IL-8 forward, 5'-ATAAAGACATACTCCAAACC-TTTCCAC-3';

IL-8 reverse, 5'-AAGCTTTACAATAATTTCTGTGTTGGC-3';

IκBα forward, 5'- GATCCGCCAGGTGAAGGG-3';

IκBα reverse, 5'- GCAATTTCTGGCTGGTTGG-3';

A20 forward, 5'- GCAGAAAAGCCGGCTGCGTG-3';

A20 reverse, 5'- CGCTGGCTCGATCTCAGTTGCT-3'.

Normalisation was performed using 18S RNA and the $\Delta\Delta C_t$ method. Primer sequence 18S forward, 5'- GTAACCCGTTGAACCCCATT-3'; 18S reverse, 5'-CCATCCAATCGGTAGTAGCG-3'.

2.2.3 Biochemistry techniques

2.2.3.1 Cell lysis

Cells were washed twice with ice-cold PBS on ice when the media was removed by aspiration. Cells were lysed with ice-cold MRC Lysis Buffer (**Table 2.1**, 0.5 ml for 10 cm dish), scraped from the plates and transferred into Eppendorf tubes. Cell lysates were clarified by centrifugation at 4 °C for 10 min at 14,000 rpm. The supernatants were taken and its protein concentration was then determined (**Section 2.2.3.2**).

2.2.3.2 Quantification of protein concentration

Protein concentration of cell lysates was determined by using the Bradford method [202]. It is a colorimetric protein assay based on an absorbance shift from 465 nm (red) to 595 nm (blue) once coomassie dye binds to proteins. A serial dilution of BSA was applied (0.03125 to 1 μg/ml, a dilution factor of 2) to generate a standard curve. Samples were diluted 10x in water and 5 μl was placed in triplicate a 96 well plate along with 250 μl Bradford reagent. The plate was incubated at RT for 5 min. The absorbance at 595 nm was measured using a 96 well plate reader, and the concentrations of samples were calculated by plotting to standard curve.

2.2.3.3 Purification of GST-fusion proteins from IL-1R* cells lacking the expression of TAB1/2/3

Cells from 5x 15 cm dishes were lyzed and clarified lysates were incubated for 4-6 h on a rotating platform at 4 °C with 1 ml Glutathione Sepharose equilibrated with MRC lysis buffer (**Table 2.1**). The Sepharose were then washed once with washing

buffer (**Table 2.1**), three times with high salt washing buffer (**Table 2.1**) and two times with PreScission protease buffer (**Table 2.1**). To cleave GST-tag and release protein, 1 ml of slurry (0.5 ml of buffer and 0.5 ml of beads) was incubated with 125 μg of PreScission protease at 4 °C overnight under gentle agitation. The slurry was then transferred to a Spin-X tube filter and spun 30 sec at top speed. The concentration of eluted protein present in the flow-through was measured, and 1 μg of protein was analysed for its purity by SDS-PAGE, while the rest was aliquoted and stored at -80 °C.

2.2.3.4 Immunoprecipitation

The cell lysate (500 μg) was incubated with 2 μg of in-house antibodies (**Table 2.3**) for 1 h at 4 °C on a rotating wheel. 10 μl Protein G-Sepharose washed with lysis buffer (**Table 2.1**) was added and incubate for extra 0.5 h. The beads were collected by brief centrifugation, washed three times with high salt washing buffer (**Table 2.1**) and once with washing buffer (**Table 2.1**). The samples were denatured in SDS sample buffer and subjected to SDS/PAGE.

2.2.3.5 Halo-NEMO/NZF_2 pulldown assays

To capture ubiquitin (Ub) chains from cell extracts, 3 mg cell extract protein was incubated with Halo-linked ubiquitin binding proteins. Halo-NEMO beads, in which the Halo-tagged full-length NEMO is bound to HaloLink resin, were used to capture Met1-Ub chains. Halo-NZF_2 beads contain two copies of Npl40 zinc finger (NZF) domain from N terminus of TAB2, and they were mainly used to capture K63-linked Ub chains [158]. Beads were kindly provided by Drs Christoph Emmerich, Sam Strickson and Siddharth Bakshi in our group. After incubation for 16 h at 4°C, the beads were washed 3 times with 1 ml of Halo resin wash buffer (**Table 2.1**) and once with 500 μl of 10 mM Tris/HCl (pH 7.5). The slurry was then transferred to a Spin-X tube filter, and after a

brief centrifuge, the dried resin was mixed with SDS sample buffer and placed on a thermomixer for 3 min at RT to release captured Ub chains. The Spin-X tube filters were briefly centrifuged again and the sample was subjected to SDS/PAGE.

2.2.3.6 *In vitro* kinase assay of IKKβ activity

IKKβ immunoprecipitates were assayed for IKKβ activity in a 50 μl reaction containing 50 mM Tris/HCl pH 7.5, 0.1 mM EGTA and 0.1% (v/v) 2-mercaptoethanol (β–ME), 1 μM microcystin (to inactivate any remaining traces of PP1γ), 0.3 mM of the peptide KKKKERLLDDRHDSGLDSMKDEEY (EP5709 in MRC-PPU database, corresponding to amino acid residues 26-42 of IκBα with multiple Lys at N terminus facilitating its association with membrane), 10 mM magnesium acetate and 0.1 mM γ^{32}P[ATP] (5 x 10^5 cpm/nmol). After incubation for 10 min at 30 ^{o}C on a shaking platform, the reaction was stopped by the addition of 5 μl EDTA (0.5 M), and 40 μl of sample was dropped into p81 membranes (2x2 cm), which were then submerged and washed extensively with 50 mM phosphoric acid. The membranes were fixed with acetone, and dried in the air. The incorporation of ^{32}P-radioactivity into peptide substrates was measured by Cerenkov counting in a scintillation counter**.**

2.2.3.7 Immunoprecipitation and dephosphorylation of IKKβ

For the overexpressed HA-tagged IKKβ in HEK293 cells, 40 μg of cell extract protein was incubated for 60 min at 4 °C with 4 μg anti-HA antibody (**Table 2.3**), whereas for the endogenous IKKβ, 0.2 mg of cell extract protein was incubated with 2.5 μg anti-IKKβ antibody (**Table 2.2**). 10 μl packed Protein G-Sepharose was added and after 30 min incubation at 4 °C, beads were collected by brief centrifugation, washed three times in cell lysis buffer plus (**Table 2.1**). The dephosphorylation included 100 μg GST-PP1γ (**Table 2.5**) for 60 min at 30 ^{o}C, and the immunoprecipitates were

collected, washed three times with high salt washing buffer, and three times with 50 mM Tris/HCl pH 7.5, 0.1 mM EGTA and 0.1% (v/v) β–ME to remove the phosphatase.

2.2.3.8 Analysis of samples/Protein resolution by electrophoresis and immunoblotting

2.2.3.8.1 SDS-polyacrylamide gel electrophoresis (SDS-PAGE)

SDS-PAGE allows the resolution of proteins based on their electrophoretic mobility in accordance with molecular weights. Sodium dodecyl sulphate (SDS) is an anionic detergent capable of coating proteins in a constant weight ratio (about 1.4 g SDS/g protein), therefore providing a net negative charge proportional to the molecular weight. The migration of a protein is a function of the logarithm of its molecular weight, as smaller proteins migrate faster and larger proteins move slower. The presence of reducing agents including SDS and β–ME broke disulphide bonds so that amino acid sequence became linear.

Samples were prepared with 1x SDS Sample Buffer (**Table 2.1**) containing 1% β–ME and heated at 95 °C for 5 min. 20 μg sample was loaded into each slot and electrophoresis was performed in 1x SDS/PAGE running buffer (**Table 2.1**) at 0.02 A for 90 min until the dye front reached the bottom of the gel. Protein samples were concentrated in the stacking gel (pH 6.8) (**Table 2.1**), which permits samples to move into the separating gel (pH 8.8) (**Table 2.1**) at the same time and ensures proteins of similar molecular weight to migrate in narrow bands. Separating gels were made of different percentages of acrylamide in order to achieve a better resolution of protein of a particular molecular weight.

Commercial precast gels were used in the studies of ubiquitin chains or proteins subjected to mass spectrometry. Commercial gels were run in MOPS running buffer (**Table 2.1**) at a constant 120 V for 1.5 h.

Both gel types were either stained with Coomassie dye (**Section 2.2.3.8.2**) or transferred onto PVDF membranes (**Section 2.2.3.8.3**).

2.2.3.8.2 Coomassie Blue staining of SDS/PAGE gels

Once SDS/PAGE finished, gels were washed with deionised water, and incubated for 1 h in 20 ml InstantBlue coomassie staining solution on a rotating platform. Gels were de-stained by repeatedly washing with deionised water.

2.2.3.8.3 Transfer of proteins from gels to PVDF membranes

Before assembling the transfer cassette, the PVDF (polyvinylidene difluoride) membrane was soaked with 100% methanol, while nylon sponge pads and the Whatmann 3-mm filter papers were equilibrated in 1x Tris-glycine transfer Buffer (**Table 2.1**). The transfer cassette was assembled as follows:

Anode (+)

Sponge pad

Whatmann paper

Membrane

Gel

Whatmann paper

Sponge pad

Cathode (-)

The transfer was run at 80 V for 80 min in 1x Tris-glycine transfer Buffer (**Table 2.1**) in Bio-Rad transfer apparatus.

2.2.3.8.4 Immunoblotting (Western blotting)

To visualize transferred proteins, PVDF membranes were stained with Ponceau S for 1 min and then washed in deionised water. The membranes were cut with a scalpel so that different proteins on the same membrane could be probed at the same time.

To avoid non-specific binding of antibodies, the PVDF membranes were blocked for 30 min with TBS-T (**Table 2.1**) containing 5% (w/v) skimmed milk at RT. After washing with TBS-T three times, the membranes were then incubated with 1 μg/ml primary antibody (**Table 2.2**) diluted in TBS-T at 4 °C overnight on a rotating roller.

The blots were then washed 3 times with TBS-T and incubated for 1 h at RT with secondary horseradish Peroxidase (HRP)-conjugated antibodies diluted in TBS-T at 1:10000. After washing as before, the membrane was incubated with enhanced chemiluminescence (ECL) reagent for 1 min, drained, placed in an X-ray cassette and exposed to X-ray films until the exposure was satisfactory. X-ray films were developed using a film automatic processor.

2.2.3.9 Measurement of cytokines by an enzyme-linked immunosorbent assay (ELISA)

IL-1R* cells were seeded into 24 well plates at a final concentration of $1.5x10^5$. The next day, the cell culture media were collected after stimulation for the times indicated. Samples were diluted 8 times with 0.05% Tween-20/0.1% BSA in PBS, and

100 µl were placed in triplicate in a 96-well plate (VWR Nunc-immuno Microwell plate, #439454) coated with capture antibody from Peprotech ELISA kits (900-K18). ABTS (2,2'-Azino-bis[3-ethylbenzothiazoline-6-sulfonicacid]- diammonium salt) was used as a substrate activated by avidin peroxidase. The ELISA reaction was stopped by the addition of 0.5 M sulphuric acid and absorbance was measured at 450 nM. A standard curve was generated by plotting the absorbance against a dilution of cytokine standards. The concentration of IL-8 in the culture medium was calculated. For statistical analysis, values were shown as means $\pm$ SEM (standard error of means). The Student's *t*-test was performed using GraphPad Prism software and the two-tailed P value was calculated.

2.2.4 Mass spectrometry

To identify novel phospho sites on TAK1 and TAB1 in the TAB2/3 DKO cells, mass spectrometry was utilized. The TAB1-TAK1 complex was immunoprecipitated from 10 mg total lysate by 10 µg of TAK1 antibody (S828A, **Table 2.3**) for 1 h at 4 ^{o}C. 50 µl slurry of Protein G-Sepharose was added and incubated for extra 30 min. The Sepharose were then collected and thoroughly washed. The bound proteins were released by denaturation in SDS, subjected to SDS/PAGE in commercial precast gel and stained with Instant Blue followed by destain with ionized water.

To avoid contamination, the sample preparation process was conducted in a laminar flow hood (Model A3VB, Bassaire Limited). The protein bands containing TAK1 and TAB1 were excised with clean scalpels from stained precast gel. Gel pieces were minced into small cubes (about 1 mm^3) and collected in a LoBind 1.5 ml tube (Eppendorf). Gel pieces were washed for 10 min with 0.5 ml water, 50% acetonitrile (ACN), and 100 mM NH_4HCO_3 followed by 50% ACN/50 mM NH_4HCO_3. After incubating

with 10 mM DTT/100 mM NH_4HCO_3 for 45 min at 65 °C to reduce disulphide bonds, gel pieces were alkylated with 50 mM iodoacetamide (IAA)/100 mM NH_4HCO_3 for 30 min at RT in the dark. It is followed by repeatedly washing with 100 mM NH_4HCO_3 and 50% ACN/50 mM NH_4HCO_3 to remove all staining dye. Gel pieces were then dehydrated with 0.3 ml ACN for 30 min at RT, and residual moisture was removed using a SpeedVac. The shrunk gel pieces were incubated with 100 µl of 25 mM Triethylammonium bicarbonate (TEABC) and pre-activated Trypsin (5 µg/ml) for 30 min at 37 °C. Extra 25 mM TEABC was added to ensure the gel pieces were covered. After incubation for 16 hours at 30 °C on a shaking platform, an equivalent volume of ACN was added and incubated for 15 min at RT. Supernatants were transferred to 1.5 ml LoBind tubes. To maximise the recovery of peptide, 150 µl of 50% ACN/ 2.5% formic acid was added to dried gel pieces for 15 min at RT. The supernatant was combined with the previous fraction, and dehydrated completely by a SpeedVac. Samples were logged in and sent to the Proteomics and Mass Spectrometry Team, MRC-PPU for analysis by David Campbell.

Tryptic peptide analysis using LC (liquid crystallography)-MS/MS (tandem MS) was conducted on an Easy-nLC HPLC coupled to an LTQ Orbitrap Classic (Thermo) and data was analysed using the Mascot search program (http://www.matrixscience.com).

Chapter 3 The activation of IKKβ is primed by TAK1 and completed by autophosphorylation

3.1 Introduction

The canonical IκB kinase (IKK) complex comprises the protein kinases IKKα and IKKβ and a polyubiquitin-binding subunit called NEMO (**Section 1.2.5**, [102–106]). It has been widely accepted that the canonical IKK complex plays a pivotal role in mediating the response to many inflammatory stimuli [135,140]. The absence of the IKK complex led to failure to activate NF-κB, and hence abolished the production of inflammatory mediators. Despite extensive studies on the biological roles of the IKK complex, the molecular mechanism of its activation remains controversial. It has been established that the activation of IKKα and IKKβ requires phosphorylation at two serine residues in their activation loops (Ser176 and Ser180 in IKKα, and Ser177 and Ser181 in IKKβ, respectively) [102,107,108]. However, whether these phosphorylation events are catalysed by "upstream" protein kinases or by the complex itself is still debatable. The TGFβ-activated kinase-1 (TAK1) complex has been reported to catalyse IKK activation *in vitro* [76], while cytokines, such as IL-1 and TNF, failed to activate IKKs in MEFs that lack TAK1 expression [83] or that express a truncated inactive version of TAK1 [84]. In addition, TAK1 inhibitors prevented the IL-1- and TNF-stimulated activation of IKKα and IKKβ in MEFs [135,148,149]. These results indicated that TAK1 triggers the phosphorylation within the activation loops of IKKα and IKKβ, therefore activating the canonical IKK complex in response to IL-1 and TNFα.

On the other hand, it has been suggested that activation of the canonical IKK complex may be mediated by an autophosphorylation mechanism, since the mutation of the two Ser residues within the activation loop of IKKβ to Asp residues led to the

auto-phosphorylation, which was prevented in the catalytically inactive form of IKKβ [102,108]. Moreover, structural analysis of human IKKβ has revealed that two surfaces required for its dimerization are also essential for its activation [203]. This suggests that, under some conditions, the interaction of ubiquitin chains with NEMO might induce dimerization and *trans*-autophosphorylation and hence activation of IKKβ. Our laboratory has reported previously that an IKKβ specific inhibitor prevented the IL-1- or TNF-induced phosphorylation of IKKβ in IKKα-deficient MEFs, employing an antibody that recognises IKKβ only when it is phosphorylated at both Ser177 and Ser181 [135]. These findings suggest that autophosphorylation might be at least part of the mechanism that activates IKKβ.

In this Chapter, I present the results of experiments that I have carried out to understand the relative importance of TAK1 and autophosphorylation in the activation of the canonical IKK complex. These studies have allowed me to propose a new model for how the IKK complex is activated.

3.2 Results

3.2.1 An IKKβ specific inhibitor prevents the phosphorylation of IKKβ at Ser181 but not Ser177.

I first carried out experiments to see whether the protein kinase activity of TAK1 was essential for the IL-1 or TNF-dependent "dual" phosphorylation of IKKβ at both Ser177 and Ser181 in IKKα-deficient MEFs. I found that phosphorylation could be prevented by two structurally unrelated TAK1 inhibitors, NG25 [199] and 5z-7-oxozeaenol [148], which do not inhibit IKKβ (**Figs 3.1A and B,** top panel, lanes 1-9). These experiments confirm that TAK1 catalytic activity is essential for IKK activation in MEFs. However, interestingly, this dual phosphorylation was also abolished when cells

were pre-treated with BI605906 [135], an IKKβ-specific inhibitor (**Figs 3.1A and B,** top panel, compare lanes 1-3 with 10-12). This phospho-specific antibody used in these experiments only recognises IKKβ when both Ser177 and Ser181 are phosphorylated. It was therefore possible that TAK1 inhibitors and /or IKKβ inhibitor only suppress the phosphorylation of just one of the two serine residues. In order to address this point, antibodies recognising IKKβ phosphorylated at either Ser177 or Ser181 were employed. Surprisingly, I found that BI605906 prevented the IL-1- or TNF-induced phosphorylation at Ser181 but not Ser177 (**Figs 3.1A and B,** second and third panels from top, lanes 10-12). In contrast, NG25 and 5Z-7-oxozeaenol suppressed the IL-1- or TNF-stimulated phosphorylation of IKKβ at both Ser177 and Ser181 (**Figs 3.1A and B,** second and third panels from top, lanes 4-9). Similar observations were made in bone marrow-derived macrophages (BMDM) from knock-in mice expressing catalytically inactive IKKα [S176A/S180A] mutant following stimulation with the TLR4 agonist LPS or the TLR1/2 agonist Pam_3CSK_4 (**Figs 3.1C and D**), indicating that these findings might be of general significance.

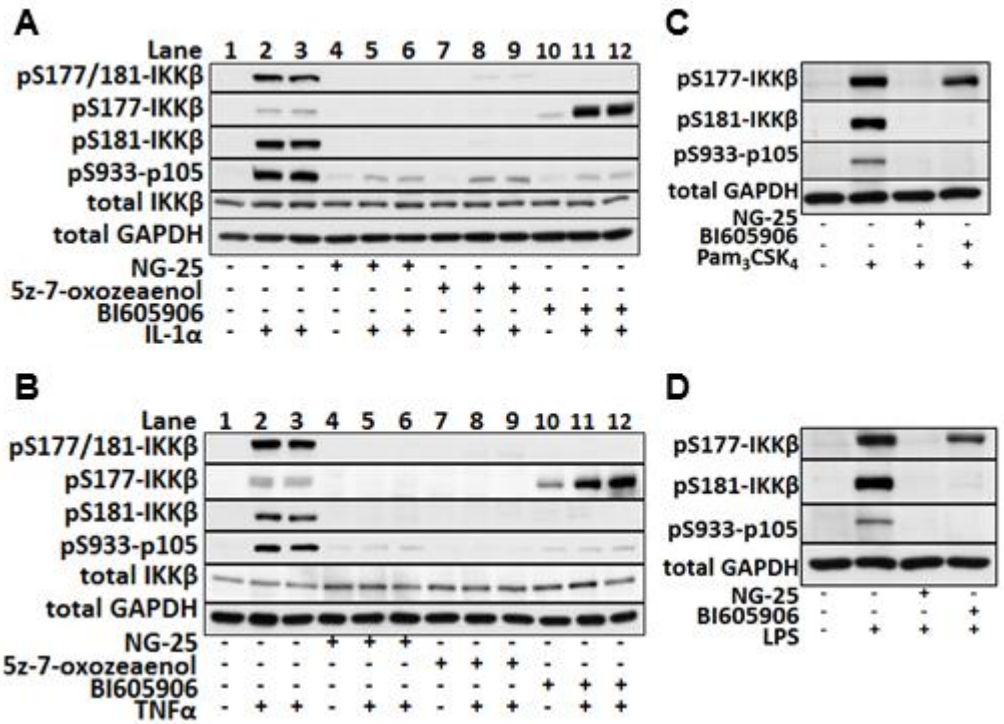

Figure 3.1 Effect of protein kinase inhibitors on the phosphorylation of IKKβ at Ser177 and/or Ser181 in MEFs lacking IKKα expression and BMDM expressing catalytically inactive IKKα. (**A**) IKKα-deficient MEFs were pre-treated for 1 h without (-) or with (+) 1 μM NG25, 1 μM 5z-7-oxozeaenol or 5 μM BI605906, and then stimulated for 10 min with 5 ng/ml IL-1α. Cell lysates (20 μg protein) were subjected to SDS/PAGE and immunoblotted with the antibodies indicated. (**B**) Same as A except that the cells were stimulated with 10 ng/ml TNFα. (**C, D**) BMDM from knock-in mice that express the catalytically inactive IKKα[S176A/S180A] mutant were pre-treated for 1 h without (-) or with (+) 2 μM NG25 or 2 μM BI605906, and then stimulated for 10 min with 1 μg/ml Pam_3CSK_4 **(C)** or 0.1 μg/ml LPS (**D**). Cell extracts (20 μg protein) were subjected to SDS/PAGE and immunoblotted with the antibodies indicated. The results are representative of at least three independent experiments.

The recognition of IKKβ by the phospho-Ser177 specific antibody showed a great enhancement in IKKα-deficient MEFs pre-treated with BI605906 and then stimulated with IL-1 or TNF (**Figs 3.1A and B,** second panel from top, compare lanes 10-12 with 1-3). One explanation for this result is that phosphorylation at Ser177 is not detected by the phospho-Ser177-specific antibody when Ser181 is phosphorylated. This was confirmed by an immunoblotting experiment using synthetic phospho-peptides corresponding to amino acid residues 171-188 of IKKβ. The mono-phosphorylated peptide carried one single phospho-serine at the position equivalent to Ser177, whereas the di-phosphorylated peptide carried phosphate at both Ser177 and Ser181. The antibody recognising phospho-Ser177 detected the mono-

phosphorylated peptide, but hardly detected the di-phosphorylated species (**Fig 3.2A**). The phospho-Ser181-specific antibody only detected the di-phosphorylated but not mono-phosphorylated peptide (**Fig 3.2B**), since Ser177 is excluded from the peptide epitope (Cys-Thr-pSer-Phe-Val) used to raise this antibody. As expected, the antibody that detects the dual-phosphorylated peptide did not recognise the peptide phosphorylated at Ser177 only (**Fig 3.2C**).

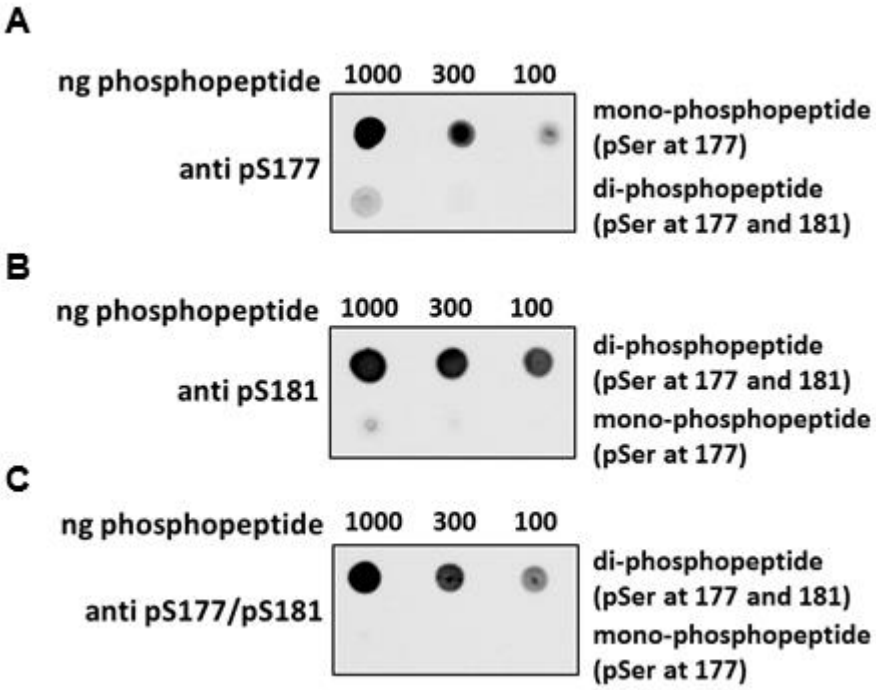

Figure 3.2 Phosphorylation at Ser181 interferes with the recognition of phospho-Ser177 by the phospho-Ser177-specific antibody. (**A**) The indicated amounts of phosphopeptides corresponding to amino acid residues 171-187 of IKKβ phosphorylated at only Ser177 or both Ser177 and Ser181 were spotted onto nitrocellulose membranes, and probed with the phospho-specific antibody recognising phospho(p)-Ser177. (**B, C**) Same as A, except that the peptides were immunoblotted with the antibody recognising IKKβ phosphorylated at Ser181 (**B**) or with the antibody only recognising the IKKβ di-phosphorylated at both Ser177 and Ser181 (**C**).

3.2.2 The expression of IKKβ[S177E] induces the IKKβ autophosphorylation of Ser181 and autoactivation.

The simplest explanation of the results shown in **Fig 3.1** was that TAK1 catalysed the phosphorylation at Ser177, allowing IKKβ to autophosphorylate itself at

Ser181. To investigate this hypothesis, I generated IKKα knock-out MEFs stably expressing different forms of HA-tagged IKKβ, including IKKβ[S177A], in which Ser177 was mutated to alanine (Ala) to prevent phosphorylation, and IKKβ[S177E] in which Ser177 was mutated to glutamic acid (Glu) to mimic the effect of phosphorylation by introducing a negative charge. After induction with doxycycline, Ser181 became phosphorylated only when the IKKβ[S177E] mutant was expressed in cells without any stimulation with IL-1 or TNF (**Fig 3.3A**). Moreover, the inclusion of BI605906 led to substantial de-phosphorylation of the IKKβ[S177E] mutant at Ser181, but incubation with the TAK1 inhibitor NG25 had no effect. Furthermore, a catalytically inactive form of IKKβ[S177E] mutant produced by the further mutation of Asp166 to Ala, prevented Ser181 from becoming phosphorylated (**Fig 3.3B**). Taken together, these lines of evidence indicate that the phospho-mimetic Ser177Glu mutation induces the autophosphorylation of Ser181.

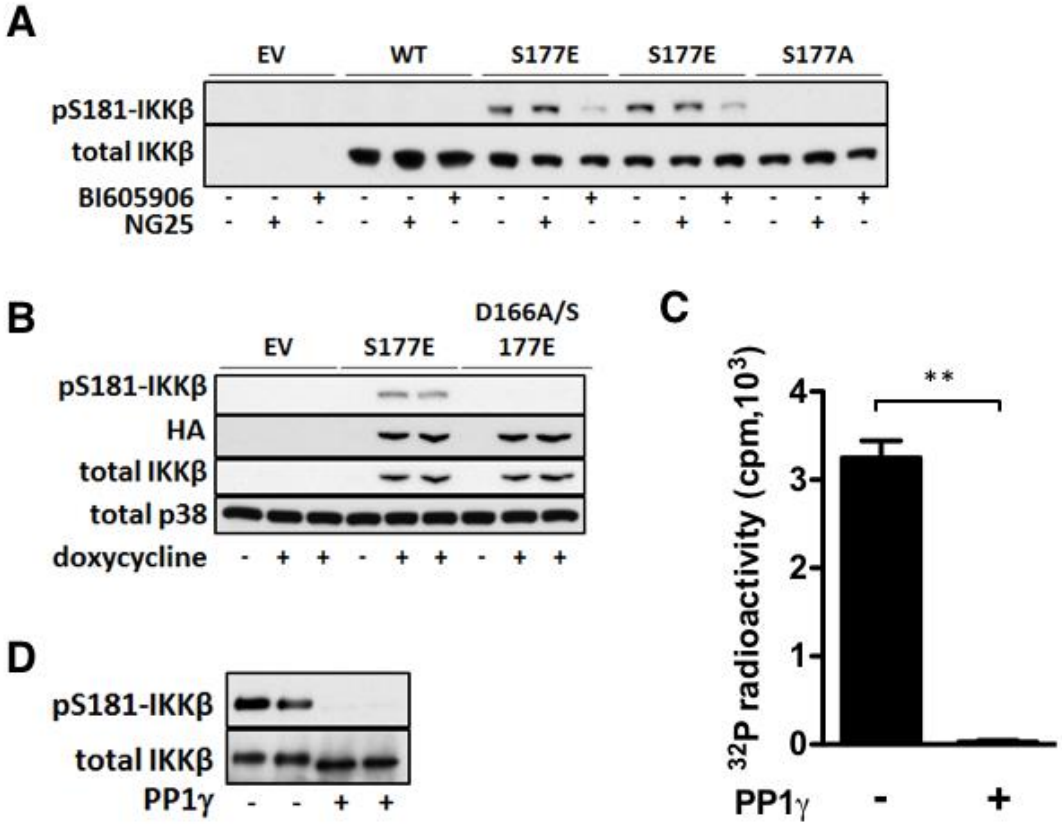

Figure 3.3 Expression of IKKβ[S177E] induces the autophosphorylation of Ser181 and activation of IKKβ. (**A**) IKKα-deficient MEFs stably expressing HA-tagged wild type IKKβ (WT), IKKβ[S177E] (S177E), IKKβ[S177A] (S177A) or empty vector (EV) were incubated for 16 h with 1 μg/ml (WT and EV), 0.2 μg/ml (S177A) or 0.1 μg/ml (S177E) doxycycline to induce the expression of these proteins, and then incubated for 1 h without (-) or with (+) 5 μM NG25 or 5 μM BI605906. Cell extracts (20 μg (EV, S177E, S177A) or 80 μg (WT) protein) were analysed by immunoblotting with the antibodies indicated. (**B**) Same as A, except that Ser181 phosphorylation was studied in MEFs stably expressing HA-IKKβ[D166A/S177E] and HA-IKKβ[S177E], and no inhibitors were used. (**C, D**) HA-tagged IKKβ[S177E] was transfected into HEK293 cells, immunoprecipitated from the cell extracts (200 μg protein) using anti-HA antibody, incubated without (-) or with (+) PP1γ and assayed for IKKβ activity (**C**) or immunoblotted with antibodies indicated (**D**). The results are representative of at least three independent experiments. **$p < 0.01$.

IKKβ activates the NF-κB signalling by phosphorylating IκBα at Ser32 and Ser36 in cells. The phosphorylation by IKKβ[S177E] of a synthetic peptide corresponding to amino acid residues 26-42 of IκBα was suppressed by BI605906 similarly to wild type IKKβ (**Fig 3.4A**), establishing that the activity being assayed was catalysed by IKKβ and not any other contaminating protein kinase in the immunoprecipitates. Phosphatase treatment inactivated the IKKβ[S177E] mutant (**Fig 3.3C**), which was consistent with the dephosphorylation of Ser181 and small increase in the electrophoretic mobility of

IKKβ (**Fig 3.3D**). These experiments suggest that the IKKβ[S177E] mutant is inactive but becomes activated when Ser181 is autophosphorylated.

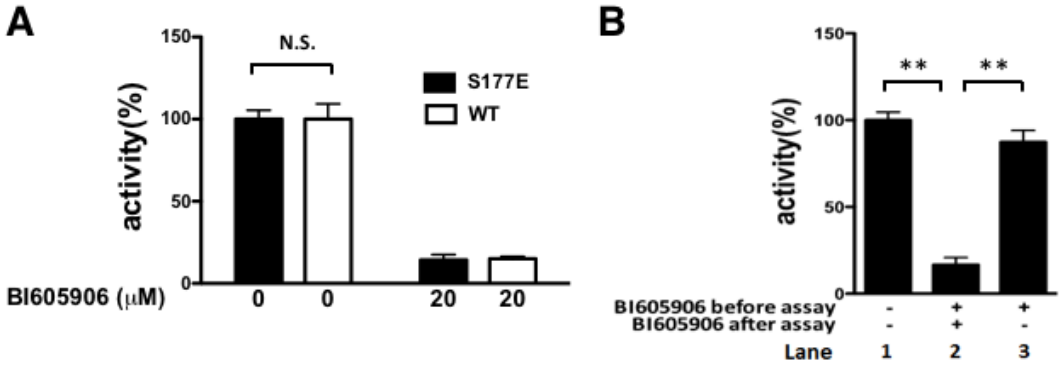

Figure 3.4 Effect of BI605906 on IKKβ kinase activity. (A) HA-tagged wild type IKKβ (WT) or IKKβ[S177E] mutant (S177E) were expressed in HEK293 cells, immunoprecipitated from the cell extracts (200 μg protein) using anti-HA antibody and assayed for activity in the absence or presence of BI605906. The activities were plotted as a percentage of that obtained in the absence of inhibitor. N.S. means not significant. **(B)** BI605906 is a reversible inhibitor of IKKβ. IKKα-deficient MEFs were stimulated for 10 min with 5 ng/ml IL-1α. The endogenous IKKβ was immunoprecipitated from cell extracts (0.2 mg protein) using anti-IKKβ antibody and incubated for 1 h at 30 ^{o}C without (-, Lane 1) or with (+, Lanes 2 and 3) 20 μM BI605906. In Lane 3 only, the immunoprecipitates were washed extensively to remove BI605906. All the immunoprecipitates were then assayed for IKKβ activity. **p < 0.01.

3.2.3 Phosphorylation of IKKβ at Ser177 induces little activity if Ser181 is not phosphorylated.

In order to investigate whether the phosphorylation at Ser177 could activate IKKβ without Ser181 phosphorylation in cells, I incubated IKKα-deficient MEFs with BI605906 to prevent the phosphorylation at Ser181, immunoprecipitated IKKβ from IL-1-stimulated IKKα-deficient cells and after washing to completely remove BI605906, the immunoprecipitates were assayed for IKKβ catalytic activity. The endogenous IKKβ phosphorylated at Ser177 alone showed much lower activity than IKKβ phosphorylated at both Ser177 and Ser181 (**Fig 3.5**). Since BI605906 is a reversible inhibitor (**Fig 3.4B**), the reduction of activity was not due to the presence of BI605906. Taken together, these experiments established that the phosphorylation of Ser177 is a requisite to permit the autophosphorylation at Ser181 on IKKβ, and the phosphorylation at Ser181

is required for the full catalytic activity of IKKβ in cells.

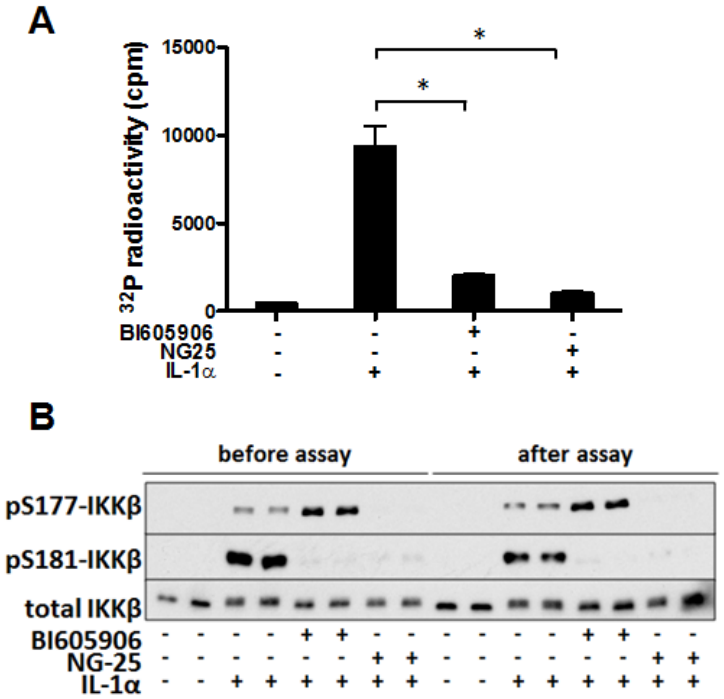

Figure 3.5 IKKβ phosphorylated at Ser177 has little activity if Ser181 is not phosphorylated. (**A**) IKKα-deficient MEFs were incubated for 1 h without (-) or with (+) 5 μM BI605906 or 2 μM NG25, and then stimulated for 10 min with 5 ng/ml IL-1α. The endogenous IKKβ was immunoprecipitated from cell extracts (0.2 mg protein) and assayed for activity. The results are representative of at least three independent experiments. *p < 0.05. (**B**) The immunoprecipitates from A were denatured before and after the assay, and aliquots of each sample were subjected to SDS/PAGE, transferred to PVDF membranes and immunoblotted with antibodies indicated.

3.2.4 Activation of the canonical IKK complex

The results presented above were carried out in IKKα-deficient MEFs or in BMDM from knock-in mice expressing the catalytically inactive IKKα[S176A/S180A] mutant. Interestingly, the phosphorylation of IKKβ at Ser181 was only decreased slightly by BI605906 in IL-1- or TNF-stimulated wild type MEFs (**Figs 3.6A and B**) and was not affected significantly in Pam_3CSK_4- or LPS-stimulated BMDM (**Fig 3.6C**). The IKKβ inhibitor BI605906 has no effect on IKKα activity [135]. This suggests that in wild type cells, in which IKKα, IKKβ and NEMO form a complex, IKKα might be able to catalyse the phosphorylation of IKKβ at Ser181 *in trans* when IKKβ activity is inhibited by BI605906, as indicated by the block of p105 phosphorylation.

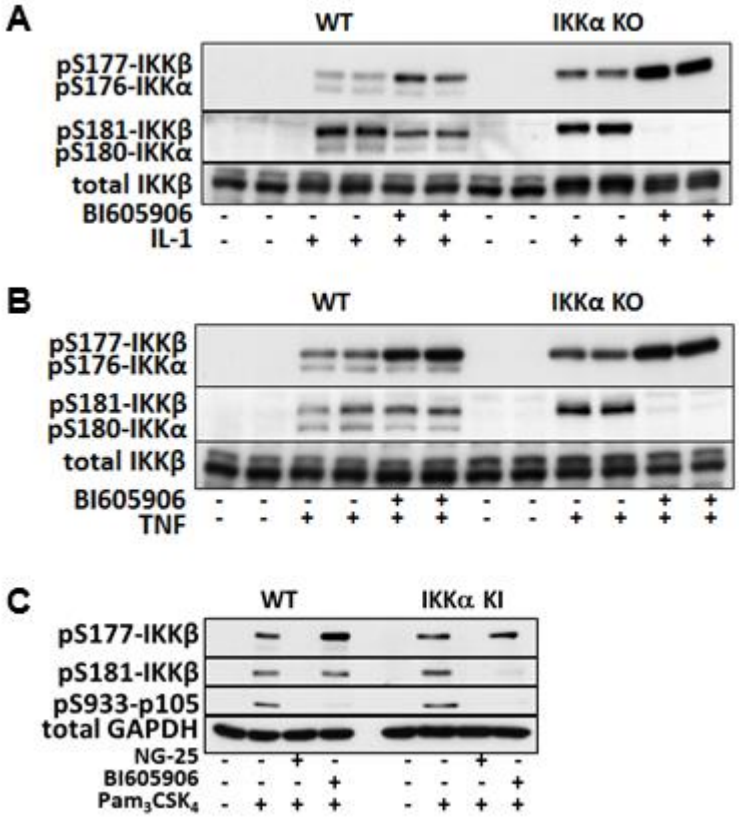

Figure 3.6 Effect of protein kinase inhibitors on the phosphorylation of IKKβ at Ser177 and Ser181 in MEFs and BMDM. (**A, B**) Wild type (WT) or IKKα-knock-out (KO) MEFs were incubated for 1 h without (-) or with (+) 5 μM BI605906 and then stimulated for 10 min with 5 ng/ml IL-1α (**A**) or 10 ng/ml TNFα (**B**). Cell extracts (20 μg protein) were subjected to SDS/PAGE and immunoblotted with antibodies indicated. (**C**) Same as A, B, except that BMDM from wild type (WT) mice and knock-in (KI) mice expressing the catalytically inactive IKKα[S176A/S180A] mutant were stimulated for 10 min with 1 μg/ml Pam_3CSK_4. The results are representative of at least three independent experiments.

3.2.5 The Met1-Ub chains and their interaction with NEMO are required for the IL-1-stimulated phosphorylation of IKKα and IKKβ.

HOIP is the catalytic subunit of the **L**inear **Ub**iquitin **A**ssembly **C**omplex (LUBAC), the only E3 ligase that generates Met1-linked (also called linear) ubiquitin (Met1-Ub) chains in response to IL-1, at least in MEFs (**Section 1.2.6**, [158]). To investigate the role of Met1-Ub chains in the phosphorylation of IKKα and IKKβ in their activation loops, I studied MEFs from knock-in mice expressing the catalytically inactive HOIP[C879S] mutant. The IL-1-stimulated phosphorylation of IKKβ at Ser177 and Ser181 or IKKα at Ser176 and Ser180 were impaired in MEFs from HOIP[C879S] knock-in mice (**Fig 3.7A**). The phosphorylation of p105 at Ser933, a physiological substrate of

IKKβ, was also decreased (**Fig 3.7A**).

The LUBAC-catalysed Met1-Ub chains associate with NEMO regulatory subunit of the canonical IKK complex (**Section 1.2.6**). To investigate the importance of this interaction in the phosphorylation of IKKβ at Ser177 and/or Ser181, I used MEFs from knock-in mice expressing the polyubiquitin-binding-defective NEMO[D311N] mutant. I found that the IL-1-stimulated phosphorylation of IKKβ at Ser177 or Ser181, or IKKα at Ser176 or Ser180 was significantly reduced (**Fig 3.7B**), similar to the results in MEFs from HOIP[C879S] knock-in mice.

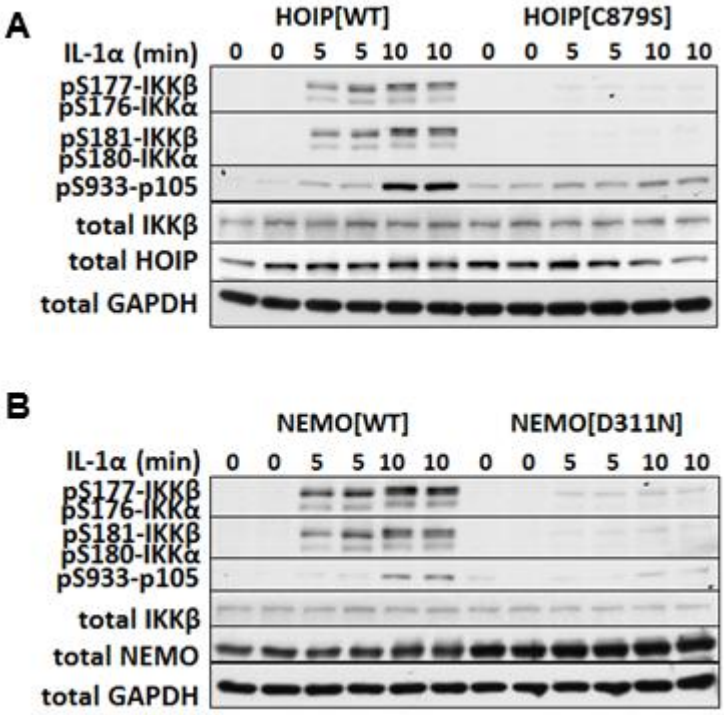

Figure 3.7 Met1-Ub chains and their interaction with NEMO are required for the IL-1-stimulated phosphorylation of IKKα and IKKβ in MEFs. (A) Cells from wild type (HOIP[WT]) or knock-in mice expressing the HOIP[C879S] mutant were stimulated with 5 ng/ml IL-1α for the times indicated. 20 μg cell extract protein was subjected to SDS/PAGE and probed with the antibodies indicated. **(B)** As in A except that the study was performed with MEFs from wild type (NEMO[WT]) or knock-in mice expressing the NEMO[D311N] mutant. The results are representative of at least three independent experiments.

The IL-1-induced phosphorylation of MAP kinases (JNK1/2 and p38α) in MEFs from HOIP[C879S] or NEMO[D311N] knock-in mice was similar to wild type MEFs (**Fig**

3.8), but was prevented by the TAK1 inhibitors NG25 or 5z-7-oxozeaenol (**Fig 3.9**). These control experiments indicate that the activation of TAK1 is not affected in MEFs from HOIP[C879S] or NEMO[D311N] knock-in mice. Furthermore, the TAK1 inhibitor NG25 did not affect the IL-1-stimulated formation of K63-Ub and Met1-Ub chains (**Fig 3.10**). This suggests that TAK1 activity is not required for the formation of poly-ubiquitin chains, and that TAK1 inhibitors do not impair the phosphorylation of IKKβ by blocking the formation of ubiquitin chains. Taken together, these findings indicate that the formation of Met1-Ub chains and their interaction with NEMO is required for TAK1 to phosphorylate IKKα at Ser176 and IKKβ at Ser177.

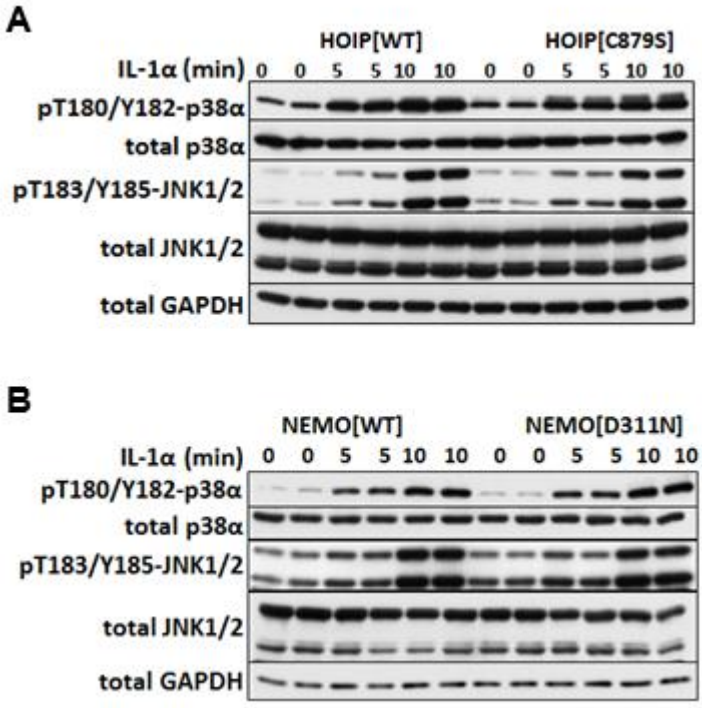

Figure 3.8 Phosphorylation of MAP kinases is not affected in HOIP[C879S] and NEMO[D311N] MEFs. (**A**) MEFs from wild type mice (HOIP[WT]) or knock-in mice expressing the inactive HOIP[C879S] mutant were stimulated with 5 ng/ml IL-1α for the times indicated. 20 µg cell extract protein was subjected to SDS/PAGE, and immunoblotted with the antibodies indicated. (**B**) Same as A except that the experiment was performed with MEFs from wild type (NEMO[WT]) or knock-in mice expressing the NEMO[D311N] mutant.

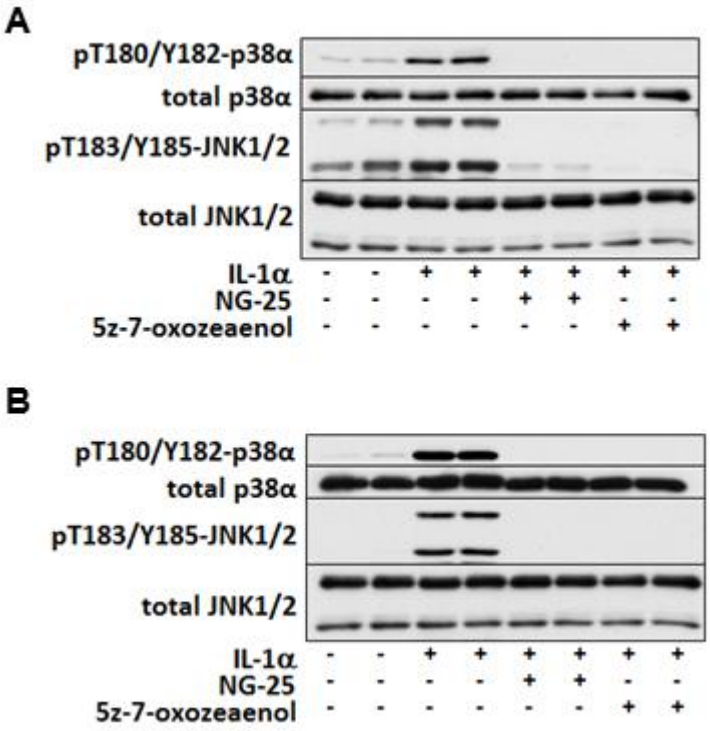

Figure 3.9 Effect of TAK1 inhibitors on the IL-1-stimulated phosphorylation of MAP kinases in HOIP[C879S] and NEMO[D311N] MEFs. (**A**) MEFs from mice expressing the HOIP[C879S] mutant were pre-treated for 1 h without (-) or with (+) the TAK1 inhibitors NG25 (1 μM) or 5z-7-oxozeaenol (1 μM) before stimulation with 5 ng/ml IL-1α for the times indicated. (**B**) Same as A except that MEFs from mice expressing the polyubiquitin-binding-deficient mutant NEMO[D311N] were used. The results are representative of at least three independent experiments.

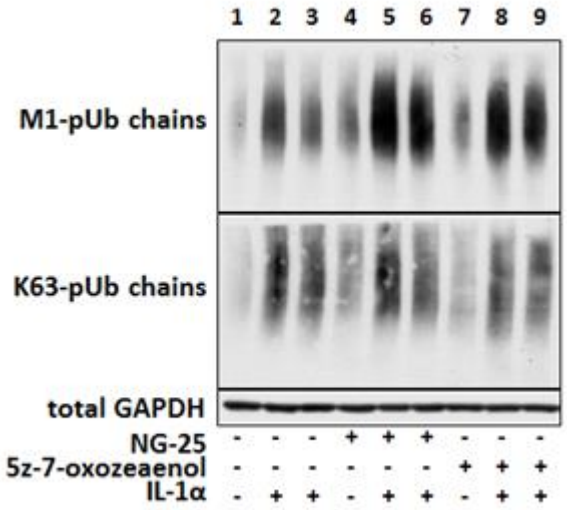

Figure 3.10 Effect of TAK1 inhibitors on the IL-1-stimulated formation of Met1-linked (M1) and Lys63-linked (K63) ubiquitin chains. Wild type MEFs were incubated for 1 h with (+) or without (-) 2 μM NG25 or 1 μM 5z-7-oxozeaenol, and then stimulated for 10 min with 5 ng/ml IL-1α. The Met1-linked and Lys63-linked ubiquitin chains in 2 mg of cell extract protein were captured on Halo-NEMO as described in Materials and Methods (**Section 2.2.3.5**), released by denaturation in SDS and immunoblotted with antibodies that recognise Met1-linked (M1) or

Lys63-linked (K63) ubiquitin chains specifically. The same cell extracts (20 μg protein) were immunoblotted with anti-GAPDH as a loading control.

Finally, it should be noted that although TAK1 complex contributes to the phosphorylation of IKKβ at Ser177 in IKKβ-NEMO complex in IKKα-deficient MEFs (**Fig 3.1**), the active TAK1 is capable of phosphorylating a catalytically inactive mutant of IKKβ at Ser177 as well as Ser181 *in vitro* (**Fig 3.11**), which does not happen in cells. It is therefore possible that the interaction of NEMO with IKKβ and/or the recruitment of the TAK1 complex to K63-Ub chains are factors that prevent TAK1 from phosphorylating Ser181 in cells.

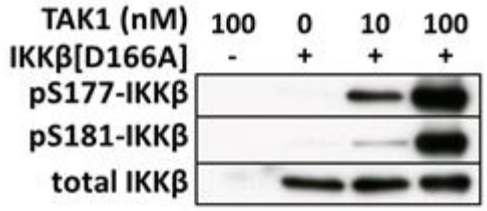

Figure 3.11 TAK1 phosphorylates IKKβ at Ser177 and Ser181 *in vitro*. Catalytically inactive IKKβ[D166A] mutant (0.8 μM) (**Section 2.1.6**) was incubated for 3 min at 30 ^{o}C with the indicated concentrations of the active TAB1-TAK1 fusion protein in 50 mM Tris/HCl pH 7.5, 0.1 mM EGTA, 2 mM dithiothreitol, 10 mM magnesium acetate and 0.1 mM ATP. Reactions were terminated by SDS denaturation. Samples were subjected to SDS/PAGE, transfer to PVDF membranes and immunoblotted with antibodies indicated.

3.3 Discussion

The activation of IKKβ requires the dual phosphorylation on both Ser177 and Ser181 [102,107]. In this Chapter, I clarified the mechanism by which the canonical IKK complex is activated. In particular, I showed that TAK1 catalyses the phosphorylation of IKKβ at Ser177, serving as a priming event which allows auto-phosphorylation at Ser181 by IKKβ itself. This two-step phosphorylation mechanism was demonstrated in IL-1- or TNF-stimulated IKKα-deficient MEFs and in TLR agonist-stimulated BMDM, suggesting that it is of general significance for IKK activation.

The phosphorylation within the activation loop of a protein kinase by two different kinases has been reported before. One example is that MAP kinase kinase 7 (MKK7) and MKK4 synergistically activate JNK by phosphorylating Thr183 and Tyr185 in the activation loop, respectively [204]. The kinase activation contributed by both 'upstream' kinases and auto-phosphorylation has been described previously for other kinases, including the phosphorylase kinase [205] and the NDR (nuclear DBF2-related) kinases [206].

3.3.1 TAK1 functions upstream of IKKβ

TAK1 is a master kinase in the MyD88 signalling pathway, at least in MEFs, where the absence of TAK1 kinase activity impairs the activation of canonical IKK complex as well as its downstream consequences and the activation of p38α and JNK MAP kinases [83,84]. In this Chapter, I have shown that two structurally unrelated TAK1 inhibitors, NG25 [199] and 5z-7-oxozeaenol [148], abolished the phosphorylation of IKKβ at Ser177 and Ser181 induced by IL-1 and TNF in MEFs and Pam_3CSK_4 and LPS in BMDM (**Fig 3.1**), confirming that TAK1 acts upstream of IKKβ in these cells.

3.3.2 The use of IKKβ inhibitor

Incubation of IKKα-deficient MEFs with the IKKβ inhibitor BI605906 caused an apparent enhancement of IKKβ phosphorylation at Ser177 in IL-1-stimulated IKKα KO MEFs (**Fig 3.1**). However, I also found that a Ser177 phospho-specific antibody displayed much better recognition of a synthetic peptide phosphorylated at Ser177 alone than a peptide phosphorylated at both Ser177 and Ser181 (**Fig 3.2A**). These experiments indicate that the phosphorylation of IKKβ at Ser181 impedes the recognition of Ser177 phosphorylation by the antibody. In contrast, the phospho-Ser181 specific antibody recognised Ser181 phosphorylation in the dual

phosphorylated peptide (**Fig 3.2B**). This is because the epitope used to raise the antibody does not include Ser177, which allowed the phosphorylation at Ser181 to be detected in IKKβ mutants where Ser177 was replaced with other amino acids.

Interestingly, Ser177 phosphorylation was elevated in the presence of the IKKβ inhibitor, even in MEFs not stimulated with IL-1 (**Figs 3.1A and B,** top panel, lanes 10). This finding could be explained in several ways. First, the binding of inhibitor to IKKβ may induce a conformational change making Ser177 of IKKβ more accessible to TAK1 or other kinase(s) that phosphorylate Ser177. Second, by blocking IKKβ-mediated basal phosphorylation at Ser181, the inhibitor encourages the de-phosphorylation of this serine residue, thus improving recognition of phospho-Ser177 by the antibody.

In BMDM from mice expressing the catalytically-inactive IKKα[S176A/S180A] mutant, I found that the IKKβ inhibitor abolished agonist-induced phosphorylation of S181, but the recognition of Ser177 phosphorylation by the phosphor-Ser177-specific antibody was slightly reduced (**Figs 3.1C and D**) in contrast to the enhancement seen in IKKα KO MEFs (**Figs 3.1A and B,** top panel, compare lanes 1-3 with 10-12). One possible explanation for this difference is that the catalytically inactive IKKα may inhibit the TAK1-catalysed phosphorylation of IKKβ at Ser177 or accelerate its de-phosphorylation by a phosphatase(s).

The present study established the mechanism of IKKβ activation based on the use of IKKβ-specific inhibitor BI605906 in IKKα-deficient MEFs. In wild type MEFs, however, BI605906 did not suppress the IL-1- or TNF-stimulated phosphorylation of IKKβ at Ser181 (**Fig 3.6**). This is presumably because the phosphorylation of IKKβ at

Ser181 can be catalysed by IKKα through *trans* auto-phosphorylation when the kinase activity of IKKβ is inhibited, and IKKα activity is unaffected by BI605906 [135].

3.3.3 Mutation of IKKβ

Since the phosphorylation of two serine residues in the activation loop is essential for IKK kinase activity, both sites have been mutated to glutamic acid in previous studies to mimic the effect of phosphorylation by introducing a negative charge, or to alanine to prevent activation [102,107]. However, the effect of mutating just one of these sites has never been studied before. Here I showed that the single mutation of Ser177 of IKKβ to Glu allowed IKKβ to auto-phosphorylate at Ser181 which triggered IKK activation in over-expression experiments even in unstimulated cells (**Fig 3.3A**). The canonical IKKs share sequence similarity with the IKK-related kinases, TBK1 and IKKε. Interestingly, the IKK-related kinases possess a glutamic acid residue at position 168 in their activation loops, which is the site equivalent to Ser176/Ser177 of IKKα/β. Ser172, the residue whose phosphorylation is required for its activation, is equivalent to Ser180/Ser181 of IKKα/IKKβ (**Fig 3.12,** [207]). This suggests that the activation of TBK1 and IKKε in TAK1-deficient MEFs occurs by an auto-phosphorylation or *trans* auto-phosphorylation mechanism (Fig 2C in [135]). However, Ser172 could also be phosphorylated by other protein kinases that have not yet been identified.

Figure 3.12 Alignment of the activation loops in the canonical IKKs and IKK-related kinases. Comparison of primary amino acid sequences of the activation loops in IKKα, IKKβ, IKKε and TBK1. The key serine residues in IKKα and IKKβ are highlighted with red asterisks.

The mutation of aspartic acid 166 in IKKβ to alanine on top of the Ser177E mutation abolished the phosphorylation of this IKKβ mutant at Ser181 (**Fig 3.3B**), indicating that IKKβ auto-phosphorylates itself at Ser181. However, it is possible that IL-1 or TNF stimulation may trigger the activation of another kinase(s) in cells phosphorylating IKKβ at Ser181. To investigate this possibility, it would be interesting to examine stimulus-induced Ser181 phosphorylation in IKKα-deficient MEFs expressing either the IKKβ[D166A/S177E] or [S177A] mutants.

The effect of mutating Ser177 of IKKβ reported in this Chapter was studied in IKKα-deficient MEFs in which the endogenous IKKβ is still expressed. To rule out interference from the endogenous IKKβ, the use of MEFs from IKKα/IKKβ double KO mice would have improved this experiment but time did not allow me to establish this cell model.

3.3.4 Role of Met1-Ub chains and NEMO in the activation of IKK complex

The activation of the canonical IKK complex requires not only the dual phosphorylation at two serine residues within its activation loop, but also the formation of both K63- and Met1-linked ubiquitin chains. It has been demonstrated that TRAF6-catalysed K63-Ub chains interact with the TAB2 and TAB3 subunits in the TAK1 complex, leading to conformational changes which induce the auto-activation of TAK1 *in vitro* [76,82,97]. The Met1-Ub chains catalysed by LUBAC [150–153] interact with NEMO [111,145,146], which is critical for the activation of the canonical IKK complex *in vitro* and the activation of NF-κB in cells [145,159]. Most of the IL-1-induced Met1-Ub chains are attached covalently to K63-Ub chains, so that both ubiquitin linkage types are present in the same hybrid polyubiquitin chains [158]. This may permit the co-localisation of TAK1 and the canonical IKK complex so that TAK1 is

able to phosphorylate the IKK complex more efficiently. The catalytically inactive HOIP mutant (HOIP[C879S]) or the knock-down of HOIP/HOIL-1 reduces the phosphorylation of p105, a physiological substrate of the canonical IKK complex (Fig 4 in [158]). Consistently, I found that the IL-1-stimulated dual phosphorylation of IKKα at Ser176/Ser180 and IKKβ at Ser177/Ser181 was suppressed not only in HOIP[C879S] MEFs, in which the Met1-Ub chains cannot be formed, but also in NEMO[D311N] MEFs, in which the Met1-Ub chains are formed but cannot bind to NEMO in the canonical IKK complex (**Fig 3.7**). As a consequence, the subsequent p105 phosphorylation mediated by IKKβ was also reduced. These observations suggest that the formation of Met1-Ub chains and their association with NEMO are required for the TAK1-catalysed phosphorylation of IKKα/IKKβ at Ser176/Ser177.

3.3.5 Downstream of the canonical IKK complex

As discussed in **section 1.2.7.2**, the activation of p38α MAP kinase is regulated by MKK3, MKK4 and MKK6 in the MyD88 signalling pathway. A recent study has shown that the activation of MKK3/6 is mediated through a direct phosphorylation catalysed by Tpl2, a kinase downstream of the IKKβ [183]. In HOIP[C879S] and NEMO[D311N] MEFs, I observed that the IL-1-stimulated phosphorylation of p38α was similar to wild type MEFs (**Fig 3.8**), despite greatly decreased activation of the canonical IKK complex (**Fig 3.7**). Since the IKK-Tpl2-MKK3/MKK6 axis should be blocked, the phosphorylation of p38α might be conducted by MKK4 in the HOIP[C879S] MEFs. It would be interesting to investigate this further by using CRISPR/Cas9 gene-editing technology to generate cells lacking any expression of MKK4 and HOIP.

Chapter 4 Studies on the mechanism by which the TAK1 complex is activated by IL-1

4.1 Introduction

As reported in **Chapter 3**, the activation of the canonical IKK complex requires the TAK1-catalysed phosphorylation at Ser176 on IKKα and Ser177 on IKKβ, respectively. TAK1 is also required for the MyD88-dependent activation of MAP kinases (**Section 1.2.7**). TAK1 is therefore a master kinase of the MyD88 signalling pathway and, for this reason, its mechanism of activation has been studied extensively (**Section 1.2.4.1**). Briefly, there are two TAK1 complexes in cells, which are the TAB1-TAK1-TAB2 complex and the TAB1-TAK1-TAB3 complex, respectively [80]. It is widely accepted that IL-1 stimulation triggers the formation of K63-Ub chains, which bind to TAB2 and TAB3 through the Npl40 zinc finger (NZF) domain at their C termini [82]. This association alters the conformation of TAK1 complex, leading to auto-phosphorylation and auto-activation of TAK1 *in vitro*. However these discoveries were made using cell free assays, but the genetic evidence needed to establish that they really operate in cells is still lacking. If the model is true, the removal of both TAB2 and TAB3 from cells should abolish the activation of TAK1 by IL-1. In this Chapter, I present the results of the experiments that I have carried out to understand the physiological roles of key components in the activation of TAK1, including TAB1, TAB2, TAB3 and TRAF6. These studies have revealed that the mechanism of activation of TAK1 is far more complex than expected.

4.2 Results

4.2.1 Generation and characterization of IL-1R* cells

As a recently developed genetic engineering approach, CRISPR/Cas9 (clustered regularly interspaced short palindromic repeat (CRISPR) associated protein 9 (Cas9)) technology is being applied successfully to knock out target genes in different cell types and in mice [208,209]. In this method, a guide RNA (gRNA), designed to specifically bind to the gene of interest, directs the Cas9 DNA endonuclease to the target site, and makes a double-strand cleavage, which disrupts the target gene. In the MRC Protein Phosphorylation and Ubiquitylation Unit (MRC-PPU), the gene encoding Cas9 has been integrated into HEK293 cell line by the laboratory of Yogesh Kulathu. These HEK293 cells inducibly expressing Flag-tagged Cas9 (HEK293_Cas9) facilitated the generation of knock-out cell lines and have been exploited extensively in the study reported in this Chapter.

The HEK293_Cas9 cell line was unresponsive to IL-1, due to the lack of expression of the IL-1 receptor (**Fig 4.1A**). I therefore transfected HEK293_Cas9 cells with virus carrying the gene encoding the IL-1 receptor (**Section 2.2.1.8.1**). I found that the newly established cell line, named IL-1R*, presented strong signal transduction in response to IL-1 stimulation, which was comparable to the previously described IL-1R cells [49], despite the far lower level of expression of the IL-1 receptor (**Fig 4.1A**). The phosphorylation of p105, JNK1/2 and p38α in the IL-1 signalling pathway were triggered rapidly after stimulation with IL-1, reaching a maximum at 10-30 min, slightly slower than IL-1R cells (**Fig 4.1B**). The compound NG25, a specific inhibitor of the TAK1 kinase [199], completely blocked signal transduction downstream of TAK1 (**Fig 4.1C**). The level of inducibly expressed Cas9 was unaffected after transfection of IL-1 receptor (**Fig 4.1D**). Taken together, IL-1R* cell line resembles IL-1R cells in its response to IL-1

stimulation, and the high level of Cas9 expression maximizes the success of knocking-out genes in this cell line.

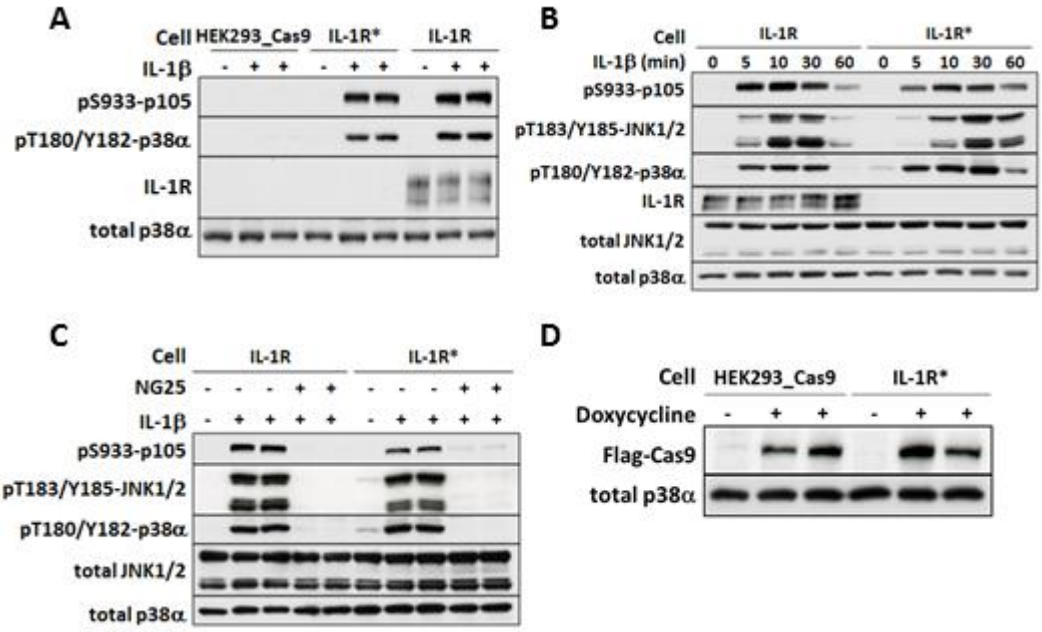

Figure 4.1 Characterization of IL-1R* cells. (A) HEK293_Cas9, IL-1R* and IL-1R cells were stimulated for 10 min with 5 ng/ml IL-1β. Cells were lysed and subjected to SDS/PAGE and immunoblotted with the antibodies indicated. (**B**) IL-1R* and IL-1R were stimulated with 5 ng/ml IL-1β for the times indicated. Cells were lysed and subjected to SDS/PAGE and immunoblotted with the antibodies indicated. (**C**) IL-1R* and IL-1R were incubated for 1 h without (-) or with (+) 5 μM NG25, and then stimulated for 5 min with 5 ng/ml IL-1β. Cells were lysed and subjected to SDS/PAGE and immunoblotted with the antibodies indicated. (**D**) HEK293_Cas9 and IL-1R* cells were incubated for 16 h with 1 μg/ml doxycycline to induce the expression of Flag-tagged Cas9, and cells were lysed, subject to SDS/PAGE and immunoblotted with the antibodies indicated. The results are representative of at least three independent experiments.

4.2.2 Generation and characterization of TAK1-null IL-1R* cells

Most previous studies of TAK1 activation have been performed in mouse embryonic fibroblasts (MEFs) [83,84]. To investigate the importance of the TAK1 catalytic subunit in IL-1R* cells, I knocked out the TAK1 gene using the CRISPR/Cas9 approach described in Materials and Methods (**Section 2.2.1.8.2**). All four clones from the first screen were TAK1 knockout (KO) cells (data not shown). I then studied the effect of TAK1 deletion on IL-1 signalling. Consistent with previous studies in MEFs, IL-1 did not induce the phosphorylation of the activation loops of canonical IKK complex, its substrate p105, and JNK1/2 and p38α/γ MAP kinases (**Fig 4.2A**), indicating that TAK1

expression is crucial for IL-1-induced signalling in the IL-1R* cell line. The signalling was restored by re-expression of wild type TAK1, but not by re-expression of the catalytically inactive TAK1[D175A] mutant in which the Asp of the Asp-Phe-Gly (DFG) motif was mutated to Ala (**Fig 4.2B**). These findings indicate that the kinase activity of TAK1 is essential for IL-1-induced signal transduction in IL-1R* cells. It was noted that the expression of TRAF6, an E3 ligase situated “upstream” of TAK1 in this signalling pathway (**Section 1.2.3**), was not affected in the TAK1 KO IL-1R* cells (**Fig 4.2C**). The formation of Met1-Ub chains was also unimpaired in two different clones TAK1 KO IL-1R* (**Fig 4.2D**), indicating that the IL-1-induced signalling upstream of TAK1 is normal, and that TAK1 expression is not required for LUBAC to catalyse Met1-Ub chain formation.

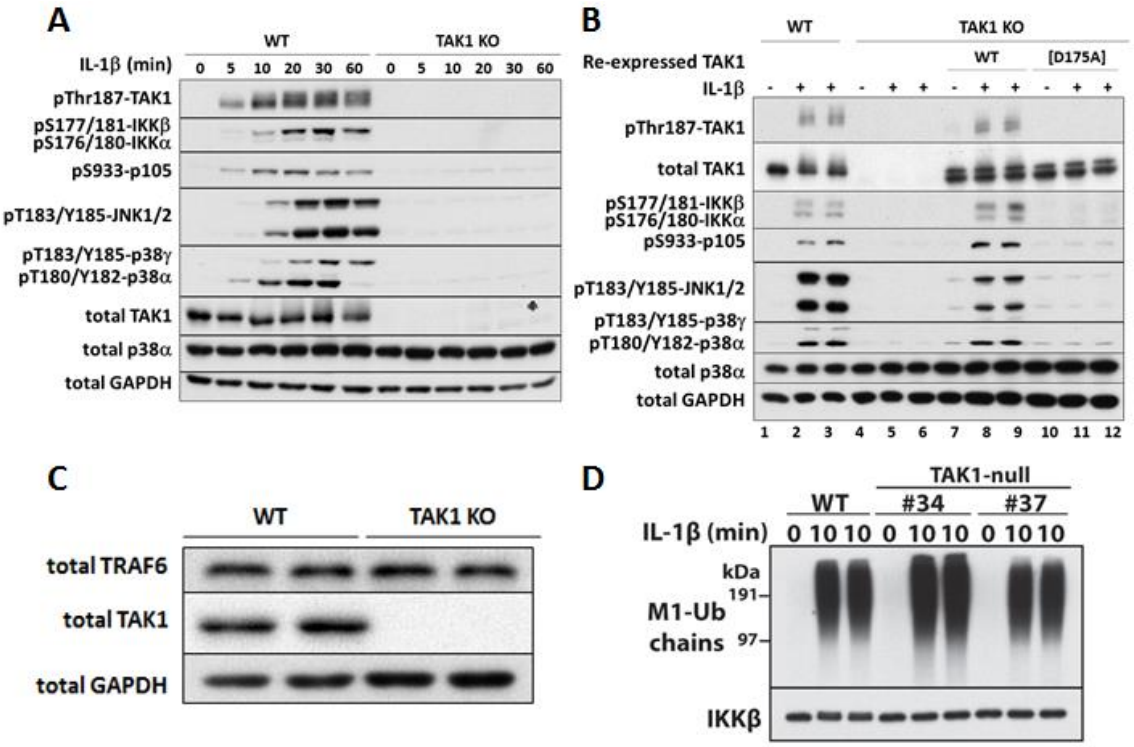

Figure 4.2 The expression and activity of TAK1 is essential for IL-1 signalling in IL-1R* cells. (A) Wild type (WT) and TAK1-knockout clone 34 (TAK1 KO) IL-1R* cells were stimulated for the times indicated with 5 ng/ml IL-1β. Cells were lysed and subjected to SDS/PAGE, followed by transfer to PVDF membranes and immunoblotting with the antibodies indicated. **(B)** TAK1-knockout clone 34 (TAK1 KO) IL-1R* cells re-expressing wild type (WT) TAK1 or the kinase-inactive TAK1[D175A] mutant were incubated for 16 h with 1 μg/ml doxycycline to induce the expression of these proteins (lanes 7-12). These cells, together with wild type (WT) and TAK1-knockout clone 34 (TAK1 KO) IL-1R* cells were stimulated for 10 min with 5 ng/ml IL-1β. Aliquots of the cell extract protein (20 μg Lanes 1-6 or (due to reduced expression of TAK1) 40 μg protein lanes 7-12) were subjected to SDS/PAGE, followed by immunoblotting with the antibodies indicated. **(C)** Wild type (WT) and TAK1-knockout clone 34 (TAK1 KO) IL-1R* cells were lysed and subjected to SDS/PAGE, followed by transfer to PVDF membranes and immunoblotting with the antibodies indicated. **(D)** Wild type (WT) and two clones (34 and 37) of TAK1-knockout (TAK1-null) IL-1R* cells were stimulated for 10 min with 5 ng/ml IL-1β. The Met1-linked ubiquitin chains in 2 mg of cell extract protein were captured on Halo-NEMO as described in Materials and Methods (**Section 2.2.3.5**), released by denaturation in SDS and immunoblotted with the antibody that recognise Met1-linked (M1) chains specifically. The same cell extracts (20 μg protein) were immunoblotted with anti-GAPDH as a loading control. This experiment was carried out by Dr Christoph Emmerich in our laboratory. The results are representative of at least three independent experiments.

4.2.3 The role of TAB1 in the IL-1-stimulated activation of TAK1 in IL-1R* cells

It has been reported that IL-1-dependent TAK1 activation occurs normally in MEFs lacking the expression of TAB1 [94]. To investigate the role of TAB1 in TAK1 activation in the human cell line, I generated TAB1-deficient IL-1R* cells (**Fig 4.3A**). In these cells, I found that the initial IL-1β-induced phosphorylation of IKKα/IKKβ and

p105 was similar to the parental IL-1R* cells despite slightly decreased TAK1 phosphorylation (**Fig 4.3B**). Consistent with these findings, the IL-1β-induced transcription of two NF-κB-dependent immediate early genes IκBα **(Fig 4.4A)** and A20 **(Fig 4.4B)**, and the production of IL-8 mRNA (**Fig 4.4C**) was similar in the TAB1 KO and parental IL-1R* cells for up to 60 min. However, the phosphorylation of TAK1, JNK1/2 and p38α/γ MAP kinases was reduced modestly, especially after prolonged stimulation (**Fig 4.3C**). These observations may explain why IL-8 mRNA production, was similar in TAB1-null and wild type IL-1R* cells up to 1 h, but IL-8 mRNA and IL-8 secretion was reduced at later time points (**Figs 4.4C and D)**. Similar results were obtained with a second clone of TAB1-null IL-1R* that was isolated independently (**Fig 4.5**).

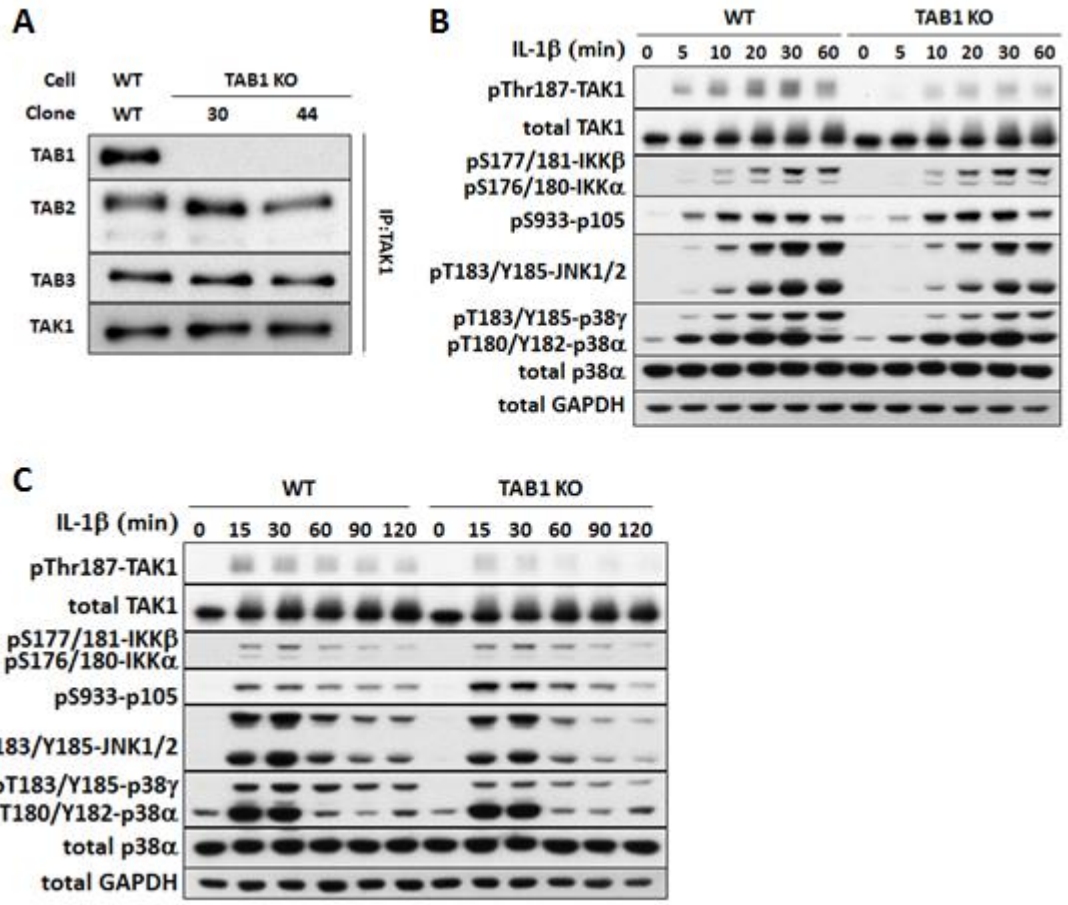

Figure 4.3 IL-1β signalling in IL-1R* cells lacking expression of TAB1. (**A**) Generation of two clones of TAB1 KO IL-1R* cells. TAK1 was immunoprecipitated from the extracts of wild type (WT) IL-1R* cells, two different clones (30 and 44) of cells devoid of TAB1 (**Section 2.2.3.4**). Immunoprecipitates were denatured in SDS, subjected to SDS-PAGE, and immunoblotted with the antibodies indicated. (**B, C**) Wild type (WT) IL-1R* cells and TAB1 KO cells (clone 44) were

stimulated for up to 1 h **(B)** or 2 h **(C)** with 5 ng/ml IL-1β . Aliquots of the cell extracts (20 μg protein) were denatured in SDS, subjected to SDS/PAGE and immunoblotted with the antibodies indicated. The results are representative of at least three independent experiments.

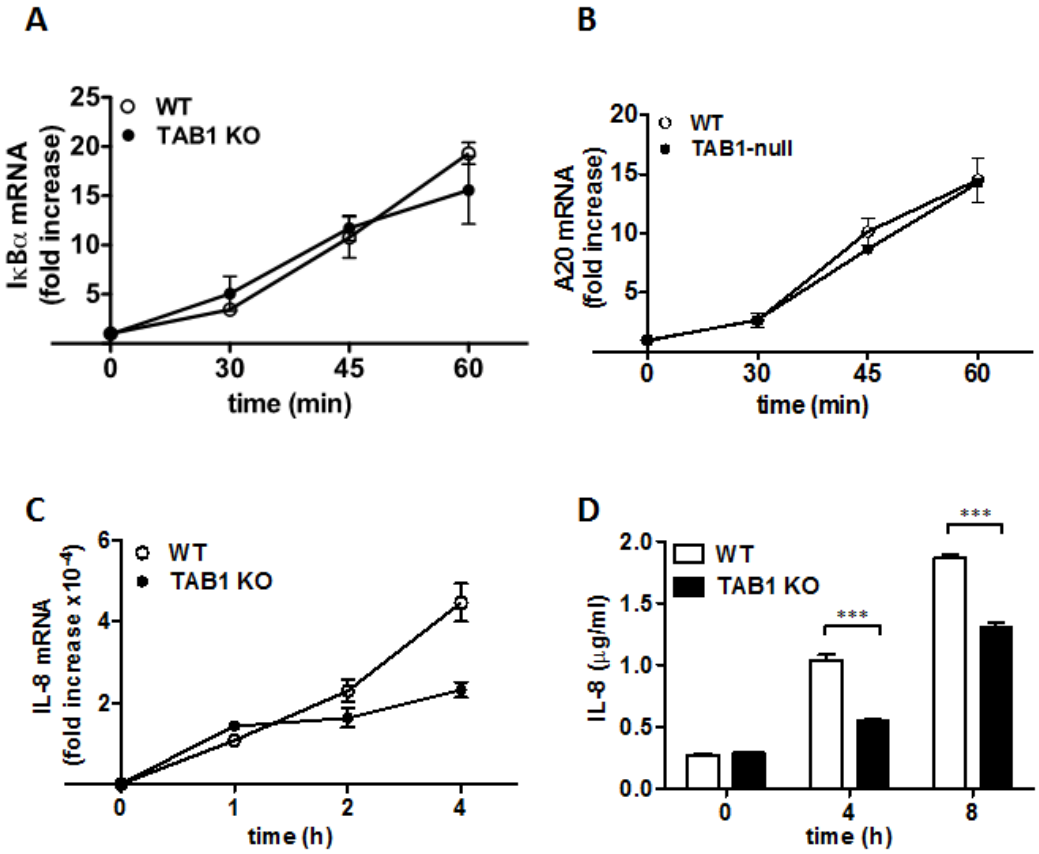

Figure 4.4 IL-1β-dependent gene expression in IL-1R* cells lacking expression of TAB1. (A-C) Cells were stimulated with IL-1β as in Fig 4.3B, and RNA was extracted from wild type (WT) IL-1R* cells and TAB1 KO cells (clone 44 from Fig 4.3A) at the times indicated. The formation of IκBα (**A**), A20 (**B**) and IL-8 (**C**) mRNA was quantitated by qRT-PCR and normalised to the level of 18S RNA (**Section 2.2.2.4**). The ordinate shows the fold-increase relative to the level present in cells not stimulated with IL-1β. **(D)** As in C, except that IL-8 secreted into the culture medium was measured by ELISA (**Section 2.2.3.9**). Data were pooled from two independent experiments. ***$p < 0.001$.

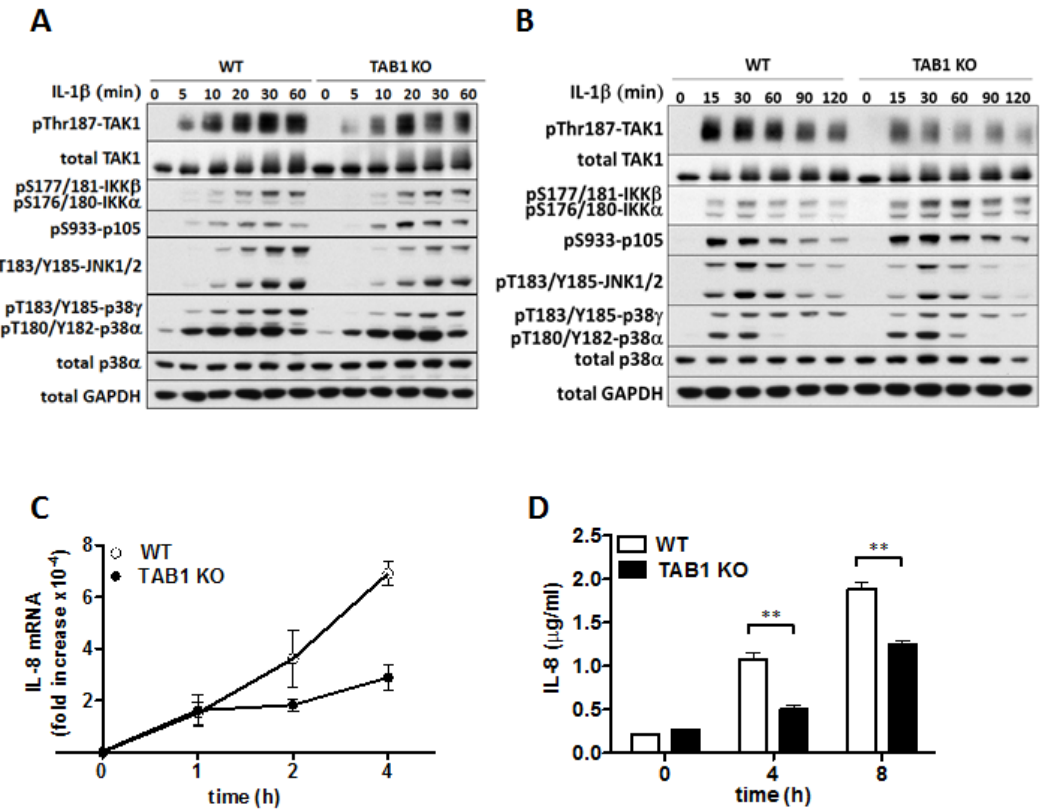

Figure 4.5 IL-1β signalling in a second clone of IL-1R* cells lacking expression of TAB1. (A, B) Same as Fig 4.3B and 4.3C, except that the studies were carried out in TAB1 KO cells clone 30 (from Fig 4.3A). **(C, D)** Same as Fig 4.4C and 4.4D, except that the experiments were carried out in TAB1 KO cells clone 30 (from Fig 4.3A). In panels A and B, the results are representative of at least three independent experiments. In panels C and D, data were pooled from two independent experiments. $^{**}p < 0.01$.

4.2.4 The role of TAB2 and TAB3 in the IL-1-stimulated activation of TAK1 in IL-1R* cells

The IL-1-induced activation of the TAK1 complex is thought to be mediated by the binding of K63-Ub chains to TAB2 and TAB3 (**Section 1.2.4.3**). To investigate this hypothesis I generated IL-1R* cells lacking any expression of TAB2 and TAB3, named "double knock-out" (DKO) cells (**Fig 4.6A,** lane 2 and 3). In these cells, TAK1 and TAB1 remained as a complex whether or not the cells were stimulated with IL-1 for up to 2 hours (**Figs 4.6A and B**). I found that IL-1 induced the phosphorylation of the activation loop of TAK1 in DKO cells, and the subsequent phosphorylation of the canonical IKK complex, its substrate p105, as well as p38α MAP kinase (**Fig 4.6C**). This demonstrates

that IL-1 can activate the TAB1-TAK1 complex by a mechanism that is independent of the binding of TAB2 and TAB3 to ubiquitin chains.

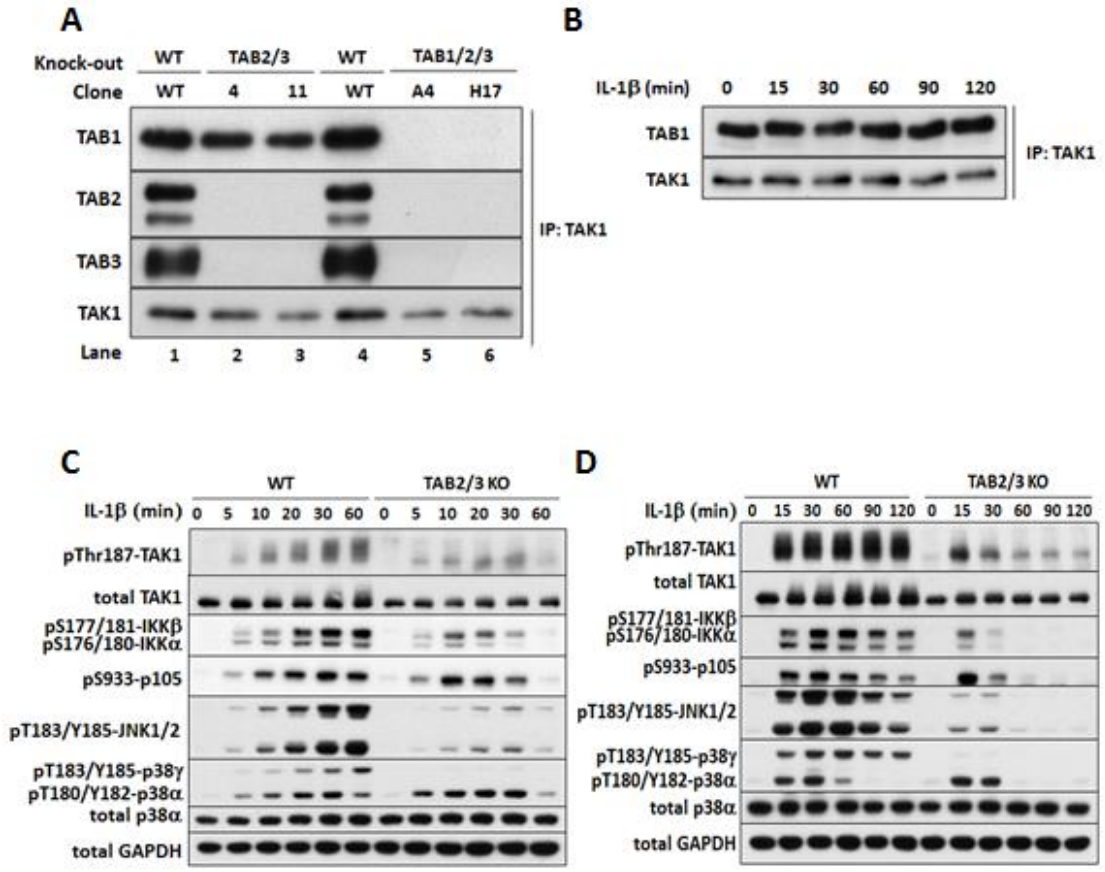

Figure 4.6 IL-1β signalling in IL-1R* cells lacking expression of TAB2 and TAB3. (A) Generation of IL-1R* cells lacking TAB2 and TAB3 or all three TAB subunits. TAK1 was immunoprecipitated from the extracts of wild type (WT) IL-1R* cells (Lane 1), two different clones (4 and 11) of cells devoid of TAB2 and TAB3 (Lanes 2 and 3) and two different clones (A4 and H17) lacking expression of all three TAB components. Immunoprecipitates were denatured in SDS, subjected to SDS-PAGE, and immunoblotted with the antibodies indicated. **(B)** TAB2/3 KO cells (clone 4 from A) were stimulated for the times indicated with 5 ng/ml IL-1β, and TAK1 was immunoprecipitated from the extracts, processed as in A and immunoblotted with the antibodies indicated. **(C, D)** Wild type (WT) IL-1R* cells or TAB2/3 KO cells (clone 4 from A) were stimulated for up to 1 h **(C)** or 2 h **(D)** as in B, and cell extracts (20 μg protein) were subjected to SDS/PAGE and immunoblotted with the antibodies indicated. The results are representative of at least three independent experiments.

Interestingly, the IL-1-dependent phosphorylation of JNK1/2 and p38γ MAP kinases was greatly reduced in the DKO cells **(Fig 4.6C)**. JNK1 and JNK2 are activated by MKK4 and MKK7 (**Section 1.2.7.2**). Therefore, this suggests that TAB2 and/or TAB3 may have a potential role in guiding the TAK1 complex to these substrates. TAB2/3 may also target TAK1 complex to the kinase(s) that activates p38γ MAP kinase.

Surprisingly, and in contrast to wild type IL-1R* cells in which signalling was sustained for up to 2h, the IL-1-dependent phosphorylation of TAK1 and IKKα/IKKβ was transient and had returned to near basal levels by 60 min in DKO cells. Consistently, the IL-1-induced transcription of two immediate early genes, IκBα (**Fig 4.7A**) and A20 (**Fig 4.7B**), was similar in the DKO cells and parental wild type IL-1R* cells for up to 60 min after stimulation, but production of the mRNA (**Fig 4.7C**) and the secretion (**Fig 4.7D**) of IL-8 was reduced drastically in the DKO cells. This might be explained by the transient activation of IKKα/IKKβ and low level of activation of JNK1/2 and p38γ MAP kinases in the DKO cells. Similar results were obtained with a second clone of DKO cells that was isolated independently (**Fig 4.8**).

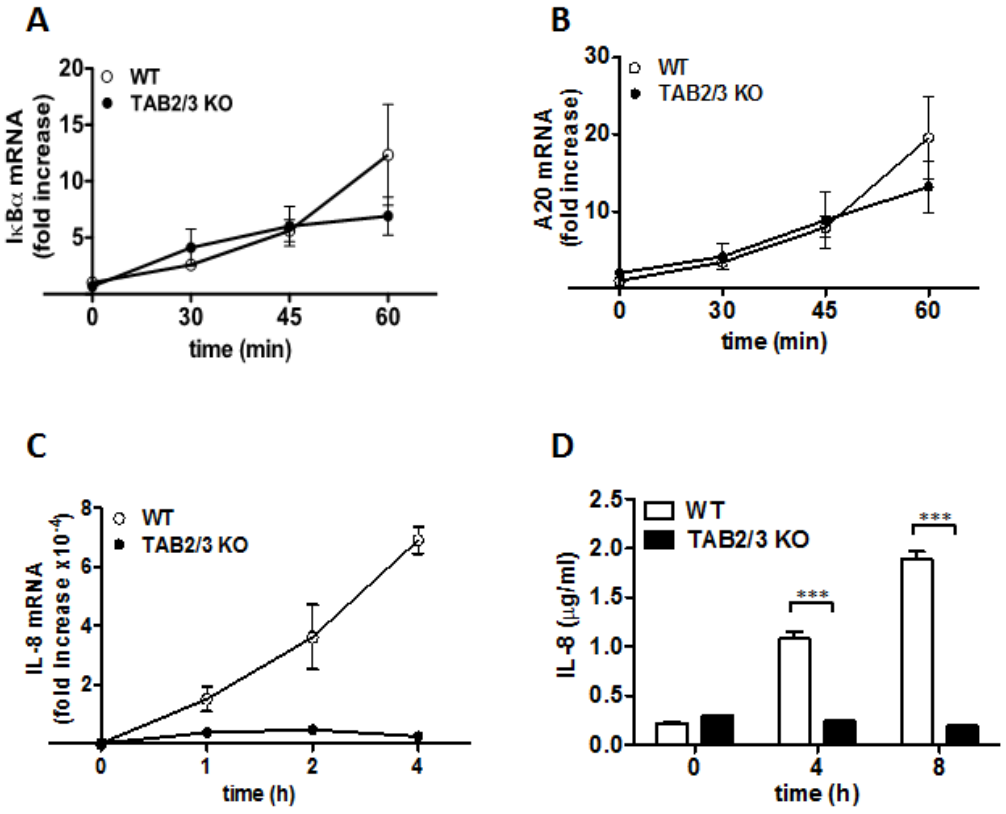

Figure 4.7 IL-1β-dependent gene expression in IL-1R* cells lacking expression of TAB2 and TAB3. (A-C) Cells were stimulated with IL-1β as in Fig 4.6, and RNA was isolated at the times indicated. The formation of mRNA encoding IκBα (**A**), A20 (**B**) and IL-8 (**C**) was quantitated by qRT-PCR and normalised to the level of 18S RNA. The ordinate shows the fold-increase relative to the level present in cells not stimulated with IL-1β. **(D)** As in C, except that IL-8 secreted into the culture medium was measured by ELISA. Data were pooled from two independent experiments. ***$p < 0.001$.

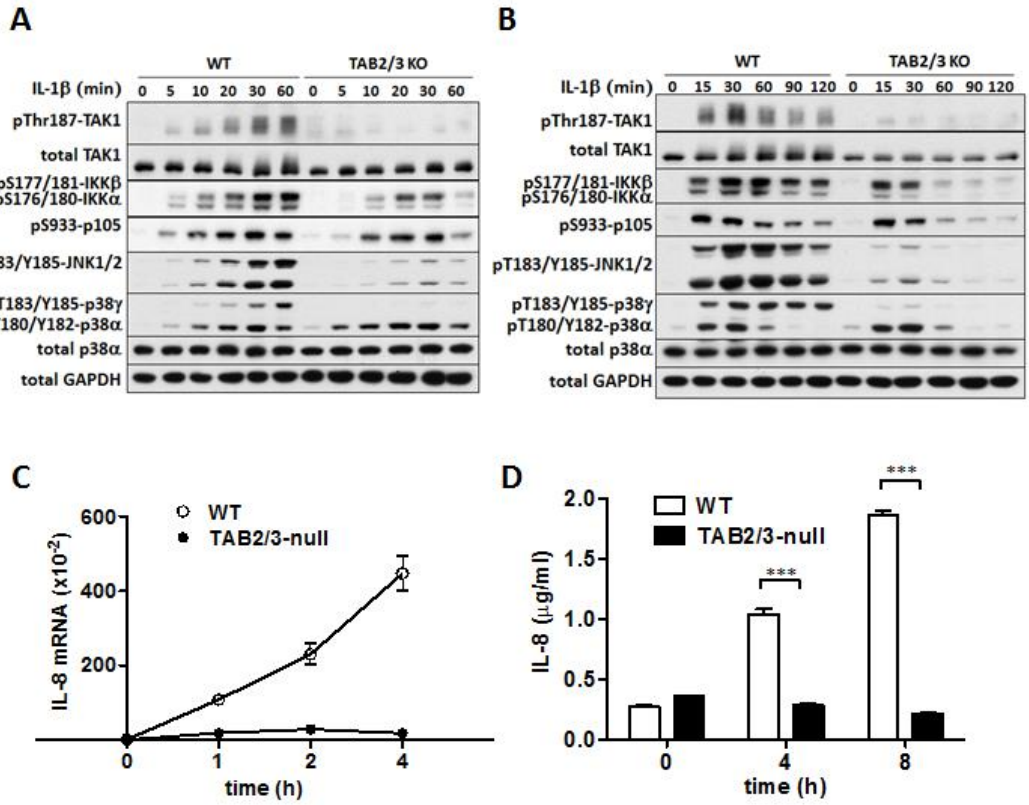

Figure 4.8 IL-1β signalling in a second clone of IL-1R* cells lacking expression of TAB2 and TAB3. (A, B) Same as Fig 4.6C and 4.6D, except that the experiments were carried out in TAB2/3 KO cells clone 11 (from Fig 4.6A). **(C, D)** Same as Fig 4.7C and 4.7D, except that the experiments were carried out in TAB2/3 KO cells clone 11 (from Fig 4.6A). In panels A and B, the results are representative of at least three independent experiments. In panels C and D, data were pooled from two independent experiments. ***$p < 0.001$.

4.2.5 A reconstitution approach to study the role of TABs in the activation of TAK1 by IL-1

To further assess the importance of TABs in the activation of the TAK1 complex, I generated IL-1R* cells lacking expression of all three TAB components, (**Fig 4.6A,** lanes 5 and 6). These triple KO cells showed neither phosphorylation of TAK1 nor activation of its downstream signalling in response to IL-1 (**Fig 4.9A).** As expected, the re-expression of wild-type TAB1 restored the activation of JNK1/2 and p38α MAP kinase (**Fig 4.9B**). These experiments confirm that TAB1 has an essential role in the IL-1-dependent activation of the TAK1 kinase in the absence of TAB2 and TAB3.

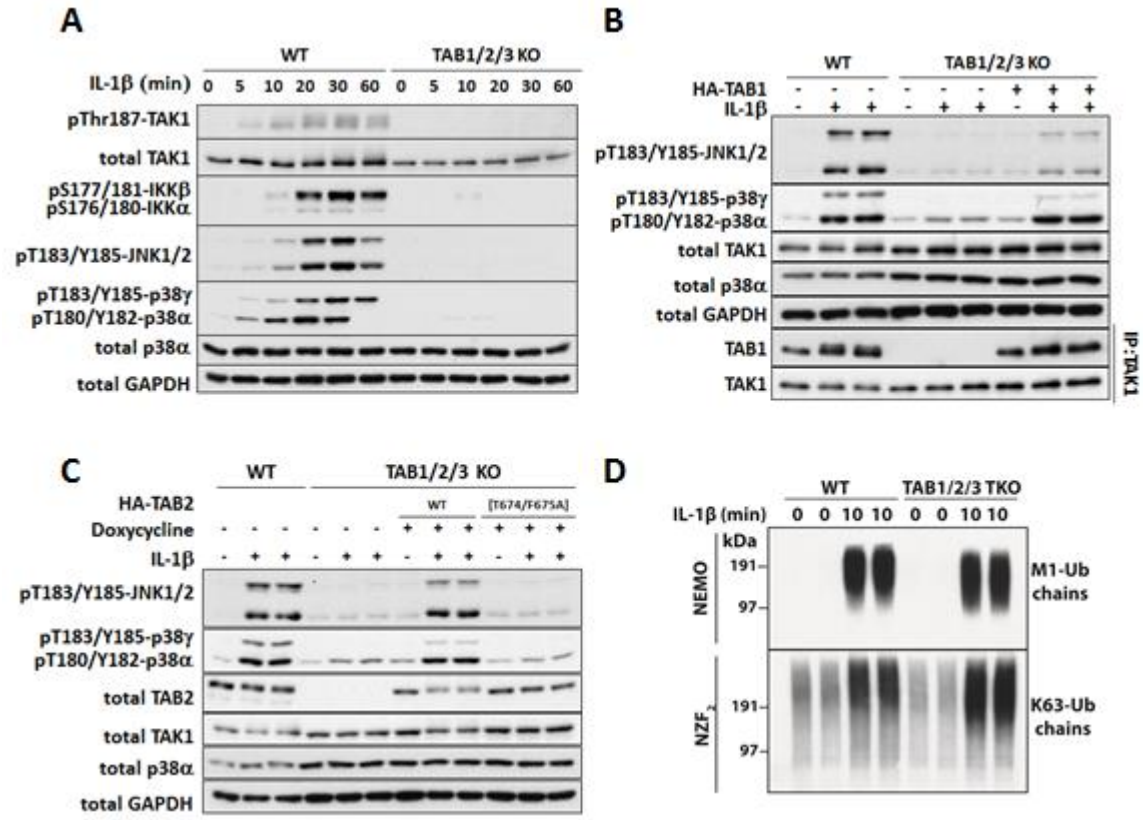

Figure 4.9 IL-1β signalling in IL-1R* cells lacking expression of TAB1, TAB2 and TAB3. (**A**) Absence of IL-1β signalling in TAB1/TAB2/TAB3 triple KO IL-1R* cells. Wild type (WT) or TAB1/2/3 triple KO (clone A4 from Fig 4.6A) IL-1R* cells were stimulated for the times indicated with 5 ng/ml IL-1β. Cell extracts (20 μg protein) were subjected to SDS/PAGE and immunoblotted with the antibodies indicated. **(B)** As in A, except TAB1/TAB2/TAB3 triple KO IL-1R* cells (clone A4 from Fig 4.6A) re-expressing HA-tagged TAB1 were incubated for 16 h with 1 μg/ml doxycycline to induce the expression of these proteins. These cells, wild type IL-1R* cells (WT) and TAB1/2/3 triple KO IL-1R* cells (clone A4 from Fig 4.6A) were stimulated for 10 min with 5 ng/ml IL-1β. Cell extracts (20 μg from wild type IL-1R* cells and (due to reduced expression of TAK1) 40 μg from TAB1/2/3-null cells) were denatured in SDS, subjected to SDS/PAGE and immunoblotted with the antibodies indicated. **(C)** HA-protein tagged TAB2 or the K63-Ub-binding-defective mutant HA-TAB2[T674/F675A] were re-expressed in TAB1/2/3 triple KO IL-1R* cells (clone A4 from Fig 4.6A) after induction for 16 h with 1μg/ml doxycycline. These cells, TAB1/2/3 KO cells not re-transfected with HA-TAB2 and wild type (WT) IL-1R* cells were stimulated for 10 min with 5 ng/ml IL-1β. Cell extracts (20 μg (WT cells) or 40 μg protein (TAB1/2/3 triple KO cells)) were subjected to SDS/PAGE and immunoblotted with the antibodies indicated. **(D)** WT IL-1R* cells or TAB1/2/3 triple KO IL-1R* cells were stimulated for 10 min with 5 ng/ml IL-1β or left unstimulated. The Met1-Ub chains or K63-Ub chains were then captured specifically from 2 mg cell extract protein on Halo-NEMO beads or Halo-NZF_2 beads respectively (**Section 2.2.3.5**), and released by denaturation in SDS and immunoblotted with the antibodies that recognise Met1-linked (M1) or Lys63-linked (K63) ubiquitin chains specifically. This experiment was carried out by Dr Christoph Emmerich in our laboratory. The results are representative of at least three independent experiments.

To investigate the importance of TAB2 in the activation of the TAK1 complex, I re-expressed TAB2 in IL-1R* cells lacking all three TAB components. The phosphorylation of JNK1/2 and p38α was restored by the re-expression of wild type

TAB2, but not by the re-expression of a TAB2 mutant, in which Thr674 and Phe675 in the C-terminal NZF motif were mutated to Ala (**Fig 4.9C**). These two sites are next to the critical Cys673 residue [82,97], therefore unable to interact with K63-Ub chains. Taken together, these experiments indicate that both the expression of TAB2 and its interaction with K63-Ub chains are essential for the IL-1-dependent activation of the TAB2-TAK1 complex in IL-1R* cells lacking expression of TAB1 and TAB3.

Notably, the IL-1-dependent formation of K63-Ub chains or Met1-Ub chains in IL-1R* cells lacking all three TAB subunits was similar to the formation of these ubiquitin chains in IL-1R* cells expressing all three TAB components (**Fig 4.9D**). Together with the findings from TAK1 KO cells, it suggests that the expression and kinase activity of TAK1 are not required for the IL-1-dependent formation of these types of ubiquitin chains.

4.2.6 The role of TRAF6 in the IL-1-induced activation of TAK1 complexes

While my experiments were in progress, Dr Sam Strickson in our laboratory showed that the IL-1-dependent activation of TAK1 was partially restored when E3 ligase-inactive versions of TRAF6 were re-expressed in TRAF6-null IL-1R* cells [210]. Since my experiments indicated that TAK1 was activated by two independent mechanisms involving TAB1 or TAB2/3, I investigated whether the TRAF6 protein and/or its E3 ligase activity were required for both pathways of TAK1 activation.

In order to investigate the role of TRAF6 in the activation of the TAB1-TAK1 complex, I first ablated TRAF6 expression in TAB2/3-null IL-1R* cells (**Fig 4.10A**). As expected, IL-1 signalling downstream of TRAF6 was abolished in these TAB2/TAB3/TRAF6 triple knock-out (TKO) cells stimulated with IL-1 for up to 2 hours (**Fig 4.10B**), but signalling upstream of TRAF6 was not impaired, since IL-1-dependent

phosphorylation of IRAK4 remains the same or increased at least in some clones (**Fig 4.10A).** These findings establish that the expression of TRAF6 is essential for the IL-1-dependent activation of the TAB1-TAK1 complex.

Next, the wild type TRAF6 and two E3 ligase-inactive mutants were re-introduced into TAB2/TAB3/TRAF6 TKO IL-1R* cells (**Fig 4.10C**). The TRAF6[L74H] mutation fails to interact with the E2 conjugating enzyme Ubc13, but its RING domain is able to coordinate zinc ions [75], while the TRAF6[C70A] mutation destroys the RING structure (**Section 1.2.3**) and is therefore unable to coordinate zinc ions [69,211]. Interestingly, the re-expression of wild type TRAF6 could restore IL-1 signalling to the TKO cells but E3 ligase-inactive TRAF6 mutants did not (**Fig 4.10C**). Similar results were obtained with a second clone of TKO cells that was isolated independently **(Fig 4.10D)**. The expression of TRAF6, as well as its E3 ligase activity, are therefore essential for the activation of the TAB1-TAK1 complex in TAB2/3 DKO IL-1R* cells.

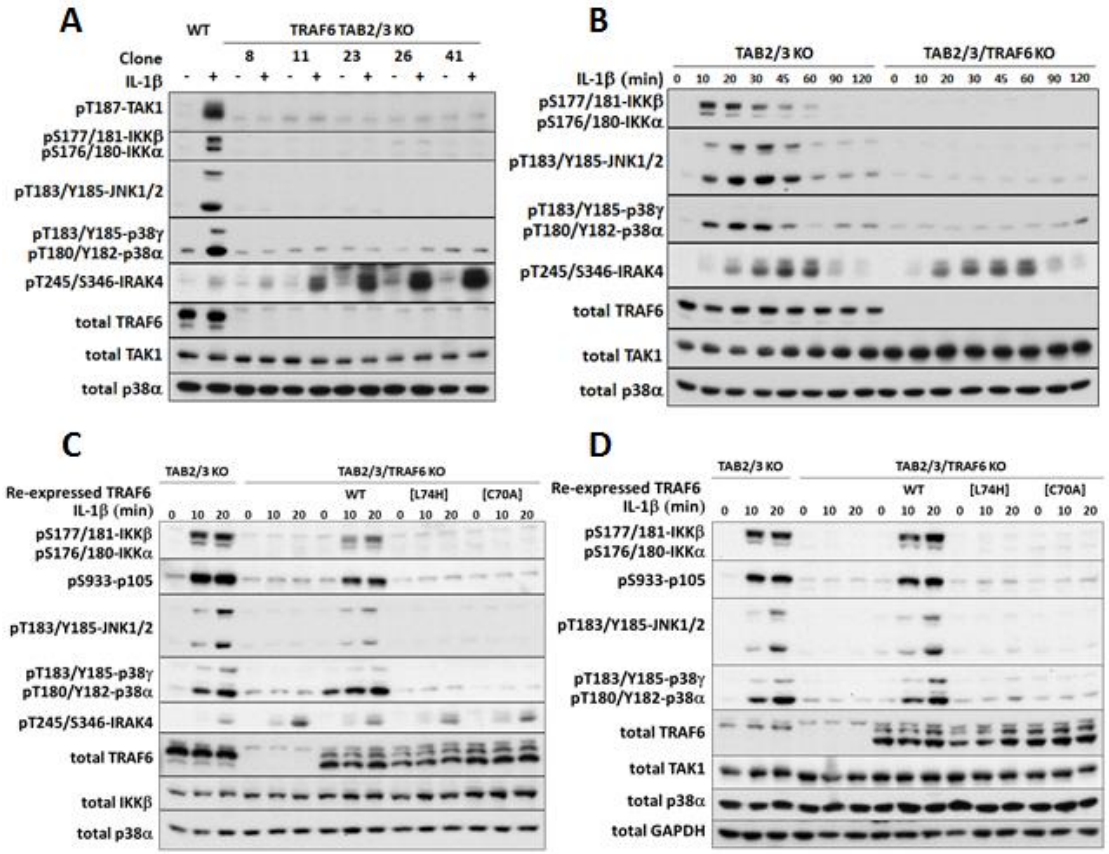

Figure 4.10 TRAF6 E3 ligase activity is required for the IL-1β-dependent activation of the TAB1-TAK1 complex in IL-1R* cells lacking expression of TAB2 and TAB3. (A) Wild type (WT) and five clones of TAB2/TAB3/TRAF6 triple KO cells (clone 8, 11, 23, 26, 41) were stimulated for 10 min with 5 ng/ml IL-1β , then subjected to SDS/PAGE and immunoblotted with the antibodies indicated. **(B)** TAB2/3 DKO (clone 4 from Fig 4.6A) and TAB2/TAB3/TRAF6 triple KO IL-1R* (clone 11 from A) were stimulated for the times indicated with 5 ng/ml IL-1β. Other details are as A. **(C)** Wild type (WT) TRAF6, two E3-ligase-inactive mutants of TRAF6, TRAF6[L74H] and TRAF6[C70A], were re-expressed in the TAB2/TAB3/TRAF6 triple KO IL-1R* (clone 11 from A) after induction for 16h with 1 μg/ml doxycycline. These cells, together with TAB2/3 DKO cells (clone 4 from Fig 4.6A) and TAB2/TAB3/TRAF6 triple KO cells (clone 11 from A) not re-transfected with TRAF6, were stimulated with 5 ng/ml IL-1β for the times indicated. Other details are as in A. **(D)** Same as C, except that experiments were carried out using a second clone (clone 41 from A) of TAB2/TAB3/TRAF6 triple KO IL-1R* cells. The results are representative of at least three independent experiments.

To assess the importance of TRAF6 in the activation of the TAB2-TAK1 and TAB3-TAK1 complexes, I also knocked out the TRAF6 gene in TAB1 KO IL-1R* cells **(Fig 4.11A)**. Consistent with previous studies, the deletion of TRAF6 abolished IL-1 signalling downstream of TRAF6 **(Fig 4.11A**). The E3 ligase inactive TRAF6[L74H] mutant and TRAF6[120-522], a truncated version of TRAF6 which lacks the N-terminal region containing the catalytic RING domain (**Section 1.2.3**), partially restored IL-1 signalling to TAB1/TRAF6 DKO cells (**Fig 4.11B**). Taken together, these experiments

show that, in contrast to the TAB1-TAK1 complex, the activation of the TAB2-TAK1 and TAB3-TAK1 complexes present in the TAB1 KO cells requires the expression but not the ligase activity of TRAF6.

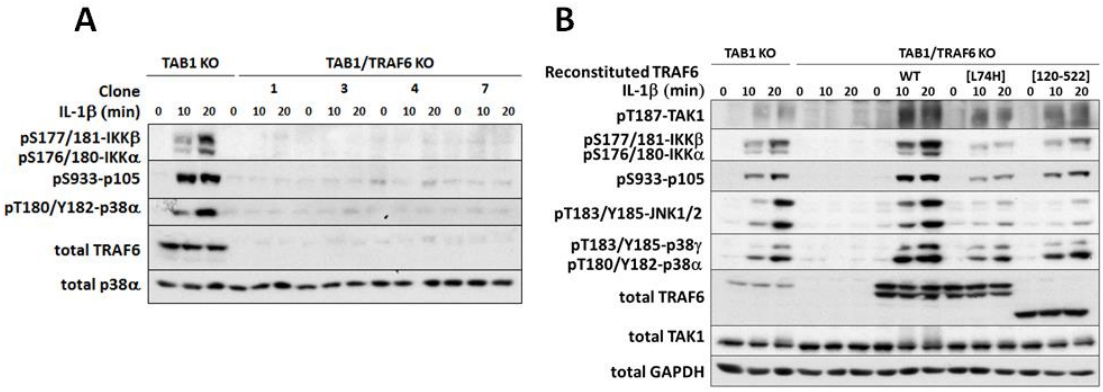

Figure 4.11 TRAF6 E3 ligase activity is not required for the IL-1β-dependent activation of the TAB2/3-TAK1 complex in IL-1R* cells lacking expression of TAB1. (A) TAB1 KO cells (clone 44 from Fig 4.3A) and four clones of TAB1/TRAF6 double KO IL-1R* cells (clone 1, 3, 4, 7) were stimulated with 5 ng/ml IL-1β for the times indicated. Cell extracts (20 μg protein) were subjected to SDS/PAGE and immunoblotted with the antibodies indicated. **(B)** Wild type (WT) TRAF6, the E3-ligase-inactive TRAF6[L74H] mutant and the TRAF6[120-522] mutant lacking the RING domain, were stably re-expressed in TAB1/TRAF6 double KO cells (clone 1 from A). These cells, together with TAB1 KO cells (clone 44 from Fig 4.3A) and TAB1/TRAF6 double KO cells not re-transfected with TRAF6 (clone 1 from A), were stimulated with 5 ng/ml IL-1β for the times indicated. Other details are as in C. The results are representative of at least three independent experiments.

4.2.7 The XIAP, cIAP1 and cIAP2 E3 ligases are not required for the IL-1-induced activation of TAB1-TAK1 complex

A major unresolved question concerned the mechanism by which the TAB1-TAK1 complex became phosphorylated at Thr187 and activated in response to IL-1. The N-terminal region of TAB1 has been shown to interact with X-linked Inhibitor of Apoptosis Protein (XIAP), which inspired a hypothesis that the dimerization of XIAP may induce the dimerization of the TAB1-TAK1 complex, leading to its trans-autophosphorylation and activation [212]. However, I did not observe any association between the endogenous XIAP and endogenous TAK1 in IL-1- stimulated wild-type or TAB2/3 DKO IL-1R* cells (**Fig 4.12A**). Moreover, I found that IL-1-signalling in the TAB2/3/XIAP triple KO cells that I made was enhanced (**Fig 4.12B**). Incubation of the

cells with SMAC (second mitochondrion-derived activator of caspase) mimetic, which results in the degradation of two other members of the IAP family, namely cIAP1 (cellular inhibitor of apoptosis protein 1) and cIAP2 [213], also did not impair IL-1 signalling in TAB2/TAB3/XIAP KO IL-1R* cells (**Fig 4.12C**). These experiments indicate that XIAP and cIAP1/2 are not essential for TAB1-TAK1 complex activation in the TAB2/3-deficient IL-1R* cells.

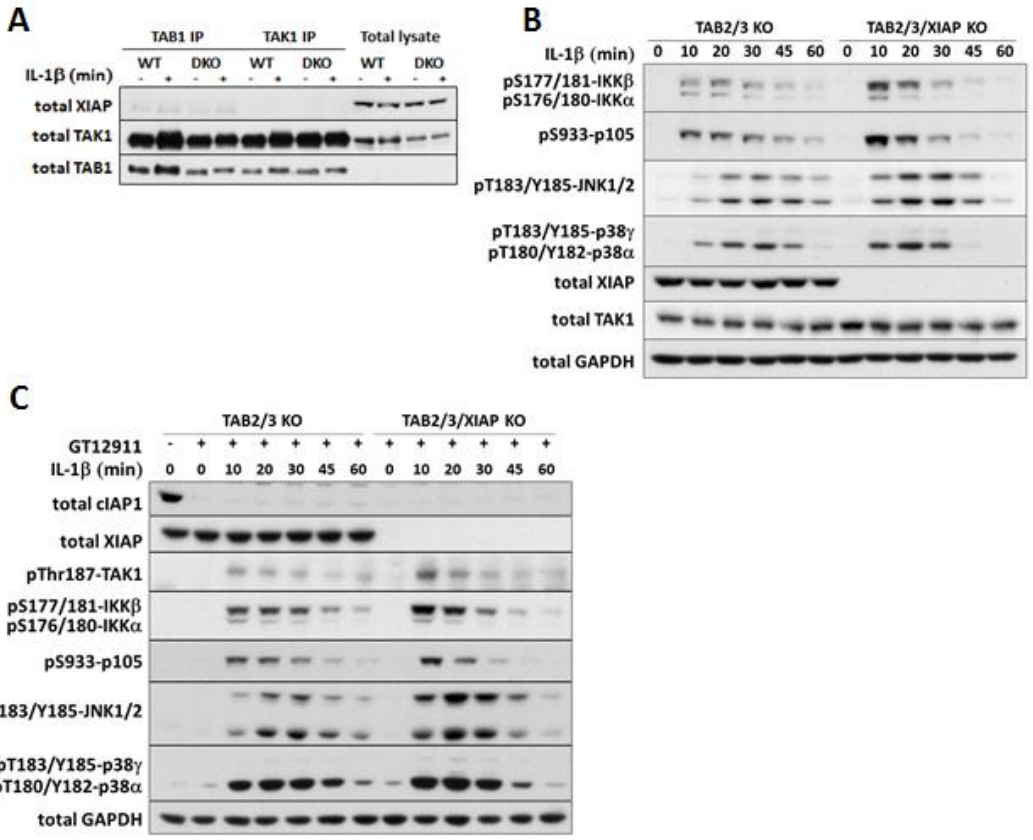

Figure 4.12 XIAP and cIAP1/2 are not required for the activation of the TAB1-TAK1 complex in IL-1R* cells lacking expression of TAB2 and TAB3. (A) IL-1R* and TAB2/3 DKO IL-1R* cells (clone 4 from Fig 4.6A) were stimulated for 10 min with 5 ng/ml IL-1β. The cell extract protein (100 μg) was incubated with the antibodies recognising TAB1 or TAK1 for 1 hour at 4 °C, followed by addition of Protein G Sepharose beads. The immunoprecipitates were denatured in SDS, subjected to SDS/PAGE, followed by transfer to PVDF membranes and immunoblotting with the antibodies indicated. **(B, C)** TAB2/3 DKO IL-1R*cells (clone 4 from Fig 4.6A) and TAB2/TAB3/XIAP triple KO (clone 9) cells were incubated for 1 h without **(B)** or with **(C)** SMAC mimetic GT12911 (100nM), and then stimulated for the times indicated with 5 ng/ml IL-1β. The cell extract protein (20 μg) was subjected to SDS/PAGE, followed by transfer to PVDF membranes and immunoblotting with the antibodies indicated.

4.2.8 The role of MAP4K family members in the IL-1-induced activation of TAB1-TAK1 complex

As TAK1 is a MAP3 kinase (**Section 1.2.4**), it is possible that the activation of TAK1 might be mediated by phosphorylation catalysed by another protein kinase, such as a MAP4 kinase. To investigate this possibility, I expressed and purified wild type TAK1 catalytic subunit from TAB1/2/3-null cells (**Section 2.2.3.3, Fig 4.13A**) in order to eliminate the influence of these binding partners. The TAK1 protein was then incubated with each of four MAP4K(s), namely MAP4K1, MAP4K2 (germinal centre kinase, GCK), MAP4K3 (GCK-like kinase, GLK) and MAP4K5 (GCK-related kinase, GCKR) (**Section 2.1.6**) to see if any of these enzymes was able to phosphorylate Thr187 in the activation loop of TAK1. I found that MAP4K2 and, to a lesser extent, MAP4K3 and MAP4K5 was able to phosphorylate wild type TAK1 at Thr187, whereas MAP4K1 could not (**Fig 4.13C**). To exclude the possibility that interaction with MAP4Ks stimulates TAK1 auto-phosphorylation, I purified the catalytically inactive TAK1 [D175A] mutant (**Fig 4.13B**). Again MAP4K2 was the only kinase that phosphorylated the TAK1 [D175A] mutant robustly (**Fig 4.13D**). These experiments suggest that MAP4K2 can directly phosphorylate the activation loop residue Thr187 of TAK1 *in vitro*.

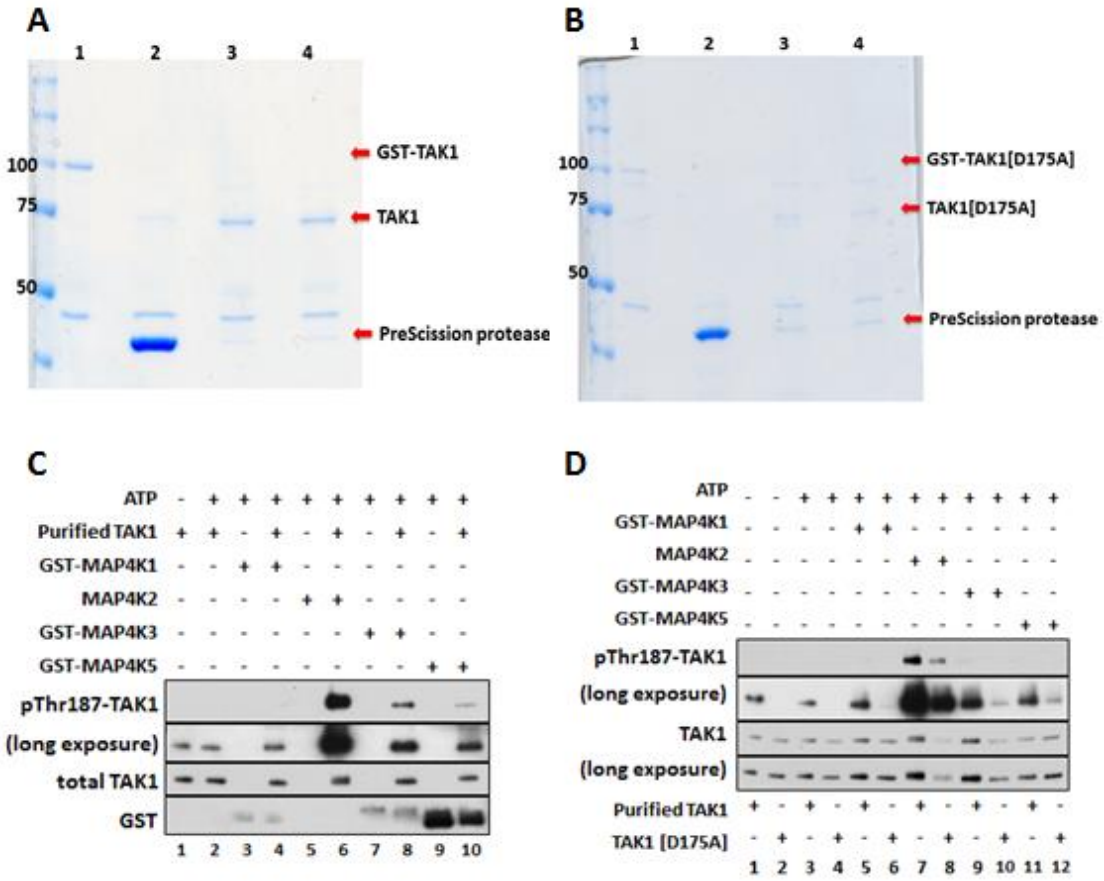

Figure 4.13 MAP4K2 phosphorylates TAK1 *in vitro.* (A, B) The GST-tagged wild type TAK1 **(A)** and catalytically inactive TAK1[D175A] mutant **(B)** were expressed in the TAB1/2/3-null cells (clone A4 from Fig 4.6A) and purified by affinity chromatography on GSH Sepharose (lane 1). After cleavage with PreScission protease that cleave GST from GST-tagged TAK1 (lane 2), the TAK1 protein was released (lane 3 and 4). Proteins were separated via SDS/PAGE and stained with Instant Blue. **(C, D)** MAP4K family members phosphorylate wildtype TAK1 and catalytically inactive TAK1[D175A] *in vitro*. 1 μM purified wildtype TAK1 (**C**) or the catalytically inactive TAK1 [D175A] mutant (**D**) were incubated for 1 h with Mg-ATP and 0.1 U MAP4Ks at 30 °C. The reactions were terminated by denaturation in SDS, and aliquots were subjected to SDS/PAGE, followed by transfer to PVDF membranes and immunoblotting with the antibodies indicated.

4.2.9 Identification of novel IL-1-stimulated phosphorylation sites in TAB1 and TAK1 in TAB2/3-null IL-1R* cells

It is also possible that in the absence of TAB2 and TAB3, IL-1-stimulation might lead to phosphorylation of one or more sites in the TAB1-TAK1 complex, which triggers the activation of this complex. To study this possibility, I used mass spectrometry to identify the amino acid residues in TAK1 and TAB1 that became phosphorylated in TAB2/TAB3 KO cells only upon IL-1 stimulation. Since TAK1 is subject to a feedback control mechanism in which p38α and ERK1/2 MAP kinases phosphorylate TAB1 at

Ser423, Thr431 and Ser438 [180], I incubated the TAB2/3 DKO IL-1R* cells with BIRB0796 (an inhibitor of all forms of p38 MAPK at the concentration used) and PD 0325901 (a potent MEK1/2 inhibitor that suppresses the phosphorylation of ERK1/2), and then stimulated the cells with IL-1 (**Fig 4.14A**). The TAB1-TAK1 complex was then immunoprecipitated and separated on SDS-PAGE gel (**Fig 4.14B**). The peptides identified by MS covered 80% of the sequence of TAK1 and 84% of the sequence of TAB1 (data not shown). Two novel IL-1-dependent phosphorylation sites (Ser417 and Thr476) on TAK1 and one (Ser469) on TAB1 were discovered (**Table 4.1**).

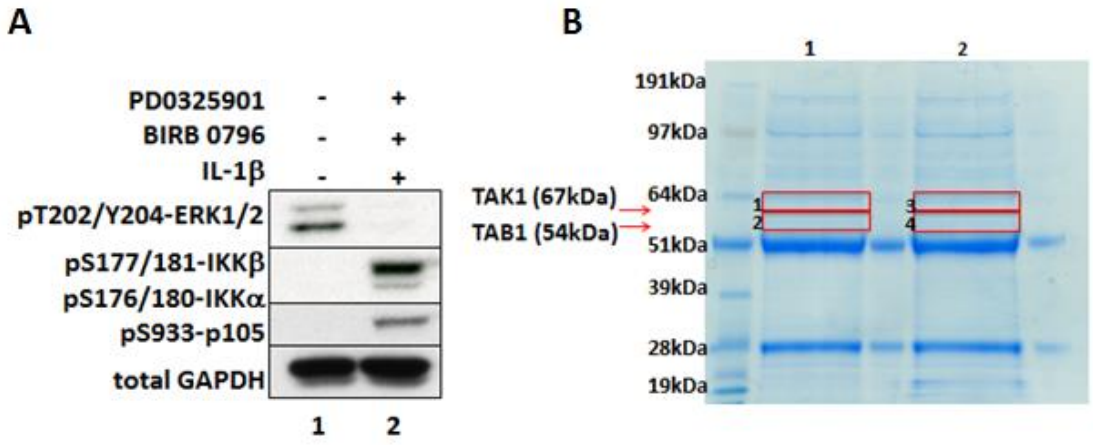

Figure 4.14 Identification of novel sites phosphorylated on TAB1-TAK1 complex using mass spectrometry. (A) TAB2/3 DKO IL-1R* cells (clone 4 from Fig 4.6A) were incubated for I h without (-) or with (+) 1 μM BIRB0796 and 0.1 μM PD0325901, and then left unstimulated (lane 1) or stimulated (lane 2) for 10 min with 5 ng/ml IL-1β. Cell extract (20 μg protein) was subjected to SDS/PAGE and immunoblotted with the antibodies indicated. **(B)** Same as A, except that 10 mg of cell extract protein from unstimulated (lane 1) and stimulated (lane 2) cells were incubated for 1 h with 10 μg of TAK1 antibody (S828A). 50 μl slurry of Protein G-Sepharose was added and incubated for 30 min at 4 ^{o}C. The Sepharose was then collected and washed thoroughly. The bound proteins were released by denaturation in SDS, subjected to SDS/PAGE and the bands located at the same position as TAK1 and TAB1 were excised, washed and digested with trypsin overnight. The dried peptide was delivered to the MS facility for analysis (**Section 2.2.4**).

Table 4.1 Summary of phospho-sites identified by mass spectrometry. Summary of phospho-sites identified on TAK1 and TAB1 in the TAB2/3 DKO cells (clone 4 from Fig 4.6A) in response to IL-1 stimulation. The novel phosphosites were highlighted in bold and in red.

TAK1	
Prior to stimulation	S367, S375, S389, S439, S454, S455
After stimulation	T187, S367, S375, S389, **S417**, S439, S454, S455, **T476**
TAB1	
Prior to stimulation	S7, S378
After stimulation	S7, S378, **S469**

4.3 Discussion

The project presented in this Chapter was initiated because the widely accepted model that the IL-1-induced activation of the TAK1 complex depended on the

association between its regulatory subunits TAB2/3 and K63-Ub chains, lacked genetic evidence. Such studies were critical to verify if the hypothesis implicit in the model really operated in cells. The unanticipated findings presented in this Chapter have shown that concerns about the model were justified and suggested that the signalling network is more complex than considered previously. In the following sections I discuss the implication of my discoveries for future studies that will be aimed at the complete elucidation of the IL-1 signalling network.

4.3.1 Application of CRISPR/Cas9 gene editing technology

The newly developed genetic engineering approach CRISPR/Cas9 technology was utilized throughout the current study. This new powerful approach makes it possible to ablate target genes much more efficiently than traditional approaches, and allowed me to generate many stable knock-out cell lines within a relatively short period of time.

At the beginning of this project, I employed the originally described CRISPR/Cas9 method to disrupt genes encoding TAB1, TAB2 and TAB3 (**Section 2.2.1.8.2**). The gene encoding Flag-tagged Cas9 endonuclease was integrated into the genome, and its expression was induced by doxycycline (**Section 4.2.1**). The stable expression of the 160 kDa Cas9 endonuclease and the straightforward transfection of one single gRNA-containing plasmid maximizes the efficiency of gene knock-out [214]. Later, I exploited an improved approach in which the Cas9[D10A] nickase mutant is utilized (**Section 2.2.1.8.2,** [198]). This mutant is directed by a pair of gRNAs to the target sites separated by an appropriate distance, and cleaves only one strand of the DNA complementary to the gRNA, forming two individual nicks. The use of paired gRNAs extends the number of specifically recognised bases for target cleavage,

thereby providing higher specificity for gene disruption [215]. If the disruption is not accomplished, the individual nick on each strand is repaired by the high-fidelity base excision repair pathway, thereby largely reducing the undesired off-target mutagenesis on double-stranded breaks (DSBs) [215,216]. The puromycin-resistance gene in the gRNA plasmid allows for the selection of transfected cells, which enhances the knock-out efficiency.

Although the CRISPR/Cas9 technology performs well in knocking out genes with high specificity and efficiency, there are at least three major issues that require particular attention. First, the gRNA is normally designed to target the first shared exon among the transcripts of genes of interest, but the destruction of the starting exon may be insufficient to create a knockout clone. Sometimes the remaining gene sequence can still be transcribed and translated, leading to the synthesis of a truncated version of the protein which may possess biological functions. Indeed, I found that this occurred during the generation of TAB2-deficient clones, in which the truncated TAB2 could be recognised by immunoblotting (data not shown). I therefore re-designed the gRNA and the new knock-out clones generated were examined by using two antibodies raised against epitopes that are far apart in the primary sequence of TAB2. Today, starting with a set of at least two gRNAs has become standard practice in the MRC-PPU in the application of CRISPR/Cas9 technology.

Second, FACS (flow-cytometry associated cell sorting) results showed that the expression level of the IL-1 receptor can vary in different knock-out clones (data not shown). Such variation makes the signal strength inconsistent, rendering data interpretation more difficult. To minimize this problem, I therefore carried out all experiments using at least two knock-out clones generated independently (**Figs 4.3-**

4.11), and kept scrutinising a read-out of the pathway located upstream of the protein of interest (e.g. the phosphorylation of IRAK4 as a readout of Myddosome formation (**Fig 4.10**)), to check that disruption of the pathway had not resulted from the loss of the IL-1R or another essential upstream element.

Third, some proteins are essential for cell life and the removal of their genes may not be achievable. For example, despite many attempts, I failed to completely knock-out the E2 conjugating enzymes Ubc13 and UbcH7. It is possible that this issue could be addressed in the future by making the conditional knock-out cells or cells where the target gene might be inducibly degraded. Thus, for example, it might be possible to combine CRISPR/Cas9 technology with the Flp/FRT and Cre/LoxP system to build an inducible knockout cell line [217], or use a modified von Hippel-Lindau (VHL) protein-dependent degradation system to direct specific endogenous target proteins for proteolysis [218].

CRISPR/Cas9 technology has the potential to edit multiple genes simultaneously, which may further speed up the generation of desired cell models. Recently, my laboratory, as well as other research groups, has demonstrated that the CRISPR/Cas9 approach can be used to make knock-in cell lines. A recent exciting study has shown that CRISPR/Cas9 technology can be used to achieve robust DNA knock-in even in non-dividing cells [219]. The generation of knock-in cell lines opens up the possibility of making selective mutations in essential genes to identify their functions without having to disrupt them completely. Biochemical studies and structural analysis carried out over the past decades has provided some understanding of the critical sites on many of the key proteins that participate in the innate immune signalling network. Many theories have been built up based on these *in vitro* experiments, which can now

be tested stringently using CRISPR/Cas9 technology to generate these mutations in cells and *in vivo*.

4.3.2 The role of TAB2 and TAB3 in regulating the phosphorylation of JNK1/2 and p38 MAP kinases

In the present study, I found that phosphorylation within the activation loops of TAK1, the canonical IKK complex and p38α MAP kinase occurred robustly in TAB2/3 DKO cells for the first 30 min after IL-1 stimulation (**Figs 4.6 and 4.8**), but the phosphorylation of JNK1/2 was greatly impaired and the phosphorylation of p38γ vanished in the TAB2/3 DKO cells (**Figs 4.6 and 4.8**). Conversely, the re-expression of TAB2 in TAB1/2/3 triple KO cells restored both JNK1/2 and p38γ phosphorylation (**Fig 4.9C**). In contrast, the activation loops of TAK1, IKK, JNK1/2 and p38α and p38γ were all phosphorylated normally in TAB1 KO cells (**Figs 4.3 and 4.5**), Taken together, these findings indicate that TAB2/3, but not TAB1, are required for the TAK1-catalysed phosphorylation of MKK4 and/or MKK7, which are the protein kinases phosphorylating the activation loop of JNK (**Section 1.2.7.2**, [171]).

However, the activation of JNK is unique among MAP kinase family members since the threonine and tyrosine residues in the activation loop are phosphorylated by distinct upstream kinases, MKK7 phosphorylating the threonine and MKK4 phosphorylating the tyrosine residue, at least *in vitro* [204,220]. Since the phospho-specific antibody used to immunoblot JNK1/2 only recognises the JNKs phosphorylated at both sites, it is unclear whether the reduced phosphorylation of JNK1/2 in TAB2/3 DKO cells results from the failure of the TAB1-TAK1 to phosphorylate MKK4, MKK7 or both kinases. This could be addressed in the future by immunoblotting extracts from wild-type and TAB2/3 DKO cells with antibodies that recognise the individual

phosphorylated site in the activation loop of JNK, or that detect the dual phosphorylation on MKK4 or MKK7, respectively. The knockout study indicated that although both MKK4 and MKK7 are required for environmental stress-induced JNK activation, the pro-inflammatory cytokines, including TNF and IL-1, trigger the activation of JNK via MKK7 alone in MEFs (Fig 5A in [184]), suggesting that the relative contribution of MKKs is highly dependent on stimulus. It would be informative to generate single or double knockout clones of MKK4 and MKK7 in IL-1R* cells, and investigate whether MKK7 is the primary regulator of JNK activation in the innate immune signalling pathway.

The dramatic reduction of JNK phosphorylation in TAB2/3 DKO cells raises another possibility that the regulatory subunits TAB2 and TAB3, in addition to their roles in interacting with K63-Ub chains (**Section 1.2.4.3**), may also participate in directing TAK1 to specific substrates, such as MKK4/7. The re-expression of TAB2 truncation mutants lacking different domains may identify which region of the protein is responsible for this targeting function. A similar guiding function has been reported for other regulatory subunits of protein kinases. For example, the C-terminal zinc finger domain of NEMO interacts with IκBα, thereby directing the canonical IKK complex to IκBα and facilitating the phosphorylation of this substrate (**Section 1.2.5,** [112]).

The disappearance of IL-1-triggered p38γ phosphorylation in TAB2/3 DKO cells may result from several reasons. First, the stability of p38γ may require TAB2 and/or TAB3. The test in the total extract of DKO cells immunoblotted with p38γ specific antibody would solve this puzzle. Second, TAB2 and/or TAB3 are needed to activate the protein kinase phosphorylating p38γ. Previous study using MKK3-deficient and

MKK6-deficient MEFs has demonstrated that both MKK3 and MKK6 are responsible for the environmental stress-induced phosphorylation of p38γ, but the disruption of MKK6 gene alone is sufficient to prevent p38γ phosphorylation in response to TNF (Fig 4E in [221]). It is necessary to investigate whether MKK6 is the major regulator in the phosphorylation of p38γ in IL-1 signalling, which could be fulfilled by generating MKK6 knockout IL-1R* cells. It is equally important to examine if MKK6 and MKK3 are activated in the IL-1-stimulated TAB2/3 DKO cells.

Besides JNK and p38, ERK1/2 MAP kinases are another classical MAP kinase tier (**Section 1.2.7.2**). The IL-1-dependent phosphorylation of ERK1/2 occurred normally in TAB2/3 DKO cells for up to 30 min (**Fig 4.15**). These MAP kinase family members are known to be activated by MKK1 and MKK2 (also known as MEK1 and MEK2), which are themselves activated by Tpl2, which is activated by IKKβ (**Section 1.2.7.1**). Consistent with this pathway, I found that Compound 1 (C1), a potent and relatively specific inhibitor of Tpl2, blocked the IL-1-dependent phosphorylation of ERK1/2 (**Fig 4.16**). Tpl2 is also reported to be the protein kinase that activates MKK3 and MKK6 in the MyD88 signalling system, at least in BMDMs [183]. However, I did not observe any reduction in the IL-1-induced phosphorylation of p38γ in the wild type IL-1R* cells nor p38α in TAB2/3 DKO cells when C1 was included in the culture medium (**Fig 4.16**). This suggests that IL-1-induced MKK4 activity is sufficient to phosphorylate p38α in these cells if MKK3 and MKK6 are not activated, and that some other kinase rather than MKK3 and MKK6 mediate the phosphorylation of p38γ, at least in IL-1R* cells. The potent and specific inhibitors of MKK3 and MKK6 are therefore essential for further investigation in the future.

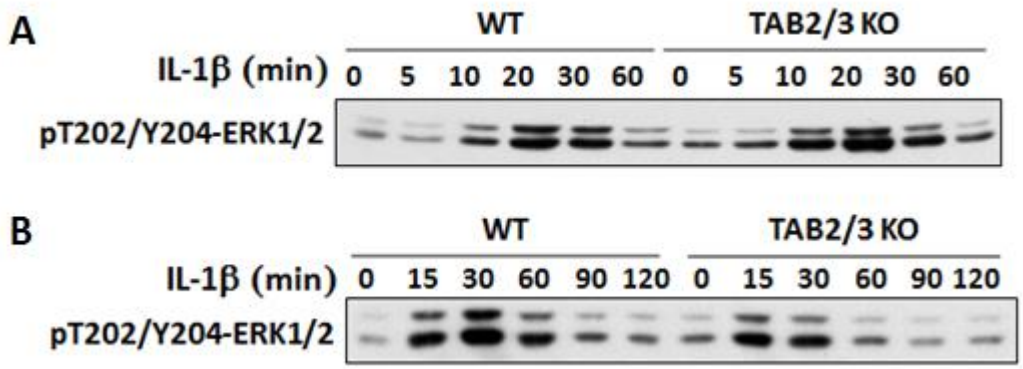

Figure 4.15 The phosphorylation of ERK1/2 in IL-1R* cells lacking expression of TAB2 and TAB3. (A, B) Wild type (WT) IL-1R* cells or TAB2/3 KO cells (clone 4 from Fig 4.6A) were stimulated for up to 60 min **(A)** or 120 min **(B)** with 5 ng/ml IL-1β. Cells were lysed and subjected to SDS/PAGE, followed by transfer to PVDF membranes and immunoblotting with the antibody recognising dual phosphorylation of ERK1/2 at Thr202 and Tyr204.

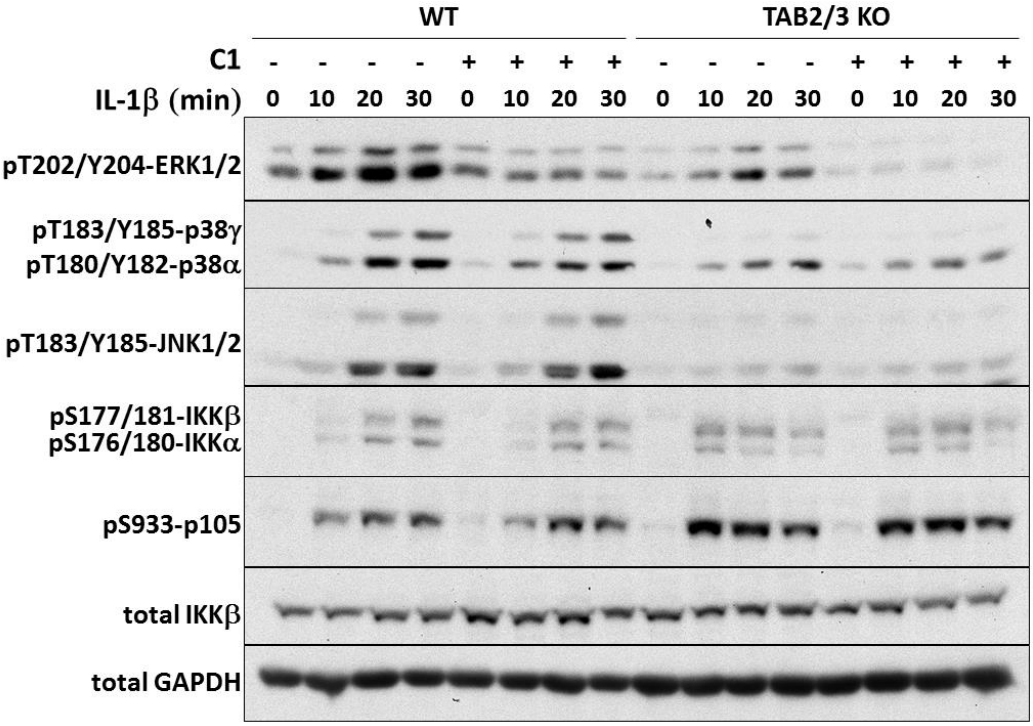

Figure 4.16 The effects of Tpl2 inhibitor C1 on IL-1β signalling in IL-1R* cells lacking expression of TAB2 and TAB3. Wild type (WT) IL-1R* cells or TAB2/3 KO cells (clone 4 from Fig 4.6A) were treated with Tpl2 inhibitor C1 (10 μM) for 60 min, and then stimulated for the times indicated with 5 ng/ml IL-1β. Cells were lysed and subjected to SDS/PAGE, followed by transfer to PVDF membranes and immunoblotting with the antibodies indicated.

4.3.3 The mechanism of activation of the TAK1 complex

The notion that the activation of the TAK1 complex is dependent on its regulatory subunits TAB2 and TAB3 has been established for many years [82]. Here I demonstrated that the IL-1-induced activation of TAK1 occurs by two different mechanisms in IL-1R* cells: the activation of TAB2/3-TAK1 complex relies on the

association between TAB2/3 and K63-Ub chains, but it does not require TRAF6 E3 ligase activity; the activation of TAB1-TAK1 complex needs the E3 ligase activity of TRAF6, but the details remain elusive.

4.3.3.1 The mechanism of activation of the TAB2/3-TAK1 complex

In the TAB1 KO cells, the IL-1-dependent activation of TAB2/3-TAK1 complex was rapid, robust and only slightly less sustained than in TAB1-expressing IL-1R* cells (**Figs 4.3 and 4.5**). The transcription of IL-8 and immediate early genes are well stimulated (**Fig 4.4**). However, the re-expression of wild type TAB2, but not an Ub-binding-deficient version of TAB2, restored IL-1-induced signalling in cells devoid of all three TABs (**Fig 4.9C**). These findings support the view that the activation of the TAB2/3-TAK1 complex is dependent on the interaction of TAB2/3 subunits with K63-Ub chains, which is consistent with the model proposed previously from studies *in vitro* [82].

Dr Sam Strickson in our laboratory recently found that the IL-1 signalling, which is lost in TRAF6-deficient IL-1R* cells, could be partially rescued by the re-expression of E3 ligase-inactive TRAF6 mutants [210], indicating that TRAF6 E3 ligase activity is not essential for IL-1 signalling. Consistent with these results, I found that the deletion of TRAF6 in the TAB1 KO IL-1R* cells eliminated TAK1 activation in response to IL-1 stimulation (**Fig 4.11A**), which was rescued by the re-expression of wild type TRAF6 and partially rescued by E3 ligase-inactive TRAF6 mutants (**Fig 4.11B**).

Sam Strickson also found that the re-expressed E3-ligase-inactive TRAF6 mutant was only able to rescue the IL-1-induced activation of the complete TAK1 complex when two other E3 ligases, termed Pellinos 1 and 2, were present [210]. Given that the E3-ligase inactive TRAF6 can rescue the IL-1-induced activation of the

TAB2/3-TAK1 complex (**Fig 4.11B**) but not TAB1-TAK1 complex in the presence of Pellinos 1 and 2 (**Fig 4.10D,** discussed below), it is proposed that Pellinos 1 and 2 are mainly involved in the activation of the TAB2/3-TAK1 complex. Previous studies showed that Pellinos 1 and 2, through their Fork-Head-Associated (FHA) domains, interact with phosphorylated threonine residues on IL-1-activated IRAK1 [52,222]. IRAK1 then phosphorylates Pellinos 1 and 2 converting them from inactive to active E3 ligases [223,224]. Taken together, these findings suggest that in cells expressing E3-inactive TRAF6 mutant, the role of TRAF6 appears to enable Pellino1/2-generated K63-Ub to activate the TAB2/3-TAK1 complex in an unknown way. This is supported by the rapid IL-1-dependent association between TAB2, TAK1 and TRAF6 in the IL-1R 293 cells (Fig 5 in [225]). To understand the physiological significance of the E3 ligase activity of Pellino1/2, our laboratory are currently crossing knock-in mice that express E3 ligase-inactive mutants of Pellino1/2 to knock-in mice that express an E3 ligase-inactive mutant of TRAF6.

The expression of the IRAK1 protein is essential for the IL-1-dependent activation of TAK1 in IL-1R* cells. Interestingly, the IL-1-stimulated ubiquitylation of IRAK1 was unaffected in Pellino1/2 KO cells, enhanced in TRAF6 KO cells and abolished in Pellino1/2/TRAF6 triple KO cells [210]. Taken together, these results indicate that Pellino1/2 and TRAF6 function redundantly in the ubiquitylation of IRAK1 and that IRAK1 ubiquitylation may be a prerequisite to activate the intact TAK1 complex.

Earlier studies in our laboratory demonstrated that the co-transfection of wild-type IRAK1 and Pellino2, but not inactive forms of these proteins, causes the formation of K63-Ub chains on IRAK1, and the transfection of Pellino2 alone triggers the polyubiquitylation of endogenous IRAK1 with K63-Ub chains (Fig 7 in [223]). Two of the

sites on IRAK1 ubiquitylated by Pellino1 *in vitro* were identified as Lys355 and Lys397 (Fig S3 in [224]). Lys134 and Lys180 have also been suggested to undergo ubiquitylation, because their mutation to arginine suppressed IL-1 signalling in MEFs (Fig 5C in [226]). Further analysis is needed to investigate whether the IL-1-dependent ubiquitylation of these four lysine residues occurs in cells [226]. It is also essential to identify the key lysine residue(s) modified by K63-Ub chains on other constituents in Myddosome and perform mutagenesis of these sites to elucidate which pools of K63-Ub chains are required for the activation of the TAB2/3-TAK1 complex. In addition, three ubiquitylation sites have been identified on Pellino 1 *in vitro* (Fig S3 in [224]), thus these potential pools of Ub chains may also contribute to the activation of TAK1 complex in cells.

Interestingly, Xia *et al* reported that the unanchored Ub chains purified from IL-1-stimulated IL-1R 293 cell line are capable of activating TAK1 complex *in vitro* (Figs 3 in [97]). If this operates in cells, the ubiquitylation on Myddosome components may not be essential. Alternatively, the working hypothesis would be that IL-1-activaed IRAK1 recruits and activates Pellinos 1/2, which catalyse the formation of free Ub chains that, with the assistance of TRAF6, are recognised and bound by TAB2 or TAB3 in TAK1 complex, leading to subsequent activation.

4.3.3.2 The mechanism of activation of the TAB1-TAK1 complex

In the current study, I found that the IL-1 induced activation of the TAB1-TAK1 complex is rapid and robust, but more transient in TAB2/3 DKO IL-1R* than that observed in TAB2/3-expressing IL-1R* cells (**Figs 4.6 and 4.8**). The transcription of immediate early genes is also stimulated, but not for IL-8 (**Fig 4.7**). In addition, the re-expression of wild type TAB1 rescued IL-1 signalling in the TAB1/2/3 triple KO cells (**Fig**

4.9B). These observations demonstrate that the TAB1-TAK1 complex can be activated transiently by IL-1, but it fails to sustain the signal after 60 min.

The additional knockout of TRAF6 in the TAB2/3 DKO IL-1R* cells prevented the IL-1-induced TAK1 activation, demonstrating an essential role of TRAF6 in activating the TAB1-TAK1 complex. However, in contrast to the TAB2/3-TAK1 complex in TAB1/TRAF6 DKO cells, the activation of the TAB1-TAK1 heterodimer was partially restored by wild type TRAF6, but not by E3-ligase-deficient TRAF6 mutants (**Fig 4.10C and D**). These findings imply that the E3 ligase activity of TRAF6, and presumably the Ub chains generated by TRAF6 are required for the activation of the TAB1-TAK1 complex. I attempted to examine the importance of K63-Ub chains in the TAB2/3 DKO IL-1R* cells by knocking down the Ubc13 E2 conjugating enzyme with specific shRNAs [158], However, as discussed earlier, the complete knock-out of Ubc13 drastically reduced the rate of cell proliferation and insufficient cells were produced for any experiments (data not shown).

Nevertheless, an *in vitro* assay found that the TAB1-TAK1 complex could not be activated by the Ub chains synthesized by TRAF6/Ube13-Uev1a *in vitro* (Fig 2a in [76]). In addition, to my knowledge, no Ub-binding domain has so far been identified and reported in either TAK1 or TAB1 [44]. It would therefore appear that an intervening step must exist which links the K63-Ub chains to the activation of the TAB1-TAK1 complex in cells. An additional component(s), including a kinase(s), E3 ligase(s), or an unidentified interacting protein(s), may be introduced into the signalling complex by the TRAF6-catalysed Ub chains, which then participates in the activation of TAB1-TAK1 complex in cells.

One possibility is that TRAF6-generated Ub chains activate another protein kinase that phosphorylates TAK1 at Thr187 and triggers its activation. In the current study, I found that MAP4K2 phosphorylates Thr187 on wild type TAK1 as well as on the catalytically inactive TAK1 [D175A] mutant in an *in vitro* kinase assay (**Figs 4.13C and D**), raising the possibility that MAP4K2 contributes to the phosphorylation and the activation of TAK1 in cells. The generation of a MAP4K2 knockout in TAB2/3 DKO IL-1R* cells should help to clarify its physiological role for the activation of TAB1-TAK1 complex. However, it may also be necessary to knock-out the closely related kinases MAP4K3 and MAP4K5 to fully address this issue.

Several previous studies suggested that TAK1 is activated by auto-phosphorylation and auto-activation [87,88]. In the current study, I found that the TAK1 inhibitor NG25 blocked the phosphorylation at Thr187 on TAK1 (**Fig 4.17**). Similarly, I discovered that the wild type TAK1, but not catalytically inactive TAK1 [D175A] mutant, restored the phosphorylation of TAK1 at Thr 187 and IL-1 signalling in the TAK1-deficient IL-1R* cells (**Fig 4.2B**). However, these results cannot completely exclude the possibility that a separate “upstream” kinase phosphorylates TAK1 at Thr187. In fact, the NG25 compound is reported as a dual inhibitor able to block not only TAK1 but also MAP4K2 [199]. The mutation of Asp175, which is in vicinity of Thr187, to Ala may result in an inhibitory conformation that prevents the recognition of Thr 187 by an upstream kinase(s). It is therefore necessary to test at least one more catalytically inactive TAK1 mutant, such as TAK1 [K63W] mutant. A new TAK1 inhibitor with higher potency and specificity would also help to clarify whether Thr187 is auto-phosphorylated in cells.

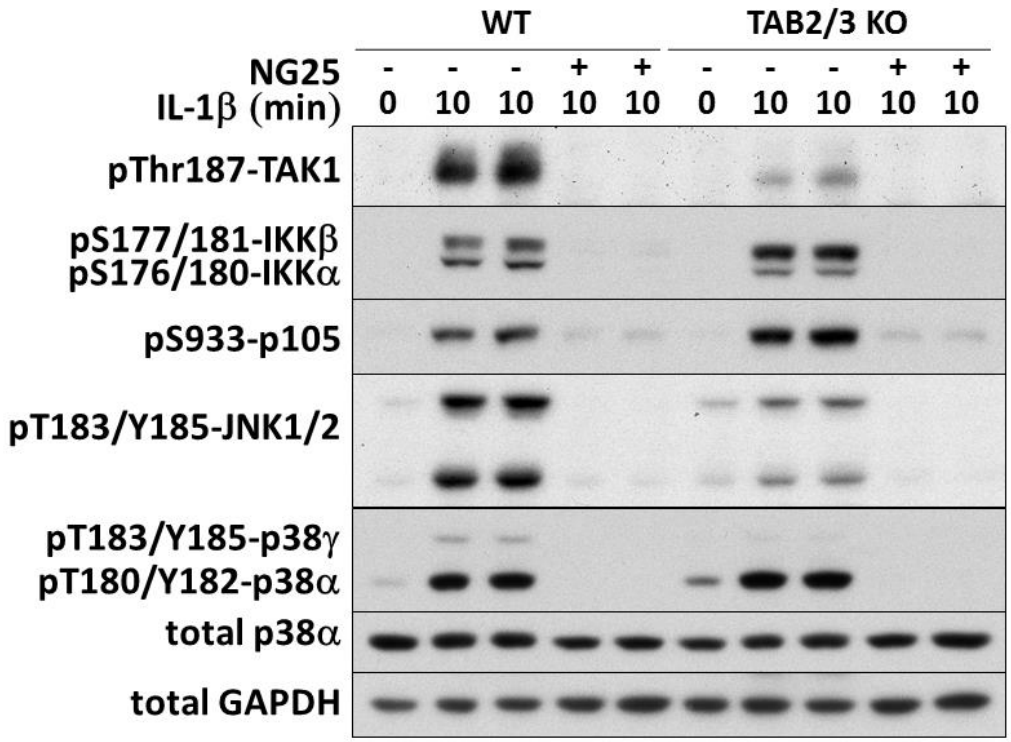

Figure 4.17 The effects of TAK1 inhibitor NG25 on IL-1β signalling in wild type IL-1R* cells and IL-1R* cells lacking expression of TAB2 and TAB3. Wild type (WT) IL-1R* cells or TAB2/3 KO cells (clone 4 from Fig 4.6A) were treated with TAK1 inhibitor NG25 (5μM) for 60 min, and then stimulated for the times indicated with 5 ng/ml IL-1β. Cells were lysed and subjected to SDS/PAGE, followed by transfer to PVDF membranes and immunoblotting with the antibodies indicated. The results are representative of at least three independent experiments.

The TAB1[F484A] mutant, which disrupts the association between TAK1 and TAB1 (**Section 1.2.4.2**, [92]), was unable to restore IL-1-signalling in TAB1/2/3 TKO cells (**Fig 4.18**), which suggests that this interaction is essential for TAK1 activation. Instead of directly phosphorylating Thr187 within the activation loop of TAK1, the putative "upstream" kinase may also phosphorylate TAB1 and/or TAK1 at other amino acid residue(s) and induce a conformational change that permits TAK1 to auto-phosphorylate Thr187. I exploited mass spectrometry to scrutinise the phosphorylation states of immunoprecipitated TAK1 and TAB1 from IL-1-stimulated TAB2/3 DKO cells. Several novel IL-1-dependent phosphorylation sites were identified (**Table 4.1**), including Ser417 and Thr476 in the TAB2/3-binding domain of TAK1. It is therefore possible that these phosphorylation events mimic the conformational change induced by the association of TAB2/3 and K63-Ub chains, leading to the auto-

phosphorylation of TAK1. In addition, I found that IL-1-induced the phosphorylation at Ser469 in the TAK1-binding region of TAB1. The phosphorylation of this site by an unknown "upstream" kinase could also promote TAK1 auto-phosphorylation via a conformational alteration. Further investigation, including the reconstitution of phospho-mimetic mutants of TAK1 and TAB1 will be necessary to reveal the biological significance of these phosphorylation events.

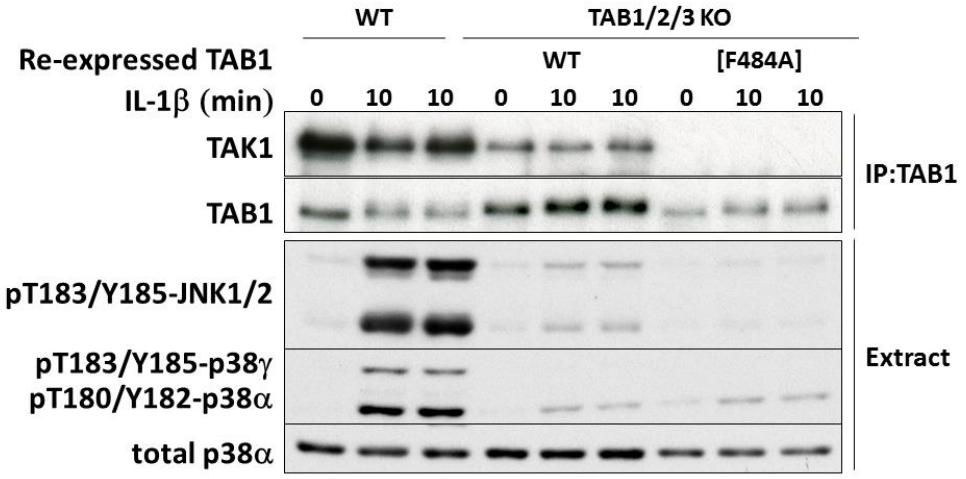

Figure 4.18 The interaction between TAK1 and TAB1 is required for IL-1β signalling. TAB1/TAB2/TAB3 triple KO IL-1R* cells (clone A4 from Fig 4.6A) re-expressing HA-tagged wild type TAB1 or TAB1[F484A] mutant were incubated for 16 h with 1 μg/ml doxycycline to induce the expression of these proteins. These cells and wild type IL-1R* cells (WT) were stimulated for 10 min with 5 ng/ml IL-1β. TAB1 was immunoprecipitated from the extracts of cells (**Section 2.2.3.4**). Immunoprecipitates and cell extracts (20 μg) were denatured in SDS, subjected to SDS/PAGE and immunoblotted with the antibodies indicated. The results are representative of at least three independent experiments.

Another hypothesis is that some other E3 ligase, working together with TRAF6, contributes to the activation of TAB1-TAK1 complex. A recent paper claimed that an E3 ligase, termed Huwe1, catalyses the formation of K48-Ub linkages on pre-formed K63-Ub oligomers synthesized by TRAF6, forming K48/K63 hybrid ubiquitin chains [227]. The knockdown of Huwe1 reduced the activation of TAK1 and its downstream signalling. These interesting data suggest a simple scenario for the activation of TAB1-TAK1 complex, namely that the TAB1-TAK1 complex binds directly binds to a unique topological structure formed by branched-Ub chains. It would be interesting to

investigate whether the TAB1-TAK1 complex is activated by K48/K63 branched-Ub chains *in vitro*. Since the association between TAK1 and TAB1 is critical for TAK1 activation, TAB1 may play an essential role in the formation of an interface between the complex and branched-Ub chains. Rapid hydrolysis of the K48-ub linkages could explain the transient activation of the TAB1-TAK1 complex.

While the current project was undergoing, Ori *et al* made conditional TAB2/3 knock-out mice and they reported that the activation of the MAP kinase cascade and the NF-κB pathway was not impaired, at least for the first 20 min after stimulation of BMDM with the TLR9 ligand CpG DNA (Fig 7H in [101]). This is consistent with the transient activation of the TAB1-TAK1 complex in the TAB2/3 DKO IL-1R* cells (**Figs 4.6 and 4.8**). Interestingly, the BMDM lacking both TAB2 and TAB3 produced IL-6, IL-12p40, and TNF in similar amounts to wild type cells in response to LPS, CpG DNA or Pam_2CSK_4 (Fig 7E in [101]). These results differ from the failure of IL-1 to induce IL-8 production in TAB2/3 DKO IL-1R* cells (**Figs 4.7C and 4.8C**). This could be a real difference and mean that activation of the TAB-TAK1 heterodimer is sustained in BMDM. However, it could also be explained, at least in part, by the Cre/LoxP-mediated conditional deletion of TAB2 being incomplete (Figs 7A,B in [101]), so that TAB2 was only partially deleted in these cells. Another possible explanation is that in BMDM, there is an alternative pathway, which can compensate for the absence of the TAK1-dependent network to produce the pro-inflammatory cytokines.

In summary, the findings in the current study allow me to draw a conclusion that the TAK1 complex is activated via two distinct mechanisms (**Fig 4.19**). The working model stated in this figure is supported by the data derived from my project and other relevant data obtained by Dr Sam Strickson in our laboratory. One mechanism is to

activate the TAB2/3-TAK1 complex, in which TRAF6 acts as an adaptor protein to couple Pellino1/2-generated K63-Ub chains (possibly on the ubiquitylated IRAK1 or other components in Myddosome) to TAB2/3-TAK1 complex. One or more of these pools of K63-Ub chains are recognised and bound by TAB2 or TAB3 in the TAK1 complex, followed by a conformational change and subsequent auto-phosphorylation and activation of TAK1. The other mechanism is TAB2/3-independent and involves the activation of the TAB1-TAK1 complex, in which TRAF6 generates K63-Ub chains to recruit and/or activate a yet identified component(s), that induces the phosphorylation and activation of TAK1.

The results presented in this Chapter provide the piece of genetic evidence that has been missing for more than ten years, which support the current established model of the TAK1 protein kinase activation. In addition, the findings on the TAB1-TAK1 complex suggest a novel activation mechanism of TAK1 in the MyD88-dependent signalling pathway. The discovery raises the question of whether this novel TAK1 activation also exists in other critical signalling pathways triggered by agonists such as TNF in innate immunity, or the antigenic stimulation in T and B cells in the adaptive immune system. It also implies that the interplay between phosphorylation and ubiquitylation is not as simple and straightforward as expected. In fact, the studies on the polyubiquitin chain-dependent activation of protein kinases could be subdivided into several aspects: 1. whether the kinase of interest is involved in different complexes; 2. whether each complex requires the same population of ubiquitin chains; 3. whether the E3 ligase(s) and its activity is needed for the activation of kinase complex. Since the cross-talk between phosphorylation and ubiquitylation has been observed and extensively investigated in many cellular events, the current study and

ideas that it has generated should be beneficial in tackling similar issues in other areas of biology.

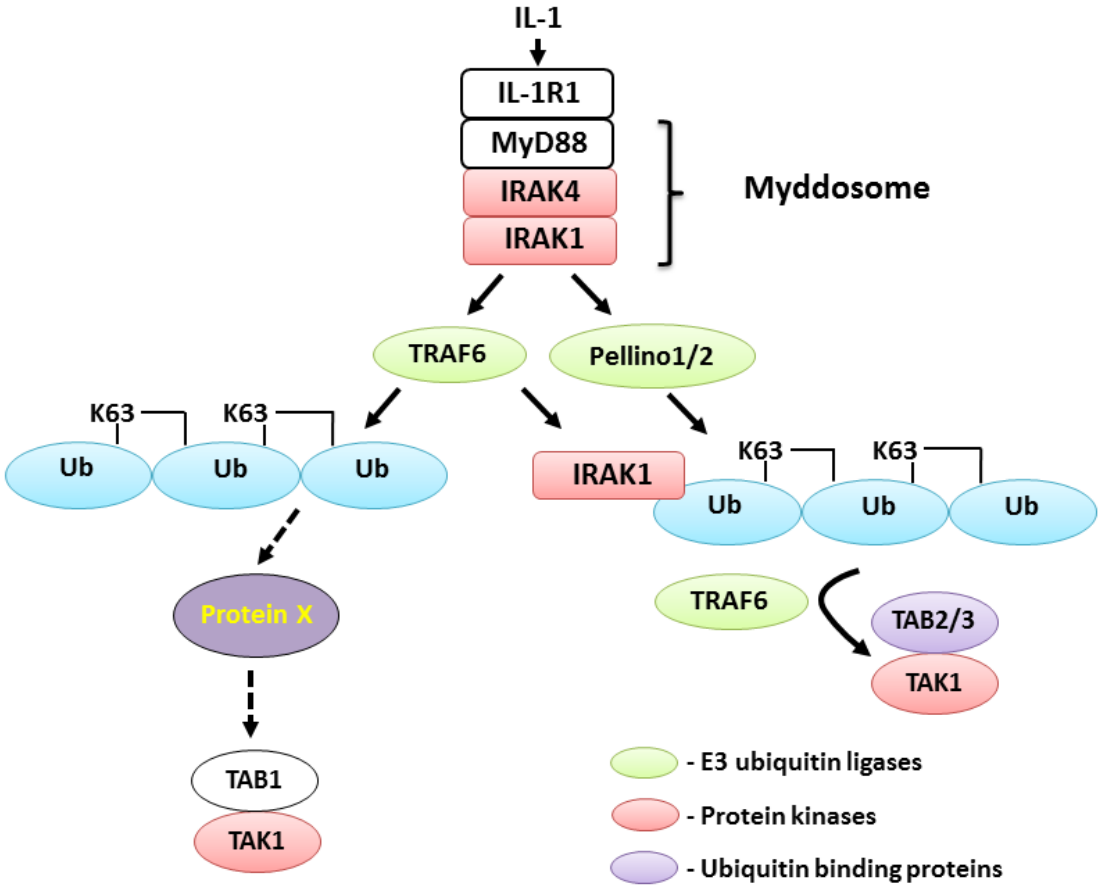

Figure 4.19 Two distinct mechanisms of TAK1 activation. IL-1-stimulation triggers the formation of the Myddosome, which recruits and activates the E3 ligases TRAF6 and Pellino1/2. In the absence of TAB2 and TAB3, TRAF6 catalyses the formation of K63-Ub chains, which transiently activate TAB1-TAK1 complex (possibly by activating a yet identified protein X). In the absence of TAB1, TRAF6 and Pellino1/2 generate K63-Ub chains on components in Myddosome. In addition, TRAF6 couples K63-Ub chains, possibly on IRAK1 or other components in Myddosome, to TAB2 and/or TAB3 regulatory subunit in TAB2/3-TAK1 complex. The association between TAB2/3 and K63-Ub chains leads to a conformational change that induces the auto-phosphorylation and activation of TAB2/3-TAK1 complex.

Chapter 5 General discussion of other mechanisms that have been proposed for the regulation of TAK1 complex and canonical IKK complex

5.1 How is phosphorylation within the activation loop of TAK1 regulated?

5.1.1 Phosphorylation of other sites on TAK1

The phosphorylation of TAK1 within its activation loop has been established to be essential for its activation [87,88]. However, phosphorylation sites outside the activation loop have also been reported to play a role in modulating TAK1 activity. Ouyang *et al* reported that Ser439 in human TAK1 (Ser412 in mouse TAK1) became phosphorylated in IL-1-stimulated IL-1R 293 cells, LPS-stimulated RAW cells and TNF-stimulated HEK293T cells (Fig 1A in [228]). The re-expression of the TAK1[Ser439Ala] mutant in TAK1 KO MEFs slightly reduced the LPS-stimulated activation of MAP kinases and NF-κB (Fig 1B, C in [228]). Furthermore, they reported that the siRNA knock-down of cAMP-dependent protein kinase catalytic subunit α (PKACα) and X-linked protein kinase (PRKX) alone and in combination suppressed the IL-1-dependent phosphorylation at Ser439 in HeLa cells and in LPS-stimulated RAW cells (Figs 6B,C in [228]). In order to test the validity of this paper, I examined the phosphorylation at Ser439 in IL-1R* cells with a validated phospho-specific antibody recognising phospho-Ser439 (**Fig 5.1A**). However, although Ser439 was phosphorylated, I found that it was phosphorylated in cells not stimulated with IL-1 and no increase in phosphorylation was observed upon stimulation with IL-1 (**Fig 5.1B**). The presence of TAK1 inhibitor NG25, which prevented TAK1 activity, did not affect the phosphorylation at Ser439 (**Fig 5.1B**). These findings suggest that the phosphorylation at Ser439 is constitutive and does not contribute significantly to the activation of TAK1, at least in IL-1R* cells. It would be essential to assess whether the re-expressed TAK1[Ser439Ala] mutant could restore IL-1 signalling in TAK1 KO IL-1R* cells.

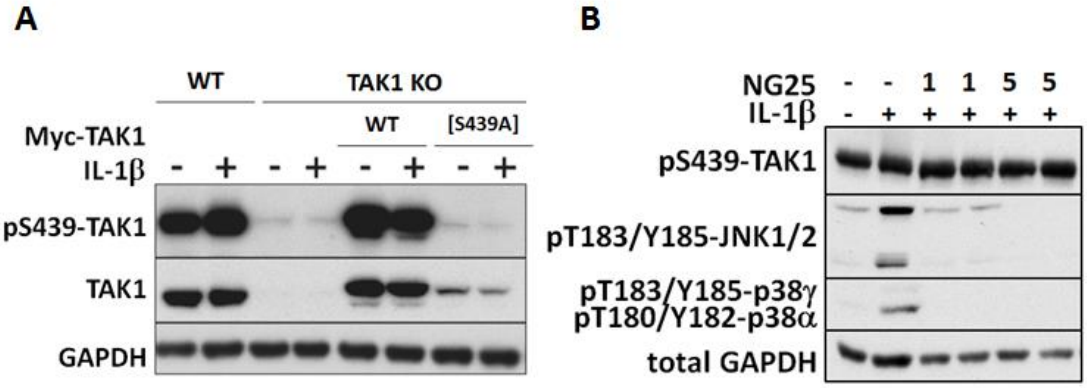

Figure 5.1 The phosphorylation of TAK1 at Ser439 has little effect on TAK1 activity. (A) Validation of phospho-specific antibody recognising phospho-Ser439 on TAK1. Myc-tagged wild type TAK1 (WT) or TAK1[S439A] mutant ([S439A]) were transiently transfected in the TAK1 KO IL-1R* cells. These cells, together with wild type IL-1R* cells (WT) and TAK1 KO cells not re-transfected with TAK1, were stimulated with 5 ng/ml IL-1β for 10 min, then subjected to SDS/PAGE and immunoblotted with the antibodies indicated. This experiment was carried out by Dr Sam Strickson. **(B)** The Ser439 was constitutively phosphorylated and not affected by TAK1 inhibitor. Wild type IL-1R* cells were incubated for 1 h without (-) or with (+) TAK1 inhibitor NG25 at indicated concentration (μM). Cells were then stimulated with 5 ng/ml IL-1β for 10 min. Other details are as in A.

5.1.2 The dephosphorylation of TAK1

Protein phosphorylation is a reversible covalent modification and the dephosphorylation of proteins is carried out by protein phosphatases. Since the activation of TAK1 requires phosphorylation at Ser and Thr residues, Ser/Thr-specific phosphatases are required to inactivate TAK1 [229].

Four major types of Ser/Thr protein phosphatases (PP1, PP2A, PP2B, and PP2C) exist in cells. Early studies reported that two isoforms of PP2C (PP2Cβ1 and PP2Cε) co-immunoprecipitated with endogenous TAK1 in 293 cells (Fig 5 in [230]) and the ectopic expression of PP2Cs suppressed IL-1-induced NF-κB activity [230,231]. However, although the TAK1 catalytic subunit can be dephosphorylated by PP2Cs *in vitro* (Fig 4 in [231]), their physiological role in regulating TAK1 in cells and the sites that they dephosphorylate on TAK1 has not yet been determined.

The PP2A-related protein phosphatase 6 (PP6) was later found to associate constitutively with endogenous TAK1 in IL-1R 293 cells (Fig 4C in [232]). Moreover, the knockdown of PP6 increased the IL-1-induced phosphorylation of TAK1 at Thr187 in IL-1R 293 cells (Fig 6B in [232]), suggesting that PP6 is involved in the dephosphorylation of TAK1 at this key phosphorylation site. In contrast, the siRNA knockdown of the PP2A catalytic subunit had no effect on the IL-1-stimulated phosphorylation of TAK1 at Thr187 in these cells (Fig 6C in [232]), indicating that PP2A does not contribute to the negative regulation of IL-1-induced TAK1 phosphorylation at least in IL-1R 293 cells.

Calyculin A, a potent inhibitor of all members of the PP1 and PP2A families, including PP6, was reported to increase TAK1 phosphorylation using a phospho-specific antibody (presumably against Thr187 but not specified in the paper) in the wild type and TAB2-deficient keratinocytes, but not in TAB1 KO keratinocytes. The re-expression of TAB1 in these cells restored the calyculin A-induced TAK1 phosphorylation (Fig 3 in [233]). The interpretation of this interesting observation is unclear but one possibility is that TAB1 recruits a TAK1-activating kinase responsible for the basal phosphorylation of TAK1 in cells where the MyD88 signalling pathway is not activated. It would be interesting to compare how calyculin A affects TAK1 phosphorylation at Thr187 in the wild type, TAB2/3 DKO and TAB1 KO IL-1R* cells that I have generated. IL-1 might activate the TAB1-TAK1 complex by inducing a transient inhibition of a PP2A family member, such as PP6.

A recent paper reported that the knockdown of PP1 reduced the phosphorylation of TAK1 at Ser439 but not Thr187 in LPS-stimulated RAW cells (Fig 2C in [234]), suggesting that PP1 may be the phosphatase that dephosphorylates this site

in cells. However, the significance of these observations is unclear because Ser439 seems to have little or no effect on TAK1 catalytic activity.

Nearly all investigations on the protein phosphatases controlling TAK1 activity have been based on the RNAi-mediated knockdown of PP6, PP2A and PP1, or the inhibitor calyculin A, which inhibits almost all members of the PPP (phosphoprotein phosphatase) family of Ser/Thr-specific phosphatases. With the development of the CRISPR/Cas9 genetic editing technology, it would be of interest to knockout these phosphatases completely in the IL-1R* cells, and study how this affects the phosphorylation of each of the components of the TAK1 complexes using advanced labelling methods, like multiplex SILAC [235] or stable isotope dimethyl labelling [236,237], as well as the powerful mass spectrometry machinery. This may enhance our understanding of the exact roles of these phosphatases in regulating TAK1 phosphorylation and activation in response to different stimuli.

5.1.3 The ubiquitylation of TAK1

Several research groups have reported that TAK1 becomes modified by ubiquitylation at different lysine residues. Lys34 of TAK1 was predicted to be a site of ubiquitylation, since this lysine residue is followed by an EIE sequence, which is similar to the KEEE motif predicted to be a preferred site of ubiquitylation by bioinformatics analysis [238]. The IL-1-induced formation of ubiquitin chains identified in TAK1 immunoprecipitates was largely reduced when the TAK1[K34R] mutant was over-expressed in HEK293T cells, and the phosphorylation of TAK1 at Thr187 and p38 MAP kinases was also impaired (Fig 5f in [239]). It is suggested from these experiments that TAK1 ubiquitylation may influence its phosphorylation and activation.

Later, Yamazaki *et al* reported that Lys209 was the predominant site of ubiquitylation on TAK1, because the TAK1[K209R] mutant, co-transfected with TRAF6 and K63Ub, failed to induce the presence of ubiquitin chains in TAK1 immunoprecipitates, in contrast to wild type TAK1 or TAK1 mutants, in which other Lys residues were mutated to Arg (Fig 1D in [240]). Moreover, the reconstitution of the TAK1[K209R] mutant in TAK1 KO MEFs only partially restored the IL-1-induced phosphorylation of TAK1 at Thr187 and the activation of the NF-κB pathway (Fig 2 in [240]). In contrast, IL-1 signalling was entirely rescued by the overexpression of wild type TAK1 and the TAK1 [K34R] mutant, suggesting that Lys34 is not the key site on TAK1, at least in the IL-1 signalling network.

However, another research group led by Jianhua Yang challenged both the above mentioned studies, claiming that it is K158 but not K34 nor K209 that is required for TRAF6-mediated TAK1 polyubiquitylation [241,242]. The reconstitution of the TAK1[K158R] mutant in TAK1 KO MEFs failed to rescue the stimulation-dependent activation of JNK1/2 and p38 MAP kinases, nor the canonical IKK complex, which were restored by the re-expression of wild type TAK1, TAK1[K34R] or TAK1[K209R] mutants in response to TGF-β or IL-1, respectively [241,242]. A similar study from the same laboratory showed that IL-1 or TNF induced the ubiquitylation of overexpressed wild type TAK1 but not overexpressed TAK1[K158R] in HeLa cells. The phosphorylation of the TAK1 mutant at Thr187 was also not detectable when Lys158 was mutated to Arg (Fig 4A, B in [243]). Given that the same cell line (TAK1 KO MEFs) and stimuli (TGF-β or IL-1) were used in all these studies, the reasons for all these different observations is unclear and may results from the over-expression of re-introduced wild type TAK1 and its mutants. Moreover, none of these studies used wild type MEFs as a positive control.

Additionally, the mutation of Lys residues to Arg may affect TAK1 regulation and activity by a mechanism that is unrelated to the loss of ubiquitylation.

To understand whether TAK1 catalytic activity is controlled by ubiquitylation, it is clearly critical to undertake a rigorous investigation to establish whether the endogenous TAK1 becomes ubiquitylated and, if so, which lysine(s) on the endogenous TAK1 plays the role of ubiquitylation in regulating TAK1. To perform these experiments TAK1 immunoprecipitates should be digested with trypsin, ubiquitylated peptides enriched with a di-Gly specific antibody should be isolated and analysed by mass spectrometry to identify possible ubiquitylation sites on TAK1 [244,245]. I immunoprecipitated the endogenous TAK1 from the IL-1-stimulated IL-1R* cells lysed with the DUB inhibitor iodoacetamide, but failed to observe any ubiquitylated TAK1 in the immunoprecipitates when I probed them with a TAK1 specific antibody (data not shown). In the published studies [239–243] the possibility was not excluded that the ubiquitin chains found associated with TAK1 immunoprecipitates were not attached covalently to TAK1, but bound non-covalently to TAB2 and TAB3 subunits. Therefore these papers do not present convincing evidence that TAK1 was ubiquitylated.

5.1.4 The deubiquitylation of TAK1

Like phosphorylation, ubiquitylation is also a reversible modification. Fan *et al* built a library of expression vectors encoding 38 human USPs (Ub-specific peptidases), which are the largest subclass of deubiquitylases (DUBs). They found that USP4 was the only DUB that inhibited NF-κB activation induced by the overexpression of TAK1 and TAB1 in 293 cells (Fig 2a in [246]). The knockdown of USP4 not only increased the ubiquitylation of Flag-TAK1 in TNF-stimulated Flag-TAK1-expressing HeLa cells, but also enhanced NF-κB activation in TNF-stimulated HeLa cells (Fig 7 in [246]), suggesting that

the deubiquitylation of TAK1 (or a component of the pathway "upstream" of TAK1) by USP4 negatively regulates TAK1 activation. Notably, CYLD, a DUB that cleaves both K63-Ub and Met1-Ub chains *in vitro* [98], did not inhibit TAK1 and TAB1 co-overexpression-induced TAK1 polyubiquitylation (Fig 1 in [246]).

In two subsequent studies, USP18 was reported to bind to the TAB1-TAK1 complex and catalyse the deubiquitylation of TAB1-TAK1 [247,248]. Liu *et al* reported that the overexpression of both TAK1 and TAB1, but not TAK1 alone, resulted in measurable ubiquitylation of immunoprecipitated TAK1 which was abolished by the overexpression of wild type USP18 but not the USP18[C16S] inactive mutant in 293T cells (Fig 9 B,C in [247]). Yang *et al* reported that USP18 deubiquitylated K63-Ub but not K48-Ub chains in the transient transfection experiments in 293T cells (Fig 5A in [248]), and that knockdown of USP18 slightly enhanced the LPS-induced activation of MAP kinases and NF-κB, and increased the transcription of genes encoding pro-inflammatory cytokines and IL-6 secretion by about 50% in the THP-1 monocyte cell line (Fig 2 in [248]). Similar to the studies on TAK1 ubiquitylation discussed earlier, what is missing in these studies is any evidence that the endogenous TAK1 is ubiquitylated and whether it affects TAK1 phosphorylation.

5.2 The regulation of TAK1 activation by the modification of its TAB subunits

5.2.1 The phosphorylation and dephosphorylation of TAB subunits

In earlier studies in our laboratory it was established that TAB1 is phosphorylated by p38α MAP kinase at Ser423, Thr431 and Ser438 *in vitro* and in IL-1-stimulated KB cells and LPS-stimulated RAW cells. The phosphorylation at Ser423 and Thr431 was prevented by a p38α specific inhibitor, coincident with the enhancement of TAK1 catalytic activity (Figs 7,8 in [180]). These studies suggest that p38α MAP

kinase-mediated TAB1 phosphorylation may serve as a negative feed-back mechanism for the regulation of TAK1 activity. The p38α-dependent phosphorylation of TAB1 at Ser423 and Thr431 was also shown to inhibit TAK1 activation in the epidermal growth factor receptor (EGFR) signalling pathway in HeLa cells [249], suggesting that this negative feedback may be a general mechanism for controlling TAK1 activity.

There is a serine rich area located near the C terminus of TAB1, in which six serine residues are clustered in the region comprising amino acid residues 449-461: HTQSSSSSSDGGL. Wolf and co-workers identified Ser452/453 and Ser456/457 as novel phosphorylation sites on TAB1 [250]. However, despite the potential role in regulating p38 MAP kinase activity and subcellular localization (Figs 4 and 5 in [250]), these phosphorylation events did not appear to affect the phosphorylation or ubiquitylation of TAK1 (Fig S3 in [250]), and therefore seem dispensable for TAK1 activation.

A further study from our laboratory identified two IL-1-stimulated phosphorylation sites on TAB2 (Ser372 and Ser524) and three on TAB3 (Ser60, Thr404 and Ser506) in IL-1R cells and MEFs [181]. Ser60 and Thr404 of TAB3 appear to be phosphorylated directly by p38α MAP kinase, while Ser506 is phosphorylated by MAPKAP-K2/MAPKAP-K3 (MAPK-activated protein kinase 2 and 3), which are protein kinases activated by p38α MAP kinase. The phosphorylation at these sites may therefore also contribute to the feedback control of TAK1. However, Ser372 and Ser524 of TAB2 are not phosphorylated by pathways dependent on p38α/β MAPKs, ERK1/2 or JNK1/2 [181]. The physiological functions of these phosphorylation events are unknown and require further investigation.

In terms of dephosphorylation of TABs, Yang *et al* reported that dual-specificity phosphatase 14 (DUSP14, also known as MAPK phosphatase 6, MKP6) interacted

constitutively with TAB1 in murine primary T cells (Fig 3D in [251]), and overexpressed DUSP14 dephosphorylated TAB1 at Ser438 in HEK293 cells (Fig 4D in [251]). Moreover, DUSP14 deficiency enhanced the phosphorylation of TAB1 at Ser438, the phosphorylation of TAK1 (presumably at Thr187 but not specified in the paper), and activated MAP kinase and NF-κB signalling in T cells stimulated by anti-CD3 plus anti-CD28 antibodies or by phorbol 12-myristate 13-acetate (PMA) plus ionomycin (Fig 5 in [251]). These observations suggest that DUSP14 negatively regulates TAK1 activation either by the dephosphorylation of TAB1 at Ser438 or TAK1 at Thr187. It would therefore be interesting and important to investigate whether DUSP14 regulates TAK1 activity in cells where TAB1 is replaced by the TAB1[S438A] mutant.

5.2.2 The ubiquitylation of TAB subunits

A recent study reported that in embryonic stem (ES) cells TGF-β or EGF induced the Lys63-linked ubiquitylation of TAB1 and that this was catalysed by the RING domain in MEKK1 (MAP kinase/ERK kinase kinase 1), the only protein kinase that possesses an E3 ligase activity in its catalytic domain [252]. An MEKK1 mutant in which the E3 ligase activity was inactivated exhibited defective TAB1 ubiquitylation (Fig 4F in [252]), as well as defective JNK and p38 activation following TGF-β stimulation (Fig 2 in [252]). The re-expression of TAB1 mutant in TAB1-deficient ES cells, in which four lysine residues were mutated to alanine (K294A, K319A, K335A and K350A), failed to restore TAK1 phosphorylation and MAP kinase activation by TGF-β (Fig 4I in [252]), suggesting that TAB1 underwent ubiquitylation at multiple sites and that one or more of these lysine residues are critical for TAK1 phosphorylation in TGF-β-stimulated ES cells. These experiments implied that ubiquitylation of TAB1 may be important for TGF-β signalling. However, in these studies the deletion of TAB1 abolished TGF-β-

induced TAK1 phosphorylation and MAP kinase activation (Fig 4G in [252]), which is entirely different from my observations in IL-1-stimulated TAB1 KO IL-1R* cells (**Section 4.2.3**). Moreover, Gopal Sapkota's lab in our Unit reported that TGFβ stimulation does not activate TAK1 and that TGFβ-induced activation of p38α MAP kinases occurs normally in TAK1 KO MEFS and in HaCaT keratinocytes where TAK1 is knocked down (Figs 1 and 4 in [253]). However, it is possible that the TAK1 activation mechanism in TGF-β signalling in ES cells differs from the MyD88 signalling network in HEK293 cells.

Theivantherian *et al* recently reported that the E3 ubiquitin ligase Itch catalysed the Lys48-linked ubiquitylation of TAB1, leading to its degradation (Fig 3 in [254]). The Itch deficiency increased TAB1 abundance and sustained p38α phosphorylation for up to 2 hours in TNF-stimulated BMDMs, but the phosphorylation of MKK3/6 was decreased. The re-expression of wild type Itch, but not E3-ligase-inactive mutant, reversed this effect (Fig 4 in [254]). Although TAK1 phosphorylation was not examined in this study, it is possible that Itch may play a role in TAK1 activation. An earlier study from the same group found that the abundance and the phosphorylation of TRAF2-associated TAK1 was sustained for up to 60 min after TNF stimulation in BMDMs that lack either Itch E3 ligase or the DUB CYLD (Fig 5a in [255]), but the phosphorylation and activation of TAK1 in the cell extracts was not investigated. They concluded that Itch and CYLD formed a complex which sequentially cleaved K63-Ub chains and catalysed the formation of K48-Ub chains on TAK1 to terminate TNF signalling.

5.2.3 Additional covalent modification of TAB subunits

TAB1 and TAB3 have been reported to be modified by glycosylation with N-acetylglucosamine (O-GlcNAcylation) [256,257]. Ser395 was identified as single O-

GlcNAcylation site on TAB1, and the expression of TAB1 [S395A] mutant led to slightly reduced IL-1-dependent phosphorylation of TAK1 at Thr187 compared to wild type TAB1 when it was re-expressed in TAB1 KO MEFs (Fig 4 in [256]). It was concluded that this modification is necessary for full activation of TAK1. However, I found that the expression of the TAB1 [S395A] mutant in TAB1/2/3 KO IL-1R* cells restored IL-1 signalling similarly to wild type TAB1 (**Fig 5.2**).

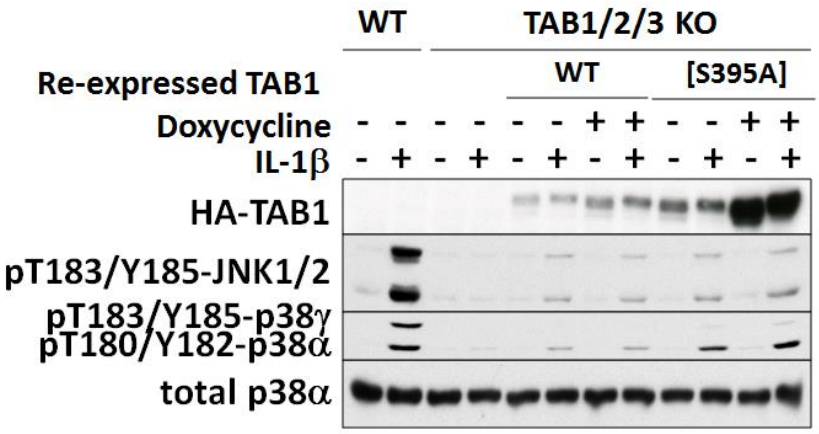

Figure 5.2 The mutation of Ser395 to Ala on TAB1 did not affect IL-1β signalling. The stable TAB1/2/3 triple KO cell lines which inducibly express HA-tagged wild-type TAB1 (WT) or TAB1[S395A] mutant ([S395A]) were established via retroviral transfection (**Section 2.2.1.8.3**). After doxycycline induction for 18 hours, cells were stimulated with 5 ng/ml IL-1β for 10 min. 20 μg total cellular extracts were loaded onto SDS-PAGE gel and transferred to PVDF membrane. Proteins were probed by indicated antibodies.

Tao *et al* recently discovered that the TAB3 was O-GlcNAcylated at Ser408 by O-GlcNAc transferase (OGT) in the triple negative breast cancer (TNBC) cells. This modification was thought to be required for the phosphorylation of TAB3 at Thr404 (Fig 4 in [257]), and the activation of TAK1 and NF-κB (Fig 3 in [257]), based on studies in IL-1 stimulated MDA-MB-231 cells involving transient transfection of TAB3. It will be of interest to test whether the reconstitution of the TAB3[S408A] mutant restores IL-1-induced TAK1 activation in TAB1/2/3 TKO cells.

5.2.4 Other TAK1 binding proteins

At least two papers reported a new TAB member, termed TAB4 [258,259]. TAB4 was initially identified as a type2A phosphatase-interacting protein (TIP). In transient transfection experiments, TAB4 co-immunoprecipitated with TAK1 but not the TAB1-TAK1 complex (Fig 3A, [259]). TAB4 was shown to bind constitutively to the TAK1/IKKα/β complex in human neutrophils [258], but the exact role of TAB4 remains elusive. In order to understand what the role of TAB4 in regulating TAK1 activation might be, it is critical to knock-out this protein in cells and investigate whether the activation of TAK1 by one or more stimuli is impaired.

TAK1 and its regulatory subunit TABs have been reported to become covalently modified in several ways, including phosphorylation beyond the activation loop, ubiquitylation, and O-GlcNAcylation. At this moment, little hard evidence is present to support if any of them contributes to the activation of TAK1 complex. It is therefore suggested that the investigation on the regulation of TAK1 activation would be an important challenge in the future.

5.3 Other mechanisms underlying the phosphorylation and activation of IKKs

5.3.1 Kinases implicated in IKK activation

It has been controversial whether TAK1 is the only kinase directly phosphorylating IKKβ in the MyD88 signalling network. Other MAP3Ks, such as members of the MEKK family, have also been proposed to phosphorylate IKKβ. Early studies revealed that MEKK1 activates IKKs *in vitro* [260], and that the overexpression of MEKK1 induced the activation of IKKα and IKKβ in cells [261]. However, IL-1-stimulated MEKK1-deficient MEFs exhibited similar NF-κB activity to wild type MEFs,

suggesting that the endogenous MEKK1 is dispensable for activation of the canonical IKK complex (Fig 5B in [262]).

Soon after, MEKK2 and MEKK3 were also shown to activate IKKα and IKKβ in transient transfection experiments [263], and the deletion of MEKK3 was reported to impair the TNF-induced phosphorylation of IκBα and the activation of NF-κB in MEFs [264]. In addition, these knockout studies demonstrated that MEKK3 is critical for the activation of IKKβ and subsequent induction of NF-κB activity in MEFs, and that MEKK3, but not MEKK2, was essential for IL-1- or LPS-induced IL-6 production in MEFs (Fig 3 in [265]). Yao *et al* reported that the IL-1-stimulated phosphorylation of IκB and activation of NF-κB was not completely abolished in the TAK1-deficient MEFs or in wild type MEFs treated with a TAK1 inhibitor, but was entirely blocked in MEKK3-deficient MEFs treated with the TAK1 inhibitor (Fig 5 in [266]). It was concluded from these studies that TAK1 and MEKK3 both contribute to the activation of IKKβ and hence NF-κB. Furthermore, they reported that it was IKKα, but not IKKβ, that was phosphorylated in the MEKK3-dependent, but TAK1-independent pathway in MEFs (Fig 7 in [266]), and that NF-κB was released from IκBα and activated without any IκBα degradation in this signalling axis (Fig 8 in [266]). Since these findings have only been reported by one laboratory, it will be important for at least one other lab to establish whether this is correct.

References

1 Charles A Janeway, J., Travers, P., Walport, M. and Shlomchik, M. J. (2001) Immunobiology: The Immune System in Health and Disease. 5th edition 5th ed., Garland Science.

2 Arthur, J. S. C. and Ley, S. C. (2013) Mitogen-activated protein kinases in innate immunity. Nat. Rev. Immunol., Nature Publishing Group **13**, 679–92.

3 Iwasaki, A. and Medzhitov, R. (2015) Control of adaptive immunity by the innate immune system. Nat. Immunol. **16**, 343–53.

4 Cooper, M. D. and Alder, M. N. (2006) The evolution of adaptive immune systems. Cell **124**, 815–22.

5 Kurosaki, T., Kometani, K. and Ise, W. (2015) Memory B cells. Nat. Rev. Immunol. **15**, 149–59.

6 Restifo, N. P. and Gattinoni, L. (2013) Lineage relationship of effector and memory T cells. Curr. Opin. Immunol. **25**, 556–63.

7 Boisson, B., Laplantine, E., Dobbs, K., Cobat, A., Tarantino, N., Hazen, M., Lidov, H. G. W. W., Hopkins, G., Du, L., Belkadi, A., et al. (2015) Human HOIP and LUBAC deficiency underlies autoinflammation, immunodeficiency, amylopectinosis, and lymphangiectasia. J. Exp. Med. **212**, 939–951.

8 Döffinger, R., Smahi, A., Bessia, C., Geissmann, F., Feinberg, J., Durandy, A., Bodemer, C., Kenwrick, S., Dupuis-Girod, S., Blanche, S., et al. (2001) X-linked anhidrotic ectodermal dysplasia with immunodeficiency is caused by impaired NF-kappaB signaling. Nat. Genet. **27**, 277–85.

9 Courtois, G. and Gilmore, T. D. (2006) Mutations in the NF-kappaB signaling pathway: implications for human disease. Oncogene **25**, 6831–43.

10 Chang, C. (2014) Autoimmunity: From black water fever to regulatory function. J. Autoimmun. **48–49**, 1–9.

11 Barnes, P. J. (2013) New anti-inflammatory targets for chronic obstructive pulmonary disease. Nat. Rev. Drug Discov. **12**, 543–559.

12 Ngo, V. N., Young, R. M., Schmitz, R., Jhavar, S., Xiao, W., Lim, K.-H., Kohlhammer, H., Xu, W., Yang, Y., Zhao, H., et al. (2011) Oncogenically active MYD88 mutations in human lymphoma. Nature, Nature Publishing Group **470**, 115–9.

13 Beutler, B. (2004) Inferences, questions and possibilities in Toll-like receptor signalling. Nature, Nature Publishing Group **430**, 257–63.

14 Rifkin, I. R., Leadbetter, E. A., Busconi, L., Viglianti, G. and Marshak-Rothstein, A. (2005) Toll-like receptors, endogenous ligands, and systemic autoimmune disease. Immunol. Rev., Munksgaard International Publishers **204**, 27–42.

15 Drexler, S. K. and Foxwell, B. M. (2010) The role of toll-like receptors in chronic inflammation. Int. J. Biochem. Cell Biol. **42**, 506–18.

16 Medzhitov, R. (2007) Recognition of microorganisms and activation of the immune response. Nature, Nature Publishing Group **449**, 819–26.

17 Kumar, H., Kawai, T. and Akira, S. (2011) Pathogen recognition by the innate immune system. Int. Rev. Immunol. **30**, 16–34.

18 Sancho, D. and Reis E Sousa, C. (2013) Sensing of cell death by myeloid C-type lectin receptors. Curr. Opin. Immunol., Elsevier Ltd **25**, 46–52.

19 Takeuchi, O. and Akira, S. (2010) Pattern recognition receptors and inflammation. Cell, Elsevier Inc. **140**, 805–20.

20 Lemaitre, B., Nicolas, E., Michaut, L., Reichhart, J. M. and Hoffmann, J. A. (1996) The dorsoventral regulatory gene cassette spätzle/Toll/cactus controls the potent antifungal response in Drosophila adults. Cell **86**, 973–83.

21 Medzhitov, R., Preston-Hurlburt, P. and Janeway, C. A. (1997) A human homologue of the Drosophila Toll protein signals activation of adaptive immunity. Nature **388**, 394–7.

22 Kawai, T. and Akira, S. (2010) The role of pattern-recognition receptors in innate immunity: update on Toll-like receptors. Nat. Immunol., Nature Publishing Group **11**, 373–84.

23 Takeda, K. and Akira, S. (2004) Microbial recognition by Toll-like receptors. J. Dermatol. Sci. **34**, 73–82.

24 Yin, Q., Fu, T.-M., Li, J. and Wu, H. (2015) Structural biology of innate immunity. Annu. Rev. Immunol. **33**, 393–416.

25 Ozinsky, a, Underhill, D. M., Fontenot, J. D., Hajjar, a M., Smith, K. D., Wilson, C. B., Schroeder, L. and Aderem, a. (2000) The repertoire for pattern recognition of pathogens by the innate immune system is defined by cooperation between toll-like receptors. Proc. Natl. Acad. Sci. U. S. A. **97**, 13766–71.

26 Matsushima, N., Tanaka, T., Enkhbayar, P., Mikami, T., Taga, M., Yamada, K. and Kuroki, Y. (2007) Comparative sequence analysis of leucine-rich repeats (LRRs) within vertebrate toll-like receptors. BMC Genomics **8**, 1–20.

27 O'Neill, L. A. J. (2008) The interleukin-1 receptor/Toll-like receptor superfamily: 10 Years of progress. Immunol. Rev. **226**, 10–18.

28 Dinarello, C. A. (2009) Immunological and inflammatory functions of the interleukin-1 family. Annu. Rev. Immunol. **27**, 519–50.

29 Garlanda, C., Dinarello, C. A. and Mantovani, A. (2013) The Interleukin-1 Family: Back to the Future. Immunity, Elsevier Inc. **39**, 1003–1018.

30 Eder, C. (2009) Mechanisms of interleukin-1beta release. Immunobiology, Elsevier **214**, 543–53.

31 Sutterwala, F. S., Haasken, S. and Cassel, S. L. (2014) Mechanism of NLRP3 inflammasome activation. Ann. N. Y. Acad. Sci. **1319**, 82–95.

32 Rubartelli, A., Cozzolino, F., Talio, M. and Sitia, R. (1990) A novel secretory pathway for interleukin-1 beta, a protein lacking a signal sequence. EMBO J. **9**, 1503–10.

33 Lamkanfi, M. and Dixit, V. M. (2012) Inflammasomes and their roles in health and disease. Annu. Rev. Cell Dev. Biol. **28**, 137–61.

34 Davis, B. K., Wen, H. and Ting, J. P.-Y. (2011) The inflammasome NLRs in immunity, inflammation, and associated diseases. Annu. Rev. Immunol. **29**, 707–35.

35 Wang, D., Zhang, S., Li, L., Liu, X., Mei, K. and Wang, X. (2010) Structural insights into the assembly and activation of IL-1β with its receptors. Nat. Immunol. **11**, 905–11.

36 Casadio, R., Frigimelica, E., Bossù, P., Neumann, D., Martin, M. U., Tagliabue, A. and Boraschi, D. (2001) Model of interaction of the IL-1 receptor accessory protein IL-1RAcP with the IL-1beta/IL-1R(I) complex. FEBS Lett. **499**, 65–8.

37 Jenkins, K. A. and Mansell, A. (2010) TIR-containing adaptors in Toll-like receptor signalling. Cytokine, Elsevier Ltd **49**, 237–244.

38 Carty, M., Goodbody, R., Schröder, M., Stack, J., Moynagh, P. N. and Bowie, A. G. (2006) The human adaptor SARM negatively regulates adaptor protein TRIF-dependent Toll-like receptor signaling. Nat. Immunol. **7**, 1074–81.

39 Peng, J., Yuan, Q., Lin, B., Panneerselvam, P., Wang, X., Luan, X. L., Lim, S. K., Leung, B. P., Ho, B. and Ding, J. L. (2010) SARM inhibits both TRIF- and MyD88-mediated AP-1 activation. Eur. J. Immunol. **40**, 1738–1747.

40 Vallabhapurapu, S. and Karin, M. (2009) Regulation and function of NF-kappaB transcription factors in the immune system. Annu. Rev. Immunol. **27**, 693–733.

41 Takaoka, A., Yanai, H., Kondo, S., Duncan, G., Negishi, H., Mizutani, T., Kano, S.-I., Honda, K., Ohba, Y., Mak, T. W., et al. (2005) Integral role of IRF-5 in the gene induction programme activated by Toll-like receptors. Nature **434**, 243–9.

42 Clark, K., MacKenzie, K. F., Petkevicius, K., Kristariyanto, Y., Zhang, J., Choi, H. G., Peggie, M., Plater, L., Pedrioli, P. G. a, McIver, E., et al. (2012) Phosphorylation of CRTC3 by the salt-inducible kinases controls the interconversion of classically activated and regulatory macrophages. Proc. Natl. Acad. Sci. U. S. A., Medical Research Council Protein Phosphorylation Unit, College of Life Sciences, Sir James Black Centre, University of Dundee, Dundee, DD1 5EH, United Kingdom. DOI - 10.1073/pnas.1215450109 SRC - Pubmed ID2 - 23033494 FG - 0 **109**, 16986–91.

43 Wesche, H., Henzel, W. J., Shillinglaw, W., Li, S. and Cao, Z. (1997) MyD88: an adapter that recruits IRAK to the IL-1 receptor complex. Immunity **7**, 837–47.

44 Napetschnig, J. and Wu, H. (2013) Molecular basis of NF-κB signaling. Annu. Rev. Biophys. **42**, 443–68.

45 Adachi, O., Kawai, T., Takeda, K., Matsumoto, M., Tsutsui, H., Sakagami, M., Nakanishi, K. and Akira, S. (1998) Targeted disruption of the MyD88 gene results in loss of IL-1- and IL- 18-mediated function. Immunity **9**, 143–150.

46 Kawai, T., Adachi, O., Ogawa, T., Takeda, K. and Akira, S. (1999) Unresponsiveness of MyD88-deficient mice to endotoxin. Immunity **11**, 115–122.

47 Motshwene, P. G., Moncrieffe, M. C., Grossmann, J. G., Kao, C., Ayaluru, M., Sandercock, A. M., Robinson, C. V., Latz, E. and Gay, N. J. (2009) An Oligomeric Signaling Platform formed by the toll-like receptor signal transducers MyD88 and IRAK-4. J. Biol. Chem., Department of Biochemistry, University of Cambridge, Cambridge CB2 1GA, United Kingdom. DOI - 10.1074/jbc.M109.022392 SRC - Pubmed ID2 - 19592493 FG - 0 **284**, 25404–25411.

48 Lin, S.-C., Lo, Y.-C. and Wu, H. (2010) Helical assembly in the MyD88-IRAK4-IRAK2 complex in TLR/IL-1R signalling. Nature, Department of Biochemistry, Weill Cornell Medical College, New York, New York 10021, USA. DOI - 10.1038/nature09121 SRC - Pubmed ID2 - 20485341 FG - 0 **465**, 885–890.

49 Cao, Z., Henzel, W. J. and Gao, X. (1996) IRAK: a kinase associated with the interleukin-1 receptor. Science **271**, 1128–31.

50 Muzio, M., Ni, J., Feng, P. and Dixit, V. M. (1997) IRAK (Pelle) family member IRAK-2 and MyD88 as proximal mediators of IL-1 signaling. Science **278**, 1612–5.

51 Wesche, H., Gao, X., Li, X., Kirschning, C. J., Stark, G. R. and Cao, Z. (1999) IRAK-M is a novel member of the Pelle/interleukin-1 receptor-associated kinase (IRAK) family. J. Biol. Chem. **274**, 19403–10.

52 Li, S., Strelow, A., Fontana, E. J. and Wesche, H. (2002) IRAK-4: a novel member of the IRAK family with the properties of an IRAK-kinase. Proc. Natl. Acad. Sci. U. S. A. **99**, 5567–5572.

53 Neumann, D., Kollewe, C., Resch, K. and Martin, M. U. (2007) The death domain of IRAK-1: An oligomerization domain mediating interactions with MyD88, Tollip, IRAK-1, and IRAK-4. Biochem. Biophys. Res. Commun. **354**, 1089–1094.

54 Ye, H., Arron, J. R., Lamothe, B., Cirilli, M., Kobayashi, T., Shevde, N. K., Segal, D., Dzivenu, O. K., Vologodskaia, M., Yim, M., et al. (2002) Distinct molecular mechanism for initiating TRAF6 signalling. Nature, Department of Biochemistry, Weill Medical College of Cornell University, New York, New York 10021, USA. DOI - 10.1038/nature00888 SRC - Pubmed ID2 - 12140561 FG - 0 **418**, 443–7.

55 Kawagoe, T., Sato, S., Jung, A., Yamamoto, M., Matsui, K., Kato, H., Uematsu, S., Takeuchi, O. and Akira, S. (2007) Essential role of IRAK-4 protein and its kinase activity in Toll-like receptor-mediated immune responses but not in TCR signaling. J. Exp. Med. **204**, 1013–24.

56 Suzuki, N., Suzuki, S., Duncan, G. S., Millar, D. G., Wada, T., Mirtsos, C., Takada, H., Wakeham, A., Itie, A., Li, S., et al. (2002) Severe impairment of interleukin-1 and Toll-like receptor signalling in mice lacking IRAK-4. Nature **416**, 750–756.

57 Koziczak-Holbro, M., Joyce, C., Glück, A., Kinzel, B., Müller, M., Tschopp, C., Mathison, J. C., Davis, C. N. and Gram, H. (2007) IRAK-4 kinase activity is required for interleukin-1 (IL-1) receptor- and toll-like receptor 7-mediated signaling and gene expression. J. Biol. Chem. **282**, 13552–13560.

58 Cheng, H., Addona, T., Keshishian, H., Dahlstrand, E., Lu, C., Dorsch, M., Li, Z., Wang, A., Ocain, T. D., Li, P., et al. (2007) Regulation of IRAK-4 kinase activity via autophosphorylation within its activation loop. Biochem. Biophys. Res. Commun. **352**, 609–616.

59 Ferrao, R., Zhou, H., Shan, Y., Liu, Q., Li, Q., Shaw, D. E., Li, X. and Wu, H. (2014) IRAK4 Dimerization and trans-Autophosphorylation Are Induced by Myddosome Assembly. Mol. Cell, Elsevier Inc. **55**, 891–903.

60 Pauls, E., Nanda, S. K., Smith, H., Toth, R., Arthur, J. S. C. and Cohen, P. (2013) Two phases of inflammatory mediator production defined by the study of IRAK2 and IRAK1 knock-in mice. J. Immunol. **191**, 2717–30.

61 Kollewe, C., Mackensen, A. C., Neumann, D., Knop, J., Cao, P., Li, S., Wesche, H. and Martin, M. U. (2004) Sequential Autophosphorylation Steps in the Interleukin-1 Receptor-associated Kinase-1 Regulate its Availability as an Adapter in Interleukin-1 Signaling. J. Biol. Chem. **279**, 5227–5236.

62 Kawagoe, T., Sato, S., Matsushita, K., Kato, H., Matsui, K., Kumagai, Y., Saitoh, T., Kawai,

T., Takeuchi, O. and Akira, S. (2008) Sequential control of Toll-like receptor-dependent responses by IRAK1 and IRAK2. Nat. Immunol. **9**, 684–91.

63 Kobayashi, K., Hernandez, L. D., Galan, J. E., Janeway Jr., C. A., Medzhitov, R. and Flavell, R. A. (2002) IRAK-M is a negative regulator of Toll-like receptor signaling. Cell **110**, 191–202.

64 Cao, Z., Xiong, J., Takeuchi, M., Kurama, T. and Goeddel, D. V. (1996) TRAF6 is a signal transducer for interleukin-1. Nature **383**, 443–6.

65 Rothe, M., Wong, S. C., Henzel, W. J. and Goeddel, D. V. (1994) A novel family of putative signal transducers associated with the cytoplasmic domain of the 75 kDa tumor necrosis factor receptor. Cell **78**, 681–692.

66 Zotti, T., Vito, P. and Stilo, R. (2012) The seventh ring: Exploring TRAF7 functions. J. Cell. Physiol. **227**, 1280–1284.

67 Lomaga, M. a, Yeh, W. C., Sarosi, I., Duncan, G. S., Furlonger, C., Ho, A., Morony, S., Capparelli, C., Van, G., Kaufman, S., et al. (1999) TRAF6 deficiency results in osteopetrosis and defective interleukin-1, CD40, and LPS signaling. Genes Dev., Department of Pharmaceutical Sciences, Faculty of Pharmacy, University of Toronto, Toronto, Ontario, Canada M5S 2S2. SRC - Pubmed ID2 - 10215628 FG - 0 **13**, 1015–24.

68 Lorick, K. L., Jensen, J. P., Fang, S., Ong, a M., Hatakeyama, S. and Weissman, a M. (1999) RING fingers mediate ubiquitin-conjugating enzyme (E2)-dependent ubiquitination. Proc. Natl. Acad. Sci. U. S. A. **96**, 11364–9.

69 Deng, L., Wang, C., Spencer, E., Yang, L., Braun, a, You, J., Slaughter, C., Pickart, C. and Chen, Z. J. (2000) Activation of the IkappaB kinase complex by TRAF6 requires a dimeric ubiquitin-conjugating enzyme complex and a unique polyubiquitin chain. Cell **103**, 351–61.

70 Walsh, M. C., Kim, G. K., Maurizio, P. L., Molnar, E. E. and Choi, Y. (2008) TRAF6 autoubiquitination-independent activation of the NFkappaB and MAPK pathways in response to IL-1 and RANKL. PLoS One **3**, e4064.

71 Lamothe, B., Besse, A., Campos, A. D., Webster, W. K., Wu, H. and Darnay, B. G. (2007) Site-specific Lys-63-linked tumor necrosis factor receptor-associated factor 6 auto-ubiquitination is a critical determinant of IκB kinase activation. J. Biol. Chem. **282**, 4102–4112.

72 Zheng, C., Kabaleeswaran, V., Wang, Y., Cheng, G. and Wu, H. (2010) Crystal Structures of the TRAF2: cIAP2 and the TRAF1: TRAF2: cIAP2 Complexes: Affinity, Specificity, and Regulation. Mol. Cell, Elsevier Ltd **38**, 101–113.

73 Muroi, M. and Tanamoto, K. (2008) TRAF6 distinctively mediates MyD88- and IRAK-1-induced activation of NF-kappaB. J. Leukoc. Biol. **83**, 702–7.

74 Baud, V., Liu, Z. G., Bennett, B., Suzuki, N., Xia, Y. and Karin, M. (1999) Signaling by proinflammatory cytokines: Oligomerization of TRAF2 and TRAF6 is sufficient for JNK and IKK activation and target gene induction via an amino-terminal effector domain. Genes Dev. **13**, 1297–308.

75 Yin, Q., Lin, S.-C., Lamothe, B., Lu, M., Lo, Y.-C., Hura, G., Zheng, L., Rich, R. L., Campos, A. D., Myszka, D. G., et al. (2009) E2 interaction and dimerization in the crystal structure of TRAF6. Nat. Struct. Mol. Biol., Weill Medical College of Cornell University, New York, New York, USA. DOI - 10.1038/nsmb.1605 SRC - Pubmed ID2 - 19465916 FG - 0 **16**,

658–666.

76 Wang, C., Deng, L., Hong, M., Akkaraju, G. R., Inoue, J. and Chen, Z. J. (2001) TAK1 is a ubiquitin-dependent kinase of MKK and IKK. Nature **412**, 346–51.

77 Yamaguchi, K., Shirakabe, K., Shibuya, H., Irie, K., Oishi, I., Ueno, N., Taniguchi, T., Nishida, E. and Matsumoto, K. (1995) Identification of a member of the MAPKKK family as a potential mediator of TGF-beta signal transduction. Science **270**, 2008–11.

78 Ninomiya-Tsuji, J., Kishimoto, K., Hiyama, A., Inoue, J., Cao, Z. and Matsumoto, K. (1999) The kinase TAK1 can activate the NIK-I kappaB as well as the MAP kinase cascade in the IL-1 signalling pathway. Nature **398**, 252–256.

79 Ajibade, A. a, Wang, H. Y. and Wang, R.-F. (2013) Cell type-specific function of TAK1 in innate immune signaling. Trends Immunol., Elsevier Ltd **34**, 307–16.

80 Cheung, P. C. F., Nebreda, A. R. and Cohen, P. (2004) TAB3, a new binding partner of the protein kinase TAK1. Biochem. J. **378**, 27–34.

81 Conner, S. H., Kular, G., Peggie, M., Shepherd, S., Schüttelkopf, A. W., Cohen, P. and Van Aalten, D. M. F. (2006) TAK1-binding protein 1 is a pseudophosphatase. Biochem. J. **399**, 427.

82 Kanayama, A., Seth, R. B., Sun, L., Ea, C.-K., Hong, M., Shaito, A., Chiu, Y.-H., Deng, L. and Chen, Z. J. (2004) TAB2 and TAB3 activate the NF-kappaB pathway through binding to polyubiquitin chains. Mol. Cell, Department of Molecular Biology, University of Texas Southwestern Medical Center, 5323 Harry Hines Boulevard, Dallas, TX 75390, USA. DOI - 10.1016/j.molcel.2004.08.008 SRC - Pubmed ID2 - 15327770 FG - 0 **15**, 535–48.

83 Shim, J.-H., Xiao, C., Paschal, A. E., Bailey, S. T., Rao, P., Hayden, M. S., Lee, K.-Y., Bussey, C., Steckel, M., Tanaka, N., et al. (2005) TAK1, but not TAB1 or TAB2, plays an essential role in multiple signaling pathways in vivo. Genes Dev. **19**, 2668–81.

84 Sato, S., Sanjo, H., Takeda, K., Ninomiya-Tsuji, J., Yamamoto, M., Kawai, T., Matsumoto, K., Takeuchi, O. and Akira, S. (2005) Essential function for the kinase TAK1 in innate and adaptive immune responses. Nat. Immunol., Akira Innate Immunity Project, Exploratory Research for Advanced Technology, Japan Science and Technology Agency. DOI - 10.1038/ni1255 SRC - Pubmed ID2 - 16186825 FG - 0 **6**, 1087–95.

85 Kishimoto, K., Matsumoto, K. and Ninomiya-Tsuji, J. (2000) TAK1 mitogen-activated protein kinase kinase kinase is activated by autophosphorylation within its activation loop. J. Biol. Chem. **275**, 7359–64.

86 Johnson, L. N., Noble, M. E. and Owen, D. J. (1996) Active and inactive protein kinases: structural basis for regulation. Cell **85**, 149–58.

87 Singhirunnusorn, P., Suzuki, S., Kawasaki, N., Saiki, I. and Sakurai, H. (2005) Critical roles of threonine 187 phosphorylation in cellular stress-induced rapid and transient activation of transforming growth factor-beta-activated kinase 1 (TAK1) in a signaling complex containing TAK1-binding protein TAB1 and TAB2. J. Biol. Chem., American Society for Biochemistry and Molecular Biology **280**, 7359–68.

88 Yu, Y., Ge, N., Xie, M., Sun, W., Burlingame, S., Pass, A. K., Nuchtern, J. G., Zhang, D., Fu, S., Schneider, M. D., et al. (2008) Phosphorylation of Thr-178 and Thr-184 in the TAK1 T-loop is required for interleukin (IL)-1-mediated optimal NFkappaB and AP-1 activation as well as IL-6 gene expression. J. Biol. Chem., American Society for Biochemistry and Molecular Biology **283**, 24497–505.

89 Shibuya, H., Yamaguchi, K., Shirakabe, K., Tonegawa, A., Gotoh, Y., Ueno, N., Irie, K., Nishida, E. and Matsumoto, K. (1996) TAB1: an activator of the TAK1 MAPKKK in TGF-beta signal transduction. Science **272**, 1179–82.

90 Sakurai, H., Miyoshi, H., Mizukami, J. and Sugita, T. (2000) Phosphorylation-dependent activation of TAK1 mitogen-activated protein kinase kinase kinase by TAB1. FEBS Lett. **474**, 141–5.

91 Sakurai, H., Nishi, A., Sato, N., Mizukami, J., Miyoshi, H. and Sugita, T. (2002) TAK1-TAB1 fusion protein: a novel constitutively active mitogen-activated protein kinase kinase kinase that stimulates AP-1 and NF-kappaB signaling pathways. Biochem. Biophys. Res. Commun., Discovery Research Laboratory, Tanabe Seiyaku Co., Ltd., 16-89 Kashima 3-chome, Yodogawa-ku, 532-8505, Osaka, Japan. SRC - Pubmed ID2 - 12372426 FG - 0 **297**, 1277–81.

92 Ono, K., Ohtomo, T., Sato, S., Sugamata, Y., Suzuki, M., Hisamoto, N., Ninomiya-Tsuji, J., Tsuchiya, M. and Matsumoto, K. (2001) An evolutionarily conserved motif in the TAB1 C-terminal region is necessary for interaction with and activation of TAK1 MAPKKK. J. Biol. Chem. **276**, 24396–400.

93 Brown, K., Vial, S. C. M., Dedi, N., Long, J. M., Dunster, N. J. and Cheetham, G. M. T. (2005) Structural basis for the interaction of TAK1 kinase with its activating protein TAB1. J. Mol. Biol. **354**, 1013–20.

94 Inagaki, M., Omori, E., Kim, J.-Y., Komatsu, Y., Scott, G., Ray, M. K., Yamada, G., Matsumoto, K., Mishina, Y. and Ninomiya-Tsuji, J. (2008) TAK1-binding protein 1, TAB1, mediates osmotic stress-induced TAK1 activation but is dispensable for TAK1-mediated cytokine signaling. J. Biol. Chem. **283**, 33080–6.

95 Takaesu, G., Kishida, S., Hiyama, A., Yamaguchi, K., Shibuya, H., Irie, K., Ninomiya-Tsuji, J. and Matsumoto, K. (2000) TAB2, a novel adaptor protein, mediates activation of TAK1 MAPKKK by linking TAK1 to TRAF6 in the IL-1 signal transduction pathway. Mol. Cell **5**, 649–58.

96 Ishitani, T., Takaesu, G., Ninomiya-Tsuji, J., Shibuya, H., Gaynor, R. B. and Matsumoto, K. (2003) Role of the TAB2-related protein TAB3 in IL-1 and TNF signaling. EMBO J. **22**, 6277–6288.

97 Xia, Z.-P., Sun, L., Chen, X., Pineda, G., Jiang, X., Adhikari, A., Zeng, W. and Chen, Z. J. (2009) Direct activation of protein kinases by unanchored polyubiquitin chains. Nature, Nature Publishing Group, Department of Molecular Biology, University of Texas, Southwestern Medical Center, Dallas, Texas 75390-9148, USA. DOI - 10.1038/nature08247 SRC - Pubmed ID2 - 19675569 FG - 0 **461**, 114–9.

98 Komander, D., Reyes-Turcu, F., Licchesi, J. D. F., Odenwaelder, P., Wilkinson, K. D. and Barford, D. (2009) Molecular discrimination of structurally equivalent Lys 63-linked and linear polyubiquitin chains. EMBO Rep., Nature Publishing Group **10**, 466–73.

99 Kulathu, Y., Akutsu, M., Bremm, A., Hofmann, K. and Komander, D. (2009) Two-sided ubiquitin binding explains specificity of the TAB2 NZF domain. Nat. Struct. Mol. Biol., Nature Publishing Group, Medical Research Council Laboratory of Molecular Biology, Cambridge, UK. DOI - 10.1038/nsmb.1731 SRC - Pubmed ID2 - 19935683 FG - 0 **16**, 1328–30.

100 Sanjo, H., Takeda, K., Tsujimura, T., Ninomiya-Tsuji, J., Matsumoto, K. and Akira, S. (2003) TAB2 is essential for prevention of apoptosis in fetal liver but not for interleukin-

1 signaling. Mol. Cell. Biol. **23**, 1231–8.

101 Ori, D., Kato, H., Sanjo, H., Tartey, S., Mino, T., Akira, S. and Takeuchi, O. (2013) Essential roles of K63-linked polyubiquitin-binding proteins TAB2 and TAB3 in B cell activation via MAPKs. J. Immunol., Laboratory of Infection and Prevention, Institute for Virus Research, Kyoto University, Kyoto 606-8507, Japan. DOI - 10.4049/jimmunol.1300173 SRC - Pubmed ID2 - 23509369 FG - 0 **190**, 4037–45.

102 Mercurio, F., Zhu, H., Murray, B. W., Shevchenko, A., Bennett, B. L., Li, J., Young, D. B., Barbosa, M., Mann, M., Manning, A., et al. (1997) IKK-1 and IKK-2: cytokine-activated IkappaB kinases essential for NF-kappaB activation. Science, American Association for the Advancement of Science **278**, 860–6.

103 Woronicz, J. D., Gao, X., Cao, Z., Rothe, M. and Goeddel, D. V. (1997) IkappaB kinase-beta: NF-kappaB activation and complex formation with IkappaB kinase-alpha and NIK. Science, American Association for the Advancement of Science **278**, 866–9.

104 Régnier, C. H., Song, H. Y., Gao, X., Goeddel, D. V, Cao, Z. and Rothe, M. (1997) Identification and characterization of an IkappaB kinase. Cell, Elsevier **90**, 373–83.

105 Rothwarf, D. M., Zandi, E., Natoli, G. and Karin, M. (1998) IKK-gamma is an essential regulatory subunit of the IkappaB kinase complex. Nature, Department of Pharmacology, University of California San Diego, La Jolla 92093-0636, USA. DOI - 10.1038/26261 SRC - Pubmed ID2 - 9751060 FG - 0 **395**, 297–300.

106 Yamaoka, S., Courtois, G., Bessia, C., Whiteside, S. T., Weil, R., Agou, F., Kirk, H. E., Kay, R. J. and Israël, A. (1998) Complementation Cloning of NEMO, a Component of the IκB Kinase Complex Essential for NF-κB Activation. Cell, Unité de Biologie Moléculaire de l'Expression Génique, URA 1773 CNRS, Institut Pasteur, Paris, France. SRC - Pubmed ID2 - 9657155 FG - 0 **93**, 1231–1240.

107 Delhase, M. (1999) Positive and Negative Regulation of IB Kinase Activity Through IKK Subunit Phosphorylation. Science (80-.). **284**, 309–313.

108 Ling, L., Cao, Z. and Goeddel, D. V. (1998) NF-kappaB-inducing kinase activates IKK-alpha by phosphorylation of Ser-176. Proc. Natl. Acad. Sci. U. S. A. **95**, 3792–7.

109 Xu, G., Lo, Y.-C., Li, Q., Napolitano, G., Wu, X., Jiang, X., Dreano, M., Karin, M. and Wu, H. (2011) Crystal structure of inhibitor of κB kinase β. Nature, Nature Publishing Group **472**, 325–30.

110 Marienfeld, R. B., Palkowitsch, L. and Ghosh, S. (2006) Dimerization of the I kappa B kinase-binding domain of NEMO is required for tumor necrosis factor alpha-induced NF-kappa B activity. Mol. Cell. Biol., American Society for Microbiology **26**, 9209–19.

111 Rahighi, S., Ikeda, F., Kawasaki, M., Akutsu, M., Suzuki, N., Kato, R., Kensche, T., Uejima, T., Bloor, S., Komander, D., et al. (2009) Specific recognition of linear ubiquitin chains by NEMO is important for NF-kappaB activation. Cell, Structural Biology Research Center, Photon Factory, Institute of Materials Structure Science, High Energy Accelerator Research Organization (KEK), Tsukuba, Ibaraki, Japan. DOI - 10.1016/j.cell.2009.03.007 SRC - Pubmed ID2 - 19303852 FG - 0 **136**, 1098–109.

112 Schröfelbauer, B., Polley, S., Behar, M., Ghosh, G. and Hoffmann, A. (2012) NEMO ensures signaling specificity of the pleiotropic IKKβ by directing its kinase activity toward IκBα. Mol. Cell, Elsevier **47**, 111–21.

113 Israël, A. (2010) The IKK complex, a central regulator of NF-kappaB activation. Cold

Spring Harb. Perspect. Biol., Cold Spring Harbor Laboratory Press **2**, a000158.

114 Tegethoff, S., Behlke, J. and Scheidereit, C. (2003) Tetrameric oligomerization of IkappaB kinase gamma (IKKgamma) is obligatory for IKK complex activity and NF-kappaB activation. Mol. Cell. Biol., American Society for Microbiology **23**, 2029–41.

115 Scheidereit, C. (2006) IkappaB kinase complexes: gateways to NF-kappaB activation and transcription. Oncogene, Nature Publishing Group **25**, 6685–705.

116 Häcker, H. and Karin, M. (2006) Regulation and function of IKK and IKK-related kinases. Sci. STKE **2006**, re13.

117 Hayden, M. S. and Ghosh, S. (2008) Shared principles in NF-kappaB signaling. Cell, Elsevier **132**, 344–62.

118 Henkel, T., Machleidt, T., Alkalay, I., Krönke, M., Ben-Neriah, Y. and Baeuerle, P. A. (1993) Rapid proteolysis of I kappa B-alpha is necessary for activation of transcription factor NF-kappa B. Nature, Nature Publishing Group **365**, 182–5.

119 Clark, K., Nanda, S. and Cohen, P. (2013) Molecular control of the NEMO family of ubiquitin-binding proteins. Nat. Rev. Mol. Cell Biol., Nature Publishing Group, Medical Research Council (MRC) Protein Phosphorylation and Ubiquitylation Unit, College of Life Sciences, Sir James Black Centre, University of Dundee, Dundee, DD1 5EH, Scotland, UK. DOI - 10.1038/nrm3644 SRC - Pubmed ID2 - 23989959 FG - 0 **14**, 673–85.

120 McCool, K. W. and Miyamoto, S. (2012) DNA damage-dependent NF-κB activation: NEMO turns nuclear signaling inside out. Immunol. Rev., Medical Scientist Training Program, University of Wisconsin-Madison, Madison, WI 53705, USA. DOI - 10.1111/j.1600-065X.2012.01101.x SRC - Pubmed ID2 - 22435563 FG - 0 **246**, 311–26.

121 Sen, R. and Baltimore, D. (1986) Multiple nuclear factors interact with the immunoglobulin enhancer sequences. Cell, Elsevier **46**, 705–16.

122 Sen, R. and Baltimore, D. (1986) Inducibility of kappa immunoglobulin enhancer-binding protein Nf-kappa B by a posttranslational mechanism. Cell, Elsevier **47**, 921–8.

123 Baeuerle, P. A. and Baltimore, D. (1988) Activation of DNA-binding activity in an apparently cytoplasmic precursor of the NF-kappa B transcription factor. Cell, Elsevier **53**, 211–7.

124 Brockman, J. A., Scherer, D. C., McKinsey, T. A., Hall, S. M., Qi, X., Lee, W. Y. and Ballard, D. W. (1995) Coupling of a signal response domain in I kappa B alpha to multiple pathways for NF-kappa B activation. Mol. Cell. Biol. **15**, 2809–18.

125 Brown, K., Gerstberger, S., Carlson, L., Franzoso, G. and Siebenlist, U. (1995) Control of I kappa B-alpha proteolysis by site-specific, signal-induced phosphorylation. Science **267**, 1485–8.

126 Chen, Z., Hagler, J., Palombella, V. J., Melandri, F., Scherer, D., Ballard, D. and Maniatis, T. (1995) Signal-induced site-specific phosphorylation targets I kappa B alpha to the ubiquitin-proteasome pathway. Genes Dev. **9**, 1586–97.

127 Spencer, E., Jiang, J. and Chen, Z. J. (1999) Signal-induced ubiquitination of IkappaBalpha by the F-box protein Slimb/beta-TrCP. Genes Dev. **13**, 284–94.

128 Yaron, A., Hatzubai, A., Davis, M., Lavon, I., Amit, S., Manning, A. M., Andersen, J. S., Mann, M., Mercurio, F. and Ben-Neriah, Y. (1998) Identification of the receptor

component of the IkappaBalpha-ubiquitin ligase. Nature **396**, 590–4.

129 Winston, J. T., Strack, P., Beer-Romero, P., Chu, C. Y., Elledge, S. J. and Harper, J. W. (1999) The SCFbeta-TRCP-ubiquitin ligase complex associates specifically with phosphorylated destruction motifs in IkappaBalpha and beta-catenin and stimulates IkappaBalpha ubiquitination in vitro. Genes Dev. **13**, 270–83.

130 Ghosh, S. and Karin, M. (2002) Missing pieces in the NF-kappaB puzzle. Cell **109 Suppl**, S81-96.

131 Sakurai, H., Chiba, H., Miyoshi, H., Sugita, T. and Toriumi, W. (1999) IkappaB kinases phosphorylate NF-kappaB p65 subunit on serine 536 in the transactivation domain. J. Biol. Chem. **274**, 30353–6.

132 Buss, H., Dörrie, A., Schmitz, M. L., Hoffmann, E., Resch, K. and Kracht, M. (2004) Constitutive and interleukin-1-inducible phosphorylation of p65 NF-{kappa}B at serine 536 is mediated by multiple protein kinases including I{kappa}B kinase (IKK)-{alpha}, IKK{beta}, IKK{epsilon}, TRAF family member-associated (TANK)-binding kinase 1 (TBK. J. Biol. Chem. **279**, 55633–43.

133 Pradère, J.-P., Hernandez, C., Koppe, C., Friedman, R. A., Luedde, T. and Schwabe, R. F. (2016) Negative regulation of NF-κB p65 activity by serine 536 phosphorylation. Sci. Signal. **9**, ra85.

134 Hu, Y., Baud, V., Delhase, M., Zhang, P., Deerinck, T., Ellisman, M., Johnson, R. and Karin, M. (1999) Abnormal morphogenesis but intact IKK activation in mice lacking the IKKalpha subunit of IkappaB kinase. Science **284**, 316–20.

135 Clark, K., Peggie, M., Plater, L., Sorcek, R. J., Young, E. R. R., Madwed, J. B., Hough, J., McIver, E. G. and Cohen, P. (2011) Novel cross-talk within the IKK family controls innate immunity. Biochem. J. **434**, 93–104.

136 Dejardin, E., Droin, N. M., Delhase, M., Haas, E., Cao, Y., Makris, C., Li, Z.-W., Karin, M., Ware, C. F. and Green, D. R. (2002) The lymphotoxin-beta receptor induces different patterns of gene expression via two NF-kappaB pathways. Immunity **17**, 525–35.

137 Claudio, E., Brown, K., Park, S., Wang, H. and Siebenlist, U. (2002) BAFF-induced NEMO-independent processing of NF-kappa B2 in maturing B cells. Nat. Immunol. **3**, 958–65.

138 Pomerantz, J. L. and Baltimore, D. (2002) Two pathways to NF-kappaB. Mol. Cell **10**, 693–5.

139 Senftleben, U., Cao, Y., Xiao, G., Greten, F. R., Krähn, G., Bonizzi, G., Chen, Y., Hu, Y., Fong, A., Sun, S. C., et al. (2001) Activation by IKKalpha of a second, evolutionary conserved, NF-kappa B signaling pathway. Science **293**, 1495–9.

140 Li, Z. W., Chu, W., Hu, Y., Delhase, M., Deerinck, T., Ellisman, M., Johnson, R. and Karin, M. (1999) The IKKbeta subunit of IkappaB kinase (IKK) is essential for nuclear factor kappaB activation and prevention of apoptosis. J. Exp. Med. **189**, 1839–45.

141 Rudolph, D., Yeh, W. C., Wakeham, A., Rudolph, B., Nallainathan, D., Potter, J., Elia, A. J. and Mak, T. W. (2000) Severe liver degeneration and lack of NF-kappaB activation in NEMO/IKKgamma-deficient mice. Genes Dev. **14**, 854–62.

142 Makris, C., Godfrey, V. L., Krähn-Senftleben, G., Takahashi, T., Roberts, J. L., Schwarz, T., Feng, L., Johnson, R. S. and Karin, M. (2000) Female mice heterozygous for IKK gamma/NEMO deficiencies develop a dermatopathy similar to the human X-linked

disorder incontinentia pigmenti. Mol. Cell **5**, 969–79.

143 Wu, C.-J., Conze, D. B., Li, T., Srinivasula, S. M. and Ashwell, J. D. (2006) Sensing of Lys 63-linked polyubiquitination by NEMO is a key event in NF-kappaB activation [corrected]. Nat. Cell Biol., Laboratory of Immune Cell Biology, National Cancer Institute, National Institutes of Health, Bethesda, MD 20892, USA. DOI - 10.1038/ncb1384 SRC - Pubmed ID2 - 16547522 FG - 0 **8**, 398–406.

144 Ea, C.-K., Deng, L., Xia, Z.-P., Pineda, G. and Chen, Z. J. (2006) Activation of IKK by TNFα Requires Site-Specific Ubiquitination of RIP1 and Polyubiquitin Binding by NEMO. Mol. Cell, Howard Hughes Medical Institute, Department of Molecular Biology, University of Texas Southwestern Medical Center, Dallas, Texas 75390, USA. DOI - 10.1016/j.molcel.2006.03.026 SRC - Pubmed ID2 - 16603398 FG - 0 **22**, 245–257.

145 Kensche, T., Tokunaga, F., Ikeda, F., Goto, E., Iwai, K. and Dikic, I. (2012) Analysis of nuclear factor-κB (NF-κB) essential modulator (NEMO) binding to linear and lysine-linked ubiquitin chains and its role in the activation of NF-κB. J. Biol. Chem., American Society for Biochemistry and Molecular Biology, Buchmann Institute for Molecular Life Sciences and Institute of Biochemistry II, Goethe University School of Medicine, Theodor-Stern-Kai 7, D-60590 Frankfurt, Main, Germany. DOI - 10.1074/jbc.M112.347195 SRC - Pubmed ID2 - 22605335 FG - 0 **287**, 23626–34.

146 Lo, Y.-C., Lin, S.-C., Rospigliosi, C. C., Conze, D. B., Wu, C.-J., Ashwell, J. D., Eliezer, D. and Wu, H. (2009) Structural basis for recognition of diubiquitins by NEMO. Mol. Cell, Elsevier Ltd **33**, 602–15.

147 Hubeau, M., Ngadjeua, F., Puel, A., Israel, L., Feinberg, J., Chrabieh, M., Belani, K., Bodemer, C., Fabre, I., Plebani, A., et al. (2011) New mechanism of X-linked anhidrotic ectodermal dysplasia with immunodeficiency: impairment of ubiquitin binding despite normal folding of NEMO protein. Blood **118**, 926–35.

148 Ninomiya-Tsuji, J., Kajino, T., Ono, K., Ohtomo, T., Matsumoto, M., Shiina, M., Mihara, M., Tsuchiya, M. and Matsumoto, K. (2003) A resorcylic acid lactone, 5Z-7-oxozeaenol, prevents inflammation by inhibiting the catalytic activity of TAK1 MAPK kinase kinase. J. Biol. Chem., Department of Molecular Biology, Graduate School of Science, Nagoya University, and CREST, Japan Science and Technology Corporation, Chikusa-ku, Nagoya 464-8602, Japan. DOI - 10.1074/jbc.M207453200 SRC - Pubmed ID2 - 12624112 FG - 0 **278**, 18485–90.

149 Pauls, E., Shpiro, N., Peggie, M., Young, E. R., Sorcek, R. J., Tan, L., Choi, H. G. and Cohen, P. (2012) Essential role for IKKbeta in production of type 1 interferons by plasmacytoid dendritic cells. J Biol Chem, MRC Protein Phosphorylation Unit, The Sir James Black Centre, College of Life Sciences, University of Dundee, Scotland DD1 5EH, United Kingdom. DOI - 10.1074/jbc.M112.345405 SRC - Pubmed ID2 - 22511786 FG - 0 **287**, 19216–19228.

150 Kirisako, T., Kamei, K., Murata, S., Kato, M., Fukumoto, H., Kanie, M., Sano, S., Tokunaga, F., Tanaka, K. and Iwai, K. (2006) A ubiquitin ligase complex assembles linear polyubiquitin chains. EMBO J., Department of Molecular Cell Biology, Graduate School of Medicine, Osaka City University, Osaka, Japan. DOI - 10.1038/sj.emboj.7601360 SRC - Pubmed ID2 - 17006537 FG - 0 **25**, 4877–87.

151 Gerlach, B., Cordier, S. M., Schmukle, A. C., Emmerich, C. H., Rieser, E., Haas, T. L., Webb, A. I., Rickard, J. a., Anderton, H., Wong, W. W.-L. W.-L., et al. (2011) Linear ubiquitination prevents inflammation and regulates immune signalling. Nature **471**, 591–6.

152 Tokunaga, F., Nakagawa, T., Nakahara, M., Saeki, Y., Taniguchi, M., Sakata, S., Tanaka, K., Nakano, H. and Iwai, K. (2011) SHARPIN is a component of the NF-κB-activating linear ubiquitin chain assembly complex. Nature, Department of Biophysics and Biochemistry, Graduate School of Medicine, Osaka University, Suita, Osaka 565-0871, Japan. DOI - 10.1038/nature09815 SRC - Pubmed ID2 - 21455180 FG - 0 **471**, 633–6.

153 Ikeda, F., Deribe, Y. L., Skånland, S. S., Stieglitz, B., Grabbe, C., Franz-Wachtel, M., van Wijk, S. J. L., Goswami, P., Nagy, V., Terzic, J., et al. (2011) SHARPIN forms a linear ubiquitin ligase complex regulating NF-κB activity and apoptosis. Nature, Frankfurt Institute for Molecular Life Sciences and Institute of Biochemistry II, Goethe University School of Medicine, Theodor-Stern-Kai 7, D-60590 Frankfurt, Main, Germany. DOI - 10.1038/nature09814 SRC - Pubmed ID2 - 21455181 FG - 0 **471**, 637–41.

154 Wenzel, D. M., Lissounov, A., Brzovic, P. S. and Klevit, R. E. (2011) UBCH7 reactivity profile reveals parkin and HHARI to be RING/HECT hybrids. Nature, Nature Publishing Group **474**, 105–8.

155 Fu, B., Li, S., Wang, L., Berman, M. A. and Dorf, M. E. (2014) The ubiquitin conjugating enzyme UBE2L3 regulates TNFα-induced linear ubiquitination. Cell Res. **24**, 376–9.

156 Stieglitz, B., Morris-Davies, A. C., Koliopoulos, M. G., Christodoulou, E. and Rittinger, K. (2012) LUBAC synthesizes linear ubiquitin chains via a thioester intermediate. EMBO Rep., Nature Publishing Group **13**, 840–6.

157 Stieglitz, B., Rana, R. R., Koliopoulos, M. G., Morris-Davies, A. C., Schaeffer, V., Christodoulou, E., Howell, S., Brown, N. R., Dikic, I. and Rittinger, K. (2013) Structural basis for ligase-specific conjugation of linear ubiquitin chains by HOIP. Nature, Nature Publishing Group **503**, 422–426.

158 Emmerich, C. H., Ordureau, A., Strickson, S., Arthur, J. S. C., Pedrioli, P. G. a., Komander, D. and Cohen, P. (2013) Activation of the canonical IKK complex by K63/M1-linked hybrid ubiquitin chains. Proc. Natl. Acad. Sci., Medical Research Council Protein Phosphorylation and Ubiquitylation Unit and Division of Cell Signaling and Immunology, Sir James Black Centre, University of Dundee, Dundee DD1 5EH, Scotland, United Kingdom. DOI - 10.1073/pnas.1314715110 SRC - Pubmed ID **110**, 15247–15252.

159 Tokunaga, F., Sakata, S., Saeki, Y., Satomi, Y., Kirisako, T., Kamei, K., Nakagawa, T., Kato, M., Murata, S., Yamaoka, S., et al. (2009) Involvement of linear polyubiquitylation of NEMO in NF-kappaB activation. Nat. Cell Biol., Department of Biophysics and Biochemistry, Graduate School of Medicine and Cell Biology and Metabolism Group, Graduate School of Frontier Biosciences, Osaka University, Suita, Osaka 565-0871, Japan. DOI - 10.1038/ncb1821 SRC - Pubmed ID2 - 19136968 FG **11**, 123–32.

160 Bloor, S., Ryzhakov, G., Wagner, S., Butler, P. J. G., Smith, D. L., Krumbach, R., Dikic, I. and Randow, F. (2008) Signal processing by its coil zipper domain activates IKK gamma. Proc. Natl. Acad. Sci. U. S. A. **105**, 1279–84.

161 Lopez-Pelaez, M., Lamont, D. J., Peggie, M., Shpiro, N., Gray, N. S. and Cohen, P. (2014) Protein kinase IKKβ-catalyzed phosphorylation of IRF5 at Ser462 induces its dimerization and nuclear translocation in myeloid cells. Proc. Natl. Acad. Sci. U. S. A., Medical Research Council Protein Phosphorylation and Ubiquitylation Unit, and. DOI - 10.1073/pnas.1418399111 SRC - Pubmed ID2 - 25326418 FG - 0 **111**, 17432–7.

162 Ren, J., Chen, X. and Chen, Z. J. (2014) IKKβ is an IRF5 kinase that instigates inflammation. Proc. Natl. Acad. Sci. U. S. A., Department of Molecular Biology and. DOI - 10.1073/pnas.1418516111 SRC - Pubmed ID2 - 25326420 FG - 0 **111**, 17438–43.

163 Waterfield, M. R., Zhang, M., Norman, L. P. and Sun, S. C. (2003) NF-kappaB1/p105 regulates lipopolysaccharide-stimulated MAP kinase signaling by governing the stability and function of the Tpl2 kinase. Mol. Cell **11**, 685–94.

164 Lang, V., Symons, A., Watton, S. J., Janzen, J., Soneji, Y., Beinke, S., Howell, S. and Ley, S. C. (2004) ABIN-2 forms a ternary complex with TPL-2 and NF-kappa B1 p105 and is essential for TPL-2 protein stability. Mol. Cell. Biol. **24**, 5235–48.

165 Waterfield, M., Jin, W., Reiley, W., Zhang, M. and Sun, S. (2004) IkappaB kinase is an essential component of the Tpl2 signaling pathway. Mol. Cell. Biol., Department of Microbiology and Immunology, Pennsylvania State University College of Medicine, 500 University Dr., Hershey, PA 17033, USA. sxs70@psu.edu DOI - 10.1128/MCB.24.13.6040-6048.2004 SRC - Pubmed ID2 - 15199157 FG - 0 **24**, 6040–8.

166 Beinke, S., Robinson, M. J., Hugunin, M. and Ley, S. C. (2004) Lipopolysaccharide activation of the TPL-2/MEK/extracellular signal-regulated kinase mitogen-activated protein kinase cascade is regulated by IkappaB kinase-induced proteolysis of NF-kappaB1 p105. Mol. Cell. Biol., National Institute for Medical Research, Division of Immune Cell Biology, The Ridgeway, Mill Hill, London NW7 1AA, United Kingdom. DOI - 10.1128/MCB.24.21.9658-9667.2004 SRC - Pubmed ID2 - 15485931 FG - 0 **24**, 9658–67.

167 Dumitru, C. D., Ceci, J. D., Tsatsanis, C., Kontoyiannis, D., Stamatakis, K., Lin, J. H., Patriotis, C., Jenkins, N. A., Copeland, N. G., Kollias, G., et al. (2000) TNF-alpha induction by LPS is regulated posttranscriptionally via a Tpl2/ERK-dependent pathway. Cell **103**, 1071–83.

168 Rousseau, S., Papoutsopoulou, M., Symons, A., Cook, D., Lucocq, J. M., Prescott, A. R., O'Garra, A., Ley, S. C. and Cohen, P. (2008) TPL2-mediated activation of ERK1 and ERK2 regulates the processing of pre-TNF alpha in LPS-stimulated macrophages. J. Cell Sci. **121**, 149–54.

169 Moss, M. L., Jin, S. L., Milla, M. E., Bickett, D. M., Burkhart, W., Carter, H. L., Chen, W. J., Clay, W. C., Didsbury, J. R., Hassler, D., et al. (1997) Cloning of a disintegrin metalloproteinase that processes precursor tumour-necrosis factor-alpha. Nature.

170 Menon, M. B. and Gaestel, M. (2016) TPL2 meets p38MAPK: emergence of a novel positive feedback loop in inflammation. Biochem. J. **473**, 2995–9.

171 Cargnello, M. and Roux, P. P. (2011) Activation and function of the MAPKs and their substrates, the MAPK-activated protein kinases. Microbiol. Mol. Biol. Rev., American Society for Microbiology **75**, 50–83.

172 Hauge, C. and Frödin, M. (2006) RSK and MSK in MAP kinase signalling. J. Cell Sci. **119**, 3021–3023.

173 Zaru, R., Ronkina, N., Gaestel, M., Arthur, J. S. C. and Watts, C. (2007) The MAPK-activated kinase Rsk controls an acute Toll-like receptor signaling response in dendritic cells and is activated through two distinct pathways. Nat. Immunol. **8**, 1227–1235.

174 Kim, C., Sano, Y., Todorova, K., Carlson, B. A., Arpa, L., Celada, A., Lawrence, T., Otsu, K., Brissette, J. L., Arthur, J. S. C., et al. (2008) The kinase p38 alpha serves cell type-specific inflammatory functions in skin injury and coordinates pro- and anti-inflammatory gene expression. Nat. Immunol. **9**, 1019–27.

175 Ananieva, O., Darragh, J., Johansen, C., Carr, J. M., McIlrath, J., Park, J. M., Wingate, A.,

Monk, C. E., Toth, R., Santos, S. G., et al. (2008) The kinases MSK1 and MSK2 act as negative regulators of Toll-like receptor signaling. Nat. Immunol. **9**, 1028–36.

176 Darragh, J., Ananieva, O., Courtney, A., Elcombe, S. and Arthur, J. S. C. (2010) MSK1 regulates the transcription of IL-1ra in response to TLR activation in macrophages. Biochem. J. **425**, 595–602.

177 Guma, M., Hammaker, D., Topolewski, K., Corr, M., Boyle, D. L., Karin, M. and Firestein, G. S. (2012) Antiinflammatory functions of p38 in mouse models of rheumatoid arthritis: advantages of targeting upstream kinases MKK-3 or MKK-6. Arthritis Rheum. **64**, 2887–95.

178 Hitti, E., Iakovleva, T., Brook, M., Deppenmeier, S., Gruber, A. D., Radzioch, D., Clark, A. R., Blackshear, P. J., Kotlyarov, A. and Gaestel, M. (2006) Mitogen-activated protein kinase-activated protein kinase 2 regulates tumor necrosis factor mRNA stability and translation mainly by altering tristetraprolin expression, stability, and binding to adenine/uridine-rich element. Mol. Cell. Biol. **26**, 2399–2407.

179 Tiedje, C., Ronkina, N., Tehrani, M., Dhamija, S., Laass, K., Holtmann, H., Kotlyarov, A. and Gaestel, M. (2012) The p38/MK2-Driven Exchange between Tristetraprolin and HuR Regulates AU-Rich Element-Dependent Translation. PLoS Genet. **8**.

180 Cheung, P. C. F., Campbell, D. G., Nebreda, A. R. and Cohen, P. (2003) Feedback control of the protein kinase TAK1 by SAPK2a/p38alpha. EMBO J., MRC Protein Phosphorylation Unit, School of Life Sciences, MSI/WTB Complex, Dow Street, University of Dundee, Dundee DD1 5EH, UK. DOI - 10.1093/emboj/cdg552 SRC - Pubmed ID2 - 14592977 FG - 0 **22**, 5793–805.

181 Mendoza, H., Campbell, D. G., Burness, K., Hastie, J., Ronkina, N., Shim, J.-H., Arthur, J. S. C., Davis, R. J., Gaestel, M., Johnson, G. L., et al. (2008) Roles for TAB1 in regulating the IL-1-dependent phosphorylation of the TAB3 regulatory subunit and activity of the TAK1 complex. Biochem. J. **409**, 711–22.

182 Morrison, D. K. (2012) MAP kinase pathways. Cold Spring Harb. Perspect. Biol. **4**, 1–5.

183 Pattison, M. J., Mitchell, O., Flynn, H. R., Chen, C.-S., Yang, H.-T., Ben-Addi, H., Boeing, S., Snijders, A. P. and Ley, S. C. (2016) TLR and TNF-R1 activation of the MKK3/MKK6-p38α axis in macrophages is mediated by TPL-2 kinase. Biochem. J. **473**, 2845–61.

184 Tournier, C., Dong, C., Turner, T. K., Jones, S. N., Flavell, R. A. and Davis, R. J. (2001) MKK7 is an essential component of the JNK signal transduction pathway activated by proinflammatory cytokines. Genes Dev. **15**, 1419–26.

185 Gupta, S., Campbell, D., Dérijard, B. and Davis, R. J. (1995) Transcription factor ATF2 regulation by the JNK signal transduction pathway. Science **267**, 389–93.

186 Davis, R. J. (2000) Signal transduction by the JNK group of MAP kinases. Cell **103**, 239–52.

187 Picard, C., von Bernuth, H., Ghandil, P., Chrabieh, M., Levy, O., Arkwright, P. D., McDonald, D., Geha, R. S., Takada, H., Krause, J. C., et al. (2010) Clinical features and outcome of patients with IRAK-4 and MyD88 deficiency. Medicine (Baltimore). **89**, 403–25.

188 Picard, C., Casanova, J.-L. and Puel, A. (2011) Infectious diseases in patients with IRAK-4, MyD88, NEMO, or IκBα deficiency. Clin. Microbiol. Rev., Study Center of Primary Immunodeficiencies, Assistance Publique Hoˆpitaux de Paris, Necker Hospital, France.

capucine.picard@inserm.fr DOI - 10.1128/CMR.00001-11 SRC - Pubmed ID2 - 21734245 FG - 0 **24**, 490–7.

189 Ben-Neriah, Y. and Karin, M. (2011) Inflammation meets cancer, with NF-κB as the matchmaker. Nat. Immunol. **12**, 715–23.

190 Hamerman, J. A., Pottle, J., Ni, M., He, Y., Zhang, Z.-Y. and Buckner, J. H. (2016) Negative regulation of TLR signaling in myeloid cells--implications for autoimmune diseases. Immunol. Rev. **269**, 212–27.

191 von Bernuth, H., Picard, C., Jin, Z., Pankla, R., Xiao, H., Ku, C. L., Chrabieh, M., Mustapha, I. B., Ghandil, P., Camcioglu, Y., et al. (2008) Pyogenic bacterial infections in humans with MyD88 deficiency. Science (80-.). **321**, 691–696.

192 Treon, S. P., Xu, L., Yang, G., Zhou, Y., Liu, X., Cao, Y., Sheehy, P., Manning, R. J., Patterson, C. J., Tripsas, C., et al. (2012) MYD88 L265P somatic mutation in Waldenström's macroglobulinemia. N. Engl. J. Med. **367**, 826–33.

193 Picard, C., Puel, A., Bonnet, M., Ku, C.-L., Bustamante, J., Yang, K., Soudais, C., Dupuis, S., Feinberg, J., Fieschi, C., et al. (2003) Pyogenic bacterial infections in humans with IRAK-4 deficiency. Science **299**, 2076–9.

194 Kim, T. W., Staschke, K., Bulek, K., Yao, J., Peters, K., Oh, K.-H., Vandenburg, Y., Xiao, H., Qian, W., Hamilton, T., et al. (2007) A critical role for IRAK4 kinase activity in Toll-like receptor-mediated innate immunity. J. Exp. Med. **204**, 1025–36.

195 Naito, A., Azuma, S., Tanaka, S., Miyazaki, T., Takaki, S., Takatsu, K., Nakao, K., Nakamura, K., Katsuki, M., Yamamoto, T., et al. (1999) Severe osteopetrosis, defective interleukin-1 signalling and lymph node organogenesis in TRAF6-deficient mice. Genes Cells **4**, 353–62.

196 Orange, J. S. and Geha, R. S. (2003) Finding NEMO: genetic disorders of NF-[kappa]B activation. J. Clin. Invest. **112**, 983–5.

197 Courtois, G., Smahi, A., Reichenbach, J., Döffinger, R., Cancrini, C., Bonnet, M., Puel, A., Chable-Bessia, C., Yamaoka, S., Feinberg, J., et al. (2003) A hypermorphic IkappaBalpha mutation is associated with autosomal dominant anhidrotic ectodermal dysplasia and T cell immunodeficiency. J. Clin. Invest. **112**, 1108–15.

198 Ran, F. A., Hsu, P. D., Wright, J., Agarwala, V., Scott, D. a and Zhang, F. (2013) Genome engineering using the CRISPR-Cas9 system. Nat. Protoc. **8**, 2281–308.

199 Tan, L., Nomanbhoy, T., Gurbani, D., Patricelli, M., Hunter, J., Geng, J., Herhaus, L., Zhang, J., Pauls, E., Ham, Y., et al. (2015) Discovery of type II inhibitors of tgfβ-activated kinase 1 (TAK1) and mitogen-activated protein kinase kinase kinase kinase 2 (MAP4K2). J. Med. Chem. **58**, 183–196.

200 Bain, J., Plater, L., Elliott, M., Shpiro, N., Hastie, C. J., McLauchlan, H., Klevernic, I., Arthur, J. S. C., Alessi, D. R. and Cohen, P. (2007) The selectivity of protein kinase inhibitors: a further update. Biochem. J., Division of Signal Transduction Therapy, College of Life Sciences, University of Dundee, Dundee DD1 5EH, Scotland, UK. DOI - 10.1042/BJ20070797 SRC - Pubmed ID2 - 17850214 FG - 0 **408**, 297–315.

201 Kuma, Y., Sabio, G., Bain, J., Shpiro, N., Márquez, R. and Cuenda, A. (2005) BIRB796 inhibits all p38 MAPK isoforms in vitro and in vivo. J. Biol. Chem. **280**, 19472–9.

202 Bradford, M. M. (1976) A rapid and sensitive method for the quantitation of microgram

quantities of protein utilizing the principle of protein-dye binding. Anal. Biochem. **72**, 248–54.

203 Polley, S., Huang, D.-B., Hauenstein, A. V, Fusco, A. J., Zhong, X., Vu, D., Schröfelbauer, B., Kim, Y., Hoffmann, A., Verma, I. M., et al. (2013) A structural basis for IκB kinase 2 activation via oligomerization-dependent trans auto-phosphorylation. PLoS Biol., Department of Chemistry & Biochemistry, University of California-San Diego, La Jolla, California, United States of America. DOI - 10.1371/journal.pbio.1001581 SRC - Pubmed ID2 - 23776406 FG - 0 **11**, e1001581.

204 Fleming, Y., Armstrong, C. G., Morrice, N., Paterson, A., Goedert, M. and Cohen, P. (2000) Synergistic activation of stress-activated protein kinase 1/c-Jun N-terminal kinase (SAPK1/JNK) isoforms by mitogen-activated protein kinase kinase 4 (MKK4) and MKK7. Biochem. J. **352 Pt 1**, 145–54.

205 Walsh, D. a, Perkins, J. P., Brosom, C. O., Ho, E. S. and Kreb, E. G. (1971) Catalysis of the phosphorylase kinase activation reaction. J. Biol. Chem. **246**, 1968–76.

206 Stegert, M. R., Hergovich, A., Tamaskovic, R., Bichsel, S. J. and Hemmings, B. a. (2005) Regulation of NDR protein kinase by hydrophobic motif phosphorylation mediated by the mammalian Ste20-like kinase MST3. Mol. Cell. Biol. **25**, 11019–29.

207 Clark, K., Plater, L., Peggie, M. and Cohen, P. (2009) Use of the pharmacological inhibitor BX795 to study the regulation and physiological roles of TBK1 and IkappaB kinase epsilon: a distinct upstream kinase mediates Ser-172 phosphorylation and activation. J. Biol. Chem. **284**, 14136–46.

208 Cong, L., Ran, F. A., Cox, D., Lin, S., Barretto, R., Habib, N., Hsu, P. D., Wu, X., Jiang, W., Marraffini, L. A., et al. (2013) Multiplex genome engineering using CRISPR/Cas systems. Science **339**, 819–23.

209 Mali, P., Yang, L., Esvelt, K. M., Aach, J., Guell, M., DiCarlo, J. E., Norville, J. E. and Church, G. M. (2013) RNA-guided human genome engineering via Cas9. Science **339**, 823–6.

210 Strickson, S., Emmerich, C. H., Goh, E. T. H., Zhang, J., Ian, K., Ortiz-Guerrero, J., Macartney, T., Hastie, J., Knebel, A., Peggie, M., et al. (2017) Identification of E3 ligase-dependent and independent roles of TRAF6. Press.

211 Lamothe, B., Campos, A. D., Webster, W. K., Gopinathan, A., Hur, L. and Darnay, B. G. (2008) The RING domain and first zinc finger of TRAF6 coordinate signaling by interleukin-1, lipopolysaccharide, and RANKL. J. Biol. Chem., Department of Experimental Therapeutics, The University of Texas M.D. Anderson Cancer Center, Houston, Texas 77030, USA. DOI - 10.1074/jbc.M802749200 SRC - Pubmed ID2 - 18617513 FG - 0 **283**, 24871–80.

212 Lu, M., Lin, S.-C., Huang, Y., Kang, Y. J., Rich, R., Lo, Y.-C., Myszka, D., Han, J. and Wu, H. (2007) XIAP induces NF-kappaB activation via the BIR1/TAB1 interaction and BIR1 dimerization. Mol. Cell **26**, 689–702.

213 Verhagen, A. M., Ekert, P. G., Pakusch, M., Silke, J., Connolly, L. M., Reid, G. E., Moritz, R. L., Simpson, R. J. and Vaux, D. L. (2000) Identification of DIABLO, a mammalian protein that promotes apoptosis by binding to and antagonizing IAP proteins. Cell **102**, 43–53.

214 Munoz, I. M., Szyniarowski, P., Toth, R., Rouse, J. and Lachaud, C. (2014) Improved Genome Editing in Human Cell Lines Using the CRISPR Method. PLoS One, Medical Research Council Protein Phosphorylation Unit, College of Life Sciences, University of

Dundee, Dundee, Scotland. DOI - 10.1371/journal.pone.0109752 SRC - Pubmed ID2 - 25303670 FG - 0 **9**, e109752.

215 Ran, F. A., Hsu, P. D., Lin, C. Y., Gootenberg, J. S., Konermann, S., Trevino, A. E., Scott, D. A., Inoue, A., Matoba, S., Zhang, Y., et al. (2013) Double nicking by RNA-guided CRISPR cas9 for enhanced genome editing specificity. Cell, Elsevier **154**, 1380–1389.

216 Shen, B., Zhang, W., Zhang, J., Zhou, J., Wang, J., Chen, L., Wang, L., Hodgkins, A., Iyer, V., Huang, X., et al. (2014) Efficient genome modification by CRISPR-Cas9 nickase with minimal off-target effects. Nat. Methods **11**, 399–402.

217 Chen, Y., Cao, J., Xiong, M., Petersen, A. J., Dong, Y., Tao, Y., Huang, C. T.-L., Du, Z. and Zhang, S.-C. (2015) Engineering Human Stem Cell Lines with Inducible Gene Knockout using CRISPR/Cas9. Cell Stem Cell, Elsevier Inc. **17**, 233–44.

218 Fulcher, L. J., Macartney, T., Bozatzi, P., Hornberger, A., Rojas-Fernandez, A. and Sapkota, G. P. (2016) An affinity-directed protein missile system for targeted proteolysis. Open Biol. **6**.

219 Suzuki, K., Tsunekawa, Y., Hernandez-Benitez, R., Wu, J., Zhu, J., Kim, E. J., Hatanaka, F., Yamamoto, M., Araoka, T., Li, Z., et al. (2016) In vivo genome editing via CRISPR/Cas9 mediated homology-independent targeted integration. Nature **540**, 144–149.

220 Lawler, S., Fleming, Y., Goedert, M. and Cohen, P. (1998) Synergistic activation of SAPK1/JNK1 by two MAP kinase kinases in vitro. Curr. Biol. **8**, 1387–1391.

221 Remy, G., Risco, A. M., Iñesta-Vaquera, F. A., González-Terán, B., Sabio, G., Davis, R. J. and Cuenda, A. (2010) Differential activation of p38MAPK isoforms by MKK6 and MKK3. Cell. Signal., Elsevier Inc. **22**, 660–667.

222 Lin, C.-C., Huoh, Y.-S., Schmitz, K. R., Jensen, L. E. and Ferguson, K. M. (2008) Pellino proteins contain a cryptic FHA domain that mediates interaction with phosphorylated IRAK1. Structure, Elsevier Ltd **16**, 1806–16.

223 Ordureau, A., Smith, H., Windheim, M., Peggie, M., Carrick, E., Morrice, N. and Cohen, P. (2008) The IRAK-catalysed activation of the E3 ligase function of Pellino isoforms induces the Lys63-linked polyubiquitination of IRAK1. Biochem. J. **409**, 43–52.

224 Smith, H., Peggie, M., Campbell, D. G., Vandermoere, F., Carrick, E. and Cohen, P. (2009) Identification of the phosphorylation sites on the E3 ubiquitin ligase Pellino that are critical for activation by IRAK1 and IRAK4. Proc. Natl. Acad. Sci. U. S. A. **106**, 4584–90.

225 Windheim, M., Stafford, M., Peggie, M. and Cohen, P. (2008) Interleukin-1 (IL-1) induces the Lys63-linked polyubiquitination of IL-1 receptor-associated kinase 1 to facilitate NEMO binding and the activation of IkappaBalpha kinase. Mol. Cell. Biol., American Society for Microbiology **28**, 1783–91.

226 Conze, D. B., Wu, C.-J., Thomas, J. A., Landstrom, A. and Ashwell, J. D. (2008) Lys63-Linked Polyubiquitination of IRAK-1 Is Required for Interleukin-1 Receptor- and Toll-Like Receptor-Mediated NF- B Activation. Mol. Cell. Biol. **28**, 3538–3547.

227 Ohtake, F., Saeki, Y., Ishido, S., Kanno, J. and Tanaka, K. (2016) The K48-K63 Branched Ubiquitin Chain Regulates NF-κB Signaling. Mol. Cell, Elsevier Inc. **64**, 251–266.

228 Ouyang, C., Nie, L., Gu, M., Wu, A., Han, X., Wang, X., Shao, J. and Xia, Z. (2014) Transforming growth factor (TGF)-β-activated kinase 1 (TAK1) activation requires phosphorylation of serine 412 by protein kinase A catalytic subunit α (PKACα) and X-

linked protein kinase (PRKX). J. Biol. Chem. **289**, 24226–37.

229 Kim, S. Il, Kwak, J. H., Wang, L. and Choi, M. E. (2008) Protein phosphatase 2A is a negative regulator of transforming growth factor-beta1-induced TAK1 activation in mesangial cells. J. Biol. Chem. **283**, 10753–63.

230 Hanada, M., Ninomiya-Tsuji, J., Komaki, K., Ohnishi, M., Katsura, K., Kanamaru, R., Matsumoto, K. and Tamura, S. (2001) Regulation of the TAK1 signaling pathway by protein phosphatase 2C. J. Biol. Chem. **276**, 5753–9.

231 Li, M. G., Katsura, K., Nomiyama, H., Komaki, K.-I., Ninomiya-Tsuji, J., Matsumoto, K., Kobayashi, T. and Tamura, S. (2003) Regulation of the interleukin-1-induced signaling pathways by a novel member of the protein phosphatase 2C family (PP2Cepsilon). J. Biol. Chem. **278**, 12013–21.

232 Kajino, T., Ren, H., Iemura, S.-I., Natsume, T., Stefansson, B., Brautigan, D. L., Matsumoto, K. and Ninomiya-Tsuji, J. (2006) Protein phosphatase 6 down-regulates TAK1 kinase activation in the IL-1 signaling pathway. J. Biol. Chem. **281**, 39891–6.

233 Omori, E., Inagaki, M., Mishina, Y., Matsumoto, K. and Ninomiya-Tsuji, J. (2012) Epithelial transforming growth factor β-activated kinase 1 (TAK1) is activated through two independent mechanisms and regulates reactive oxygen species. Proc. Natl. Acad. Sci. U. S. A. **109**, 3365–70.

234 Gu, M., Ouyang, C., Lin, W., Zhang, T., Cao, X., Xia, Z. and Wang, X. (2014) Phosphatase Holoenzyme PP1/GADD34 Negatively Regulates TLR Response by Inhibiting TAK1 Serine 412 Phosphorylation. J. Immunol. **192**, 2846–56.

235 Hilger, M., Bonaldi, T., Gnad, F. and Mann, M. (2009) Systems-wide analysis of a phosphatase knock-down by quantitative proteomics and phosphoproteomics. Mol. Cell. Proteomics **8**, 1908–20.

236 Boersema, P. J., Aye, T. T., Van Veen, T. A. B., Heck, A. J. R. and Mohammed, S. (2008) Triplex protein quantification based on stable isotope labeling by peptide dimethylation applied to cell and tissue lysates. Proteomics **8**, 4624–4632.

237 Boersema, P. J., Raijmakers, R., Lemeer, S., Mohammed, S. and Heck, A. J. R. (2009) Multiplex peptide stable isotope dimethyl labeling for quantitative proteomics. Nat. Protoc., Nature Publishing Group **4**, 484–94.

238 Catic, A., Collins, C., Church, G. M. and Ploegh, H. L. (2004) Preferred in vivo ubiquitination sites. Bioinformatics **20**, 3302–7.

239 Sorrentino, A., Thakur, N., Grimsby, S., Marcusson, A., von Bulow, V., Schuster, N., Zhang, S., Heldin, C.-H. and Landström, M. (2008) The type I TGF-beta receptor engages TRAF6 to activate TAK1 in a receptor kinase-independent manner. Nat. Cell Biol. **10**, 1199–207.

240 Yamazaki, K., Gohda, J., Kanayama, A., Miyamoto, Y., Sakurai, H., Yamamoto, M., Akira, S., Hayashi, H., Su, B. and Inoue, J. (2009) Two mechanistically and temporally distinct NF-kappaB activation pathways in IL-1 signaling. Sci. Signal. **2**, ra66.

241 Mao, R., Fan, Y., Mou, Y., Zhang, H., Fu, S. and Yang, J. (2011) TAK1 lysine 158 is required for TGF-β-induced TRAF6-mediated Smad-independent IKK/NF-κB and JNK/AP-1 activation. Cell. Signal., Elsevier Inc. **23**, 222–7.

242 Fan, Y., Yu, Y., Mao, R., Zhang, H. and Yang, J. (2011) TAK1 Lys-158 but not Lys-209 is

required for IL-1β-induced Lys63-linked TAK1 polyubiquitination and IKK/NF-κB activation. Cell. Signal. **23**, 660–5.

243 Fan, Y., Yu, Y., Shi, Y., Sun, W., Xie, M., Ge, N., Mao, R., Chang, A., Xu, G., Schneider, M. D., et al. (2010) Lysine 63-linked polyubiquitination of TAK1 at lysine 158 is required for tumor necrosis factor alpha- and interleukin-1beta-induced IKK/NF-kappaB and JNK/AP-1 activation. J. Biol. Chem. **285**, 5347–60.

244 Udeshi, N. D., Svinkina, T., Mertins, P., Kuhn, E., Mani, D. R., Qiao, J. W. and Carr, S. A. (2013) Refined preparation and use of anti-diglycine remnant (K-ε-GG) antibody enables routine quantification of 10,000s of ubiquitination sites in single proteomics experiments. Mol. Cell. Proteomics **12**, 825–31.

245 Udeshi, N. D., Mertins, P., Svinkina, T. and Carr, S. A. (2013) Large-scale identification of ubiquitination sites by mass spectrometry. Nat. Protoc., Nature Research **8**, 1950–60.

246 Fan, Y.-H., Yu, Y., Mao, R.-F., Tan, X.-J., Xu, G.-F., Zhang, H., Lu, X.-B., Fu, S.-B. and Yang, J. (2011) USP4 targets TAK1 to downregulate TNFα-induced NF-κB activation. Cell Death Differ. **18**, 1547–60.

247 Liu, X., Li, H., Zhong, B., Blonska, M., Gorjestani, S., Yan, M., Tian, Q., Zhang, D.-E., Lin, X. and Dong, C. (2013) USP18 inhibits NF-κB and NFAT activation during Th17 differentiation by deubiquitinating the TAK1-TAB1 complex. J. Exp. Med. **210**, 1575–90.

248 Yang, Z., Xian, H., Hu, J., Tian, S., Qin, Y., Wang, R.-F. and Cui, J. (2015) USP18 negatively regulates NF-κB signaling by targeting TAK1 and NEMO for deubiquitination through distinct mechanisms. Sci. Rep., Nature Publishing Group **5**, 12738.

249 Shin, M.-S., Shinghirunnusorn, P., Sugishima, Y., Nishimura, M., Suzuki, S., Koizumi, K., Saiki, I. and Sakurai, H. (2009) Cross interference with TNF-alpha-induced TAK1 activation via EGFR-mediated p38 phosphorylation of TAK1-binding protein 1. Biochim. Biophys. Acta, Elsevier B.V. **1793**, 1156–64.

250 Wolf, A., Beuerlein, K., Eckart, C., Weiser, H., Dickkopf, B., Müller, H., Sakurai, H. and Kracht, M. (2011) Identification and functional characterization of novel phosphorylation sites in TAK1-binding protein (TAB) 1. PLoS One **6**, e29256.

251 Yang, C.-Y., Li, J.-P., Chiu, L.-L., Lan, J.-L., Chen, D.-Y., Chuang, H.-C., Huang, C.-Y. and Tan, T.-H. (2014) Dual-specificity phosphatase 14 (DUSP14/MKP6) negatively regulates TCR signaling by inhibiting TAB1 activation. J. Immunol. **192**, 1547–57.

252 Charlaftis, N., Suddason, T., Wu, X., Anwar, S., Karin, M. and Gallagher, E. (2014) The MEKK1 PHD ubiquitinates TAB1 to activate MAPKs in response to cytokines. EMBO J. **33**, 2581–96.

253 Sapkota, G. P. (2013) The TGFbeta-induced phosphorylation and activation of p38 mitogen-activated protein kinase is mediated by MAP3K4 and MAP3K10 but not TAK1. Open Biol. **3**, 130067.

254 Theivanthiran, B., Kathania, M., Zeng, M., Anguiano, E., Basrur, V., Vandergriff, T., Pascual, V., Wei, W., Massoumi, R. and Venuprasad, K. (2015) The E3 ubiquitin ligase Itch inhibits p38α signaling and skin inflammation through the ubiquitylation of Tab1. Sci. Signal. **8**, ra22.

255 Ahmed, N., Zeng, M., Sinha, I., Polin, L., Wei, W.-Z., Rathinam, C., Flavell, R., Massoumi, R. and Venuprasad, K. (2011) The E3 ligase Itch and deubiquitinase Cyld act together to regulate Tak1 and inflammation. Nat. Immunol. **12**, 1176–83.

256 Pathak, S., Borodkin, V. S., Albarbarawi, O., Campbell, D. G., Ibrahim, A. and van Aalten, D. M. (2012) O-GlcNAcylation of TAB1 modulates TAK1-mediated cytokine release. EMBO J. **31**, 1394–404.

257 Tao, T., He, Z., Shao, Z. and Lu, H. (2016) TAB3 O-GlcNAcylation promotes metastasis of triple negative breast cancer. Oncotarget **7**, 1–12.

258 Ear, T., Fortin, C. F., Simard, F. a and McDonald, P. P. (2010) Constitutive association of TGF-beta-activated kinase 1 with the IkappaB kinase complex in the nucleus and cytoplasm of human neutrophils and its impact on downstream processes. J. Immunol. **184**, 3897–906.

259 Prickett, T. D., Ninomiya-Tsuji, J., Broglie, P., Muratore-Schroeder, T. L., Shabanowitz, J., Hunt, D. F. and Brautigan, D. L. (2008) TAB4 stimulates TAK1-TAB1 phosphorylation and binds polyubiquitin to direct signaling to NF-kappaB. J. Biol. Chem. **283**, 19245–54.

260 Lee, F. S., Hagler, J., Chen, Z. J. and Maniatis, T. (1997) Activation of the IkappaB alpha kinase complex by MEKK1, a kinase of the JNK pathway. Cell **88**, 213–22.

261 Lee, F. S., Peters, R. T., Dang, L. C. and Maniatis, T. (1998) MEKK1 activates both IkappaB kinase alpha and IkappaB kinase beta. Proc. Natl. Acad. Sci. U. S. A. **95**, 9319–24.

262 Yujiri, T., Ware, M., Widmann, C., Oyer, R., Russell, D., Chan, E., Zaitsu, Y., Clarke, P., Tyler, K., Oka, Y., et al. (2000) MEK kinase 1 gene disruption alters cell migration and c-Jun NH2-terminal kinase regulation but does not cause a measurable defect in NF-kappa B activation. Proc. Natl. Acad. Sci. U. S. A. **97**, 7272–7.

263 Zhao, Q. and Lee, F. S. (1999) Mitogen-activated protein kinase/ERK kinase kinases 2 and 3 activate nuclear factor-kappaB through IkappaB kinase-alpha and IkappaB kinase-beta. J. Biol. Chem. **274**, 8355–8.

264 Yang, J., Lin, Y., Guo, Z., Cheng, J., Huang, J., Deng, L., Liao, W., Chen, Z., Liu, Z. and Su, B. (2001) The essential role of MEKK3 in TNF-induced NF-kappaB activation. Nat. Immunol. **2**, 620–4.

265 Huang, Q., Yang, J., Lin, Y., Walker, C., Cheng, J., Liu, Z. and Su, B. (2004) Differential regulation of interleukin 1 receptor and Toll-like receptor signaling by MEKK3. Nat. Immunol. **5**, 98–103.

266 Yao, J., Kim, T. W., Qin, J., Jiang, Z., Qian, Y., Xiao, H., Lu, Y., Qian, W., Gulen, M. F., Sizemore, N., et al. (2007) Interleukin-1 (IL-1)-induced TAK1-dependent Versus MEKK3-dependent NFkappaB activation pathways bifurcate at IL-1 receptor-associated kinase modification. J. Biol. Chem. **282**, 6075–89.